Center for
Advanced Nuclear
Energy Systems

Massachusetts Institute of Technology
77 Massachusetts Avenue, 24-215
Cambridge, MA 02139-4307

(617) 452-2660
canes@mit.edu
canes.mit.edu

Advanced Nuclear Power Program

Feasibility Study of Decentralized Hydrogen Production Using Nuclear Batteries

Emile Germonpre and Jacopo Buongiorno

Department of Nuclear Science and Engineering
Massachusetts Institute of Technology

MIT-ANP-TR-199
January 2024

Feasibility study of decentralized hydrogen production using nuclear batteries

Emile Germonpre
MIT Nuclear Science and Engineering Department
11/27/23

Executive summary

Nuclear batteries (NBs) are an innovative class of nuclear microreactors with a thermal output below 30 MWth. They promise to provide energy as a service to customers with minimal staff and site preparation requirements, with rapid deployment – on the order of days to weeks – owing to their compactness (size of one or multiple shipping containers) and autonomous plug-and-play nature. In addition, the possibility for colocation of the NBs with customers and their high targeted reliability (capacity factors upwards of 90%) limits the need for costly transmission and storage systems. This is especially appealing in the context of hydrogen production, as the hydrogen transport and dispensing costs are prohibitively high for the development of a hydrogen economy – in 2017, the hydrogen transport and dispensing costs were 14.4 – 15.6 $/kg [1].

This work aims to identify the requirements NBs must satisfy for decentralized electricity or hydrogen production and their ability to do so. This report outlines the current state of research and identifies key areas of future work.

A set of requirements has been identified in the context of both hydrogen production and the use of NBs in offshore power generation – which is part of the broader scope of this project sponsored by Shell, Equinor and Exxon Mobil – but the set is only treated qualitatively for now. No system requirements have been identified that are unique or more stringent for electrolysis than for grid electricity production. Thus, the limiting requirement for the viability of NB-power electrolysis is its economics, which is why the study has focused mainly on the economics of hydrogen production using NBs.

For the economic analysis, several projects starting in 2030 in California (CA) are considered, see Table 1. The projects either buy electricity from the grid, or produce it using NBs. In the latter case, the more efficient, high-temperature Solid Oxide Electrolysis Cells (SOEC) are considered alongside the mature low-temperature Polymer Electrolyte Membrane (PEM) electrolysis. CA is chosen because many hydrogen projects have been developed there already, and hence, data on costs and price projections is readily available. Two types of decentralized hydrogen production are considered, one is a community-scale facility that is close to the demand and the other is on-site production using a single NB – hereafter referred to as **centralized** and **distributed** production, respectively. Note that the community-scale facility can be referred to as a semi-centralized facility under the nomenclature or Reddi et al. [2], but is called a centralized facility in this report.

The capacity of the community-scale facilities represents an electrical demand of roughly 60 MWe for PEM electrolysis and 45 MWe for SOEC electrolysis, well within the reasonable range for a multiple-NB project. For the distributed production, a capacity of 1600 kg/d is chosen based on the capacity of the currently-largest hydrogen fueling station in CA [3].

The economic analysis is based on simple levelized cost models to compare the levelized cost of electricity (LCOE) and hydrogen (LCOH2). Reported costs result from Monte Carlo simulations and in addition, sensitivity analyses are performed for each project. Moreover, multiple ways of claiming subsidies under the Inflation Reduction Act (IRA) are considered for each case considered in Table 1. Finally, a doubling of the capacity of the distributed projects to two NBs is also considered to highlight economies of scale in the NB projects.

Table 1 The cases considered in the economic analysis

Paradigm	Method	Capacity [kg/d]	Transportation method
Community-scale/centralized	Grid + PEM	25 000	Truck delivery
	NB + PEM	25 000	Truck delivery
	NB + SOEC	25 000	Truck delivery
Distributed	Grid + PEM	1600	None
	NB + PEM	1600	None
	NB + SOEC	1600	None

In both distributed and community-scale electricity production, the LCOE of the NBs far exceeds the projected 2030 wholesale electricity price in CA, Figure 1. However, colocation of the NB with the demand avoids most of the high transmission and distribution costs, and as a result, the LCOE of the NBs in community-scale production is competitive compared to the average projected retail electricity price. Yet, the same does not hold in smaller-scale distributed production due to the high levelized O&M costs due to ensuring on-site security, i.e., armed guards. As these costs are fixed to the NB site (not their power), they have a larger influence at these smaller scales.

The site-specific security costs can be diluted by increasing the generation capacity of a NB project. Indeed, the LCOE decreases significantly when adding a second and third NB, Figure 2. However, increasing the number of NBs yields diminishing returns and adding a fifth or seventh NB only decreases the LCOE by 2% or 1%, respectively. Given that NBs compete with larger-scale technologies that benefit from economies of scale, it is unlikely that NB projects with high capacities will be economical. The mid-range of a handful – e.g., four – of NBs thus seems optimal.

The extent to which the facility size influences the LCOE depends on the required number of on-site guards (full-time employees, FTEs), Figure 3. If the regulator does not demand the presence of an on-site security force, then there is no scaling of the LCOE with facility size – within our cost model. The eventual regulations about on-site security requirements will thus significantly affect the economics of small-scale NB projects.

Given that the centralized NBs facility can supply cheaper electricity than the grid, it is no surprise that the LCOH2 for centralized production is lower than the grid benchmark, Figure 4. The LCOH2 can be lowered further by capitalizing on the high-temperature heat production of the NBs with efficient SOEC electrolysis, resulting in an LCOH2 of 3.67 $/kg, which is on par with what is expected for solar-powered electrolysis in CA – i.e., 3.2 – 3.8 $/kg after correction for the IRA subsidies [4]. The economics of distributed generation with NBs look much bleaker due to the high cost of on-site security, Figure 4.

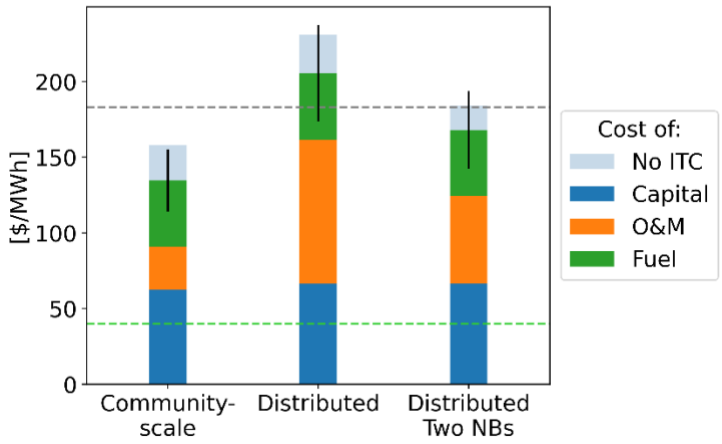

Figure 1 Comparison of the LCOE for electricity production with NBs to the projected 2030 wholesale electricity price in CA (green) and retail price (grey) [5]. The light blue bar shows the LCOE in case no Investment Tax Credits (ITC) are claimed under the Inflation Reduction Act (IRA)

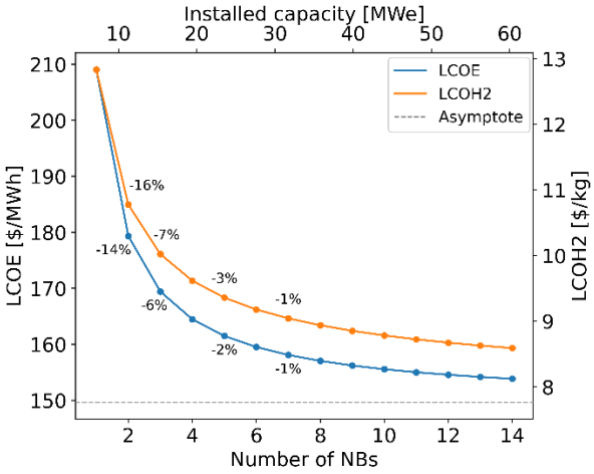

Figure 2 The evolution of the LCOE and LCOH2 as a function of the number of installed NBs in a centralized PEM model. The data labels represent the percentage decline compared to the previous data point and the grey line corresponds to the asymptote at infinite number of NBs

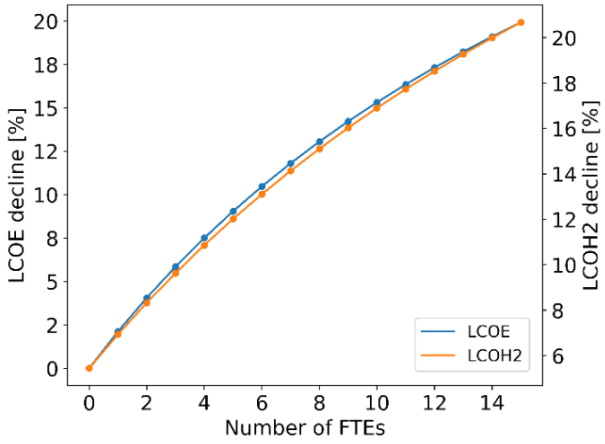

Figure 3 The percentage decrease in the LCOE and LCOH2 upon adding a second NB as a function of the number of required on-site guards

A basic optimization is performed to consider flexible operation of the hydrogen production plant – i.e., allowing for the sale of electricity to the grid in times of high prices. Based on our preliminary results, off-grid operation seems more attractive for NBs, as their high marginal production cost would lead to infrequent operation with the revenue from grid participation not able to compensate for the loss in capacity factor. However, a more comprehensive study of potential revenue streams and a more elaborate optimization are needed to decisively rule out grid participation for NBs.

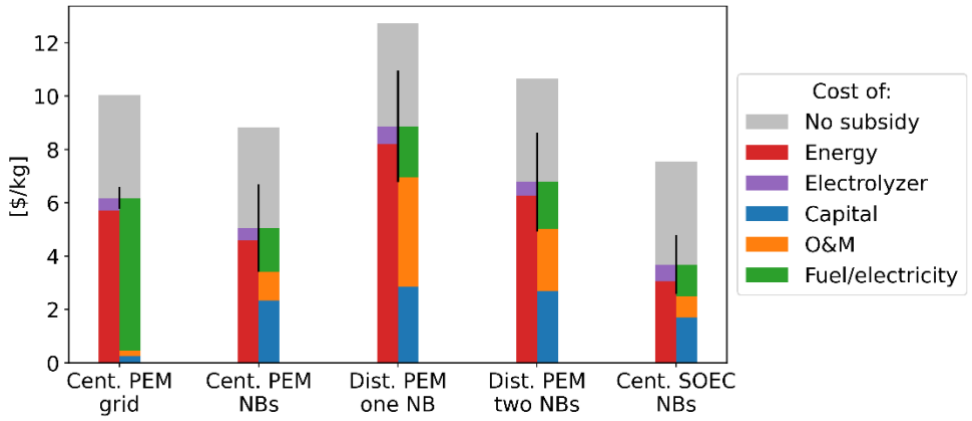

Figure 4 Comparison of the lowest LCOH2 estimates for with different technologies, the LCOH2 is broken up in two columns for each case to show share of the levelized cost of the electrolyzers versus energy and to show the distribution between the levelized costs of capital, O&M, and fuel. The grey bars show the LCOH2 in case no subsidies are claimed under the IRA

Importantly, the discussion so far only considers the production cost of hydrogen, not the total cost, which ignores the benefit of on-site hydrogen production in the distributed case. Estimating the value of on-site hydrogen production is, unfortunately, not as simple as for electricity production, as estimates for the cost of hydrogen storage, distribution and dispensing vary significantly in the literature. Hence, a rudimentary hydrogen cost model was developed in this work to estimate the supply chain cost difference between distributed and centralized hydrogen production based on a partial levelized cost of hydrogen distribution (pLCOH2).

Although the transport and dispensing costs themselves are very large, the cost difference between the distributed and centralized production is rather small at 1.14 $/kg because the community-scale facility is located relatively close to demand, and the distributed production needs more storage onsite. As a result, the production cost differences are most important, and centralized production is cheaper, Figure 5. When distributed production is done at a larger-scale with two NBs, the production costs come down and there is no longer a clear winner between centralized and distributed production, Figure 6.

In all cases with NBs, the levelized cost of capital is high, and even more so for first-of-a-kind (FOAK) NBs, where the economics are not attractive, Figure 7. It is thus unlikely that NBs will see their first use in an application such as hydrogen production. The learning rates in the production of more NBs will thus be key to reaching sufficiently low costs – capital costs in particular – to enable widespread use of NBs. Although aggressive cost declines are needed, a recent study by Abou-Jaoude et al. [6] supports that idea that factory production and assembly can drive down costs significantly, even in near-term NB production scenarios. Another conclusion to be drawn from Figure 7 is that the fuel type used (UO_2 vs. TRISO fuel) does not significantly change the economics – to the first order, secondary effects on, e.g., licensing are not considered.

It is important to acknowledge the crucial role of the IRA subsidies in the comparison of the LCOH2 of different technologies. At present, there are still many grey areas in the legislation, e.g., how lifecycle emissions will be counted and what the emissions of grid electricity are. For example, if grid electricity emissions are counted via the average carbon intensity of the electricity producers, the PEM electrolysis with energy from the grid is not eligible for IRA subsidies, resulting in higher costs for non-nuclear

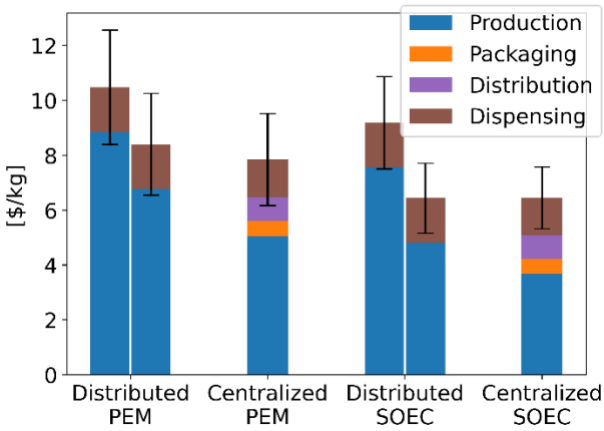

Figure 5 Comparison of the total LCOH2 between centralized and distributed production with PEM and SOEC. For the distributed production, the left bar represents production with a single NB and the right bar represents production with two NBs

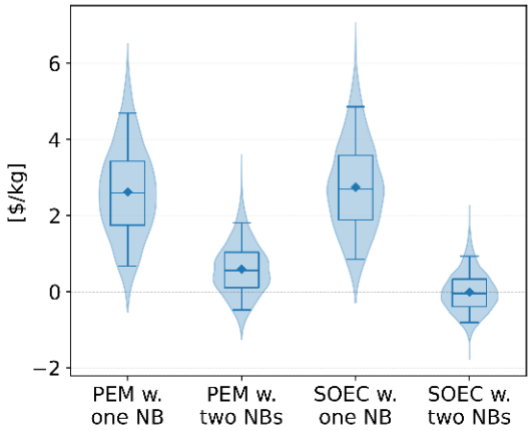

Figure 6 Box plots of the total LCOH2 difference between distributed and centralized production as determined from Monte Carlo simulations with consistent sampling. Centralized PEM/SOEC production is the reference for the differences, with the labels denoting what type of distributed production is used

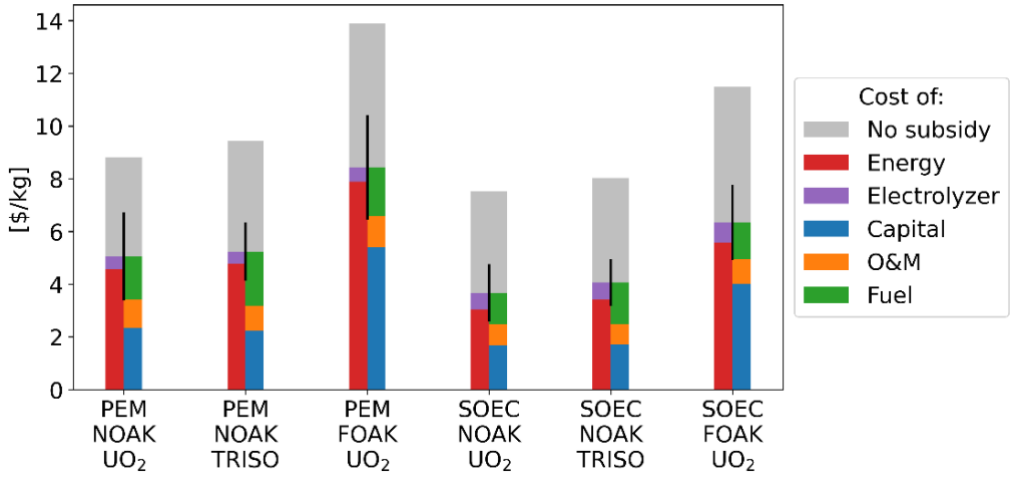

Figure 7 Comparison of the lowest LCOH2 estimates for centralized production with NOAK and FOAK NBs and different fuel types, the LCOH2 is broken up in two columns for each case to show share of the levelized cost of the electrolyzers versus energy and to show the distribution between the levelized costs of capital, O&M, and fuel. The grey bars show the LCOH2 in case no subsidies are claimed under the IRA

distributed production than with energy supplied by NBs, Figure 4. However, in case lifecycle emissions for electricity from the grid can be avoided through power-purchase agreements with renewable generators, the IRA subsidies can be claimed and the NBs are no longer the cheapest option. In the current default Greenhouse gases, Regulated Emissions, and Energy use in Technology (GREET) model, nuclear energy is unfairly disadvantaged compared to renewables in terms of emissions accounting. The eventual implementation of the IRA subsidies can thus seriously alter the bottom line of this study.

Figure 8 Figure 9 show the distribution of cost differences between different scenarios as determined via Monte Carlo simulations that sample shared cost items consistently. They give a better view of the cost differences than the bar charts of Figure 4 Figure 7 and compare all influences side-by-side.

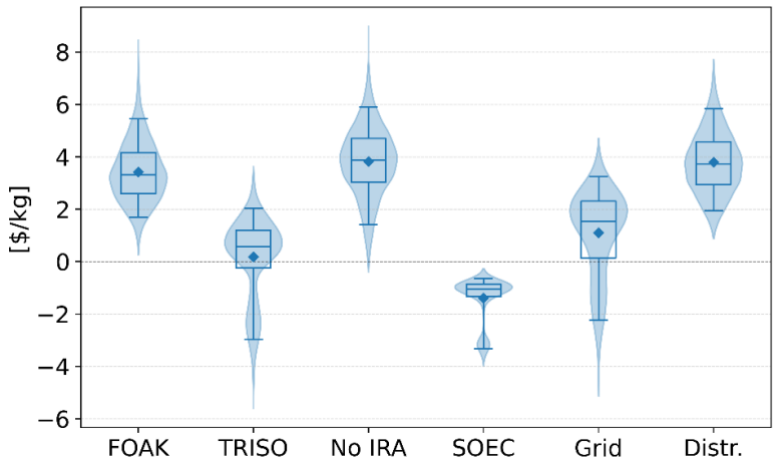

Figure 8 Boxplots of the LCOH2 difference distributions resulting from coupled Monte Carlo simulations. For each boxplot, one assumption is changed compared to the reference, which is a community-scale PEM facility using UO_2-fueled NOAK NBs and claiming mixed subsidies

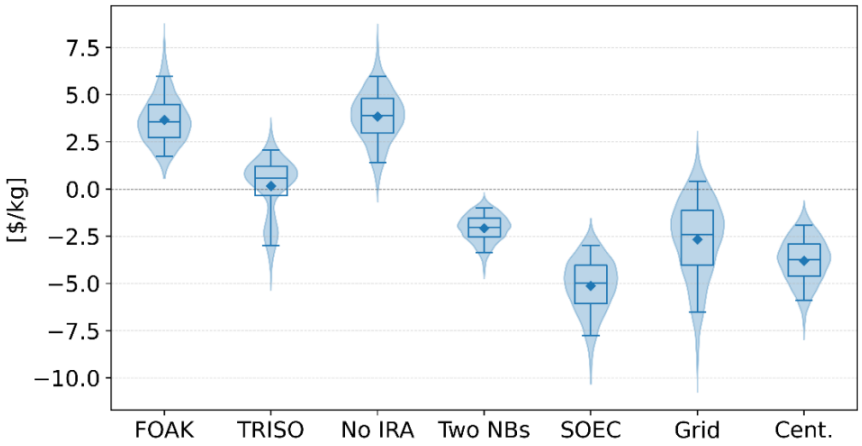

Figure 9 Boxplots of the LCOH2 difference distributions resulting from coupled Monte Carlo simulations. For each boxplot, one assumption is changed compared to the reference, which is on-site production using PEM electrolyzers with a single UO_2-fueled NOAK NB and claiming mixed subsidies

In conclusion, the need for cost competitiveness with other decentralized hydrogen production technologies is the only potentially inhibiting requirement identified for the viability of decentralized hydrogen production using NBs. The preliminary results suggest community-scale hydrogen production with NBs can be cost competitive. However, the diseconomies of scale in the physical security requirements results in unattractive costs for distributed (onsite) production with a single NB. Overall, the competitiveness of a NB-based hydrogen project is especially dependent on:

1. Policy and regulation through clean energy subsidies and the requirement of on-site guards.
2. The learning rates in the economies of multiples that must lower NB capital costs overtime.
3. The efficient leveraging of NB capabilities, specifically the high-temperature heat production and capability of standalone operation in remote off-grid and energy constrained areas.
4. The benefit of local production, which is decisive for electricity production with NBs compared to buying electricity from the grid by allowing to avoid the high electricity tariffs. Yet, in case of hydrogen production, the avoided distribution costs for on-site distributed production are not sufficient to offset the higher production costs compared to centralized production.

CANES Publications

Topical and progress reports are published under seven series:

Advances in Nuclear Energy Disciplines (ANED) Series

Advanced Nuclear Power Technology (ANP) Series

Nuclear Fuel Cycle Technology and Policy (NFC) Series

Nuclear Systems Enhanced Performance (NSP) Series

MIT Reactor Redesign (MITRR) Series

Nuclear Energy and Sustainability (NES) Series

Nuclear Space Applications (NSA) Series

Please visit our website (mit.edu/canes/) to view more publication lists.

MIT-ANP-TR-197	Matthew Chew and Jacopo Buongiorno, **A Cybersecurity Framework for Nuclear Microreactors** (June 2023).
MIT-ANP-TR-196	Paul E. Roege(MIT ANPEG), Alexander L. Schoonen(INL), James R. Case (INL), Corey L. Beebe(INL), Ryan Cumings (MIT LL), Zachary A. Collier (Collier Research Systems), **Assessment of Potential Ground Force Capability Enhancement Using Nuclear Microreactors** (August 2022).
MIT-ANP-TR-194	W. Robb Stewart and K. Shirvan (MIT), **Capital Cost Evaluation of Advanced Water-Cooled Reactor Designs With Consideration of Uncertainty and Risk** (June 2022).
MIT-ANP-TR-193	K. Shirvan (MIT), **Overnight Capital Cost of the Next AP1000** (March 2022).
MIT-ANP-TR-192	R. MacDonald and J. Parsons (MIT), **The Value of Nuclear Microreactors in Providing Heat and Electricity to Alaskan Communities** (October 2021).
MIT-ANP-TR-191	C. W. Forsberg (MIT) and A. W. Foss (INL), **Markets and Economic Requirements for Fission Batteries and Other Nuclear Systems** (March 2021).
MIT-ANP-TR-190	J. Buongiorno (MIT), **An Economic Evaluation of Micro-Reactors for the State of Washington** (January 2021).
MIT-ANP-TR-189	C. W. Forsberg (MIT), P. Sabharwall (INL)and A. Sowder (EPRI), **Separating Nuclear Reactors from the Power Block with Heat Storage:** A New Power Plant Design Paradigm (November 2020).
MIT-ANP-TR-188	X. Zhao and M. Golay, **Symptom-Based Conditional Failure Probability Estimation for Selected Structures, Systems, and Components:** Minor Milestone Report: Project on Design of Risk-Informed Autonomous Operation for Advanced Reactors DOE/EXT- DE-NE0008873 Project number: 19-17435 (July 2020).
MIT-ANP-TR-187	J. Buongiorno, K. Shirvan, E. Baglietto, C. Forsberg, M. Driscoll, W. Robb Stewart, Enrique Velez-Lopez (MIT), H. Einstein (Civil & Environmental Engineering), Iain

Macdonald (ArtEZ), Kennard Johnston (Morgan State Univ.) and Go Hashimoto (Univ. of Tokyo), **Japan's Next Nuclear Energy System (JNext)** (March 2020).

MIT-ANP-TR-186 Y. Cai and M. W. Golay, **A Framework for Analyzing Nuclear Power Multiunit Accident Scenarios and Providing Accident Mitigation and Site Improvement Suggestions** (September 2019).

MIT-ANP-TR-185 C. W. Forsberg (MIT), P. Sabharwall and H. D. Gougar (INL), **Heat Storage Coupled to Generation IV Reactors for Variable Electricity from Base-load Reactors: Changing Markets, Technology, Nuclear-Renewables Integration and Synergisms with Solar Thermal Power Systems** INL/EXT-19-54909 (September 2019).

MIT-ANP-TR-184 C. W. Forsberg, **Implications of Carbon Constraints on (1) the Electricity Generation Mix For the United States, China, France and United Kingdom and (2) Future Nuclear System Requirements** (March 2019).

MIT-ANP-TR-183 C. W. Forsberg, **Fluoride-Salt-Cooled High-temperature Reactor (FHR) Temperature Control Options: Removing Decay Heat and Avoiding Salt Freezing** (January 2019).

MIT-ANP-TR-182 J. Buongiorno, N. Sepulveda and L. Rush, **White Paper: Potential Applications of the Modern Nuclear Fuel Cycle to (South) Australia** (November 2018).

MIT-ANP-TR-181 C. Forsberg and P. Sabharwall, **Heat Storage Options for Sodium, Salt and Helium Cooled Reactors to Enable Variable Electricity to the Grid and Heat to Industry with Base-Load Reactor Operations** (September 2018).

MIT-ANP-TR-180 C. W. Forsberg, et al. **Integrated FHR Technology Development Final Report: Tritium Management, Materials Testing, Salt Chemistry Control, Thermal Hydraulics and Neutronics with Associated Benchmarking** (September 2018).

MIT-ANP-TR-179 C. W. Forsberg, N. Sepulveda and K. Dawson **Implications of Carbon Constraints on Electricity Generation Mix For the United States, China, France and United Kingdom** (August 2018).

MIT-ANP-TR-178 C. W. Forsberg, N. Sepulveda and K. Dawson **Commercialization Basis for Fluoride-salt-cooled High-Temperature Reactors (FHRs): Base-load Reactor with Heat Storage for Variable Electricity and High-Temperature Heat to Industry** (August 2018).

MIT-ANP-TR-177 S.T. Lam, C. W. Forsberg, and R. Ballinger **Understanding Hydrogen/Tritium Behavior on Carbon to Predict and Control Tritium in Salt Reactors: Experiments, Modeling and Simulation** (August 2018).

MIT-ANP-TR-176 J. Conway, N. Todreas, and J. Buongiorno **Security and the Offshore Nuclear Plant (ONP): Security Simulation Testing and Analysis of the Multi-Layer Security System** (August 2018).

MIT-ANP-TR-175 P. A. Champlin, D. Petti, and J. Buongiorno **Techno-Economic Evaluation of Cross-Cutting Technologies for Cost Reduction in Nuclear Power Plants** (August 2018).

Table of contents

Executive summary i
CANES Publications vii
Table of contents ix
List of Abbreviations xi
List of Tables xii
List of Figures xiv
1. Introduction 1
2. Nuclear battery requirements 2
3. Case studies 5
4. Hydrogen production cost analysis 8
4.1. Cost modeling methodology 8
4.2. The Inflation Reduction Act subsidies 11
4.3. PEM electrolysis with grid electricity 13
4.3.1. Community-scale production 13
4.3.2. Distributed production 15
4.4. PEM electrolysis with nuclear batteries 17
4.4.1. Community-scale production 17
4.4.2. Distributed production 26
4.5. SOEC electrolysis with nuclear batteries 31
4.5.1. Community-scale production 31
4.5.2. Distributed production 35
4.6. TRISO fuel 39
4.7. Effect of facility sizing 42
4.8. Revenue from grid participation 44
4.9. Production cost comparison and discussion 48
5. Partial hydrogen storage, distribution, and dispensing costs 53
5.1. Modeling scope 53
5.2. Cost modeling methodology 55
5.3. Modeling the storage and transport of hydrogen 57
5.4. Distributed production 62
5.5. Centralized production 65

5.6. Total hydrogen cost comparison and discussion 70
6. Conclusion and future work 74
7. References 76
Appendix A Waste and refueling cost calculations A-1
A.1 Waste cost A-1
A.2 Refueling cost A-5
Appendix B LCOE Results B-8
B.1 Nuclear batteries B-8
B.1.1 Community-scale production B-8
B.1.2 Distributed production B-9
B.1.3 Distributed production with two NBs B-10
B.2 Nuclear batteries used in SOEC electrolysis B-11
B.2.1 Distributed production B-11
Appendix C LCOH2 Results C-13
C.1 PEM electrolysis with grid electricity C-13
C.1.1 Community-scale production C-13
C.1.2 Distributed production C-14
C.2 PEM electrolysis with nuclear batteries C-15
C.2.1 Community-scale production C-15
C.2.2 Distributed production C-18
C.2.3 Distributed production with two NBs C-21
C.3 SOEC electrolysis with nuclear batteries C-24
C.3.1 Community-scale production C-24
C.3.2 Distributed production C-27
C.3.3 Distributed production with two NBs C-30

List of Abbreviations

CA	California
CANDU	Canadian deuterium uranium
EOL	End-of-life
FOAK	First-of-a-kind
FTE	Full-time employee
GHG	Greenhouse gas
GREET	Greenhouse gases, Regulated Emissions, and Energy use in Technology
INL	Idaho National Laboratory
IRA	Inflation Reduction Act
IRC	Internal Revenue Code
ITC	Investment tax credit
HM	Heavy metal
LCOE	Levelized cost of electricity
LCOH	Levelized cost of heat
LCOH2	Levelized cost of hydrogen
MC	Monte Carlo
NB	Nuclear battery
NEA	Nuclear Energy Agency
NOAK	Nth-of-a-kind
NRC	Nuclear Regulatory Commission
O&M	Operations and maintenance
PEM	Polymer Electrolyte Membrane
pLCOH2	Partial levelized cost of hydrogen
PTC	Production tax credit
PWR	Pressurized water reactor
SNF	Spent nuclear fuel
SOEC	Solid oxide electrolysis cell
SMR	Steam methane reforming
SWU	Separative work unit

List of Tables

Table 1 The cases considered in the economic analysis ii
Table 2 Qualitative assessment of the requirements for the NBs when used in hydrogen production and offshore power generation: green indicates the requirement is highly relevant to the application, yellow indicates moderate relevance, and orange means the requirement is either not strict or not applicable .2
Table 3 The cases considered in the economic analysis 7
Table 4 The base clean hydrogen credit under the IRA as a function of the hydrogen production emissions 12
Table 5 Model assumptions for a community-scale PEM facility with electricity bought from the grid 13
Table 6 Model assumptions for distributed PEM electrolysis with electricity bought from the grid 16
Table 7 NOAK model assumptions for a community-scale PEM facility with electricity produced by NBs, FOAK NB capital costs are shown in red 17
Table 8 NOAK model assumptions for distributed PEM electrolysis with electricity produced by NBs, FOAK capital costs are shown in red 26
Table 9 NOAK model assumptions for a community-scale SOEC facility with electricity and heat provided by NBs, FOAK capital costs are shown in red 31
Table 10 NOAK model assumptions for distributed PEM electrolysis with electricity and heat provided by NBs, FOAK capital costs are shown in red 35
Table 11 A list of NB designs that are being developed 40
Table 12 Model assumptions for on-site hydrogen production using NBs 62
Table 13 Model assumptions for community-scale hydrogen production with gaseous truck delivery 65
Table 14 Geometric parameters of the fuel assemblies of different reactor types A-1
Table 15 Assumptions for the central facility cost model A-6
Table 16 LCOE breakdown for community-scale PEM electrolysis with UO_2-fueled NBs, LCOE given in $/MWh as μ ± σ [m, M] B-8
Table 17 LCOE breakdown for community-scale PEM electrolysis with TRISO-fueled NBs, LCOE given in $/MWh as μ ± σ [m, M] B-8
Table 18 LCOE breakdown for distributed PEM electrolysis with UO_2-fueled NBs, LCOE given in $/MWh as μ ± σ [m, M] B-9
Table 19 LCOE breakdown for distributed PEM electrolysis with TRISO-fueled NBs, LCOE given in $/MWh as μ ± σ [m, M] B-9
Table 20 LCOE breakdown for distributed PEM electrolysis with two UO_2-fueled NBs, LCOE given in $/MWh as μ ± σ [m, M] B-10
Table 21 LCOE breakdown for distributed PEM electrolysis with two TRISO-fueled NBs, LCOE given in $/MWh as μ ± σ [m, M] B-10
Table 22 LCOE breakdown for distributed SOEC electrolysis with UO_2-fueled NBs, LCOE given in $/MWh as μ ± σ [m, M] B-11
Table 23 LCOE breakdown for distributed SOEC electrolysis with TRISO-fueled NBs, LCOE given in $/MWh as μ ± σ [m, M] B-12
Table 24 LCOH2 for PEM electrolysis using grid electricity in $/kg as μ ± σ [m, M] C-13
Table 25 LCOH2 breakdown for community-scale PEM electrolysis with UO_2-fueled NBs, LCOH2 given in $/kg as μ ± σ [m, M] C-15

Table 26 LCOH2 breakdown for community-scale PEM electrolysis with TRISO-fueled NBs, LCOH2 given in $/kg as μ ± σ [m, M] C-16
Table 27 LCOH2 breakdown for distributed PEM electrolysis with UO_2-fueled NBs, LCOH2 given in $/kg as μ ± σ [m, M] C-18
Table 28 LCOH2 breakdown for distributed PEM electrolysis with TRISO-fueled NBs, LCOH2 given in $/kg as μ ± σ [m, M] C-19
Table 29 LCOH2 breakdown for distributed PEM electrolysis with two UO_2-fueled NBs, LCOH2 given in $/kg as μ ± σ [m, M] C-21
Table 30 LCOH2 breakdown for distributed PEM electrolysis with two TRISO-fueled NBs, LCOH2 given in $/kg as μ ± σ [m, M] C-22
Table 31 LCOH2 breakdown for community-scale SOEC electrolysis with UO_2-fueled NBs, LCOH2 given in $/kg as μ ± σ [m, M] C-24
Table 32 LCOH2 breakdown for community-scale SOEC electrolysis with TRISO-fueled NBs, LCOH2 given in $/kg as μ ± σ [m, M] C-25
Table 33 LCOH2 breakdown for distributed SOEC electrolysis with UO_2-fueled NBs, LCOH2 given in $/kg as μ ± σ [m, M] C-27
Table 34 LCOH2 breakdown for distributed SOEC electrolysis with TRISO-fueled NBs, LCOH2 given in $/kg as μ ± σ [m, M] C-28
Table 35 LCOH2 breakdown for distributed SOEC electrolysis with two UO_2-fueled NBs, LCOH2 given in $/kg as μ ± σ [m, M] C-30
Table 36 LCOH2 breakdown for distributed SOEC electrolysis with two TRISO-fueled NBs, LCOH2 given in $/kg as μ ± σ [m, M] C-31

List of Figures

Figure 1 Comparison of the LCOE for electricity production with NBs to the projected 2030 wholesale electricity price in CA (green) and retail price (grey) [5]. The light blue bar shows the LCOE in case no Investment Tax Credits (ITC) are claimed under the Inflation Reduction Act (IRA) iii
Figure 2 The evolution of the LCOE and LCOH2 as a function of the number of installed NBs in a centralized PEM model. The data labels represent the percentage decline compared to the previous data point and the grey line corresponds to the asymptote at infinite number of NBs iii
Figure 3 The percentage decrease in the LCOE and LCOH2 upon adding a second NB as a function of the number of required on-site guards iii
Figure 4 Comparison of the lowest LCOH2 estimates for with different technologies, the LCOH2 is broken up in two columns for each case to show share of the levelized cost of the electrolyzers versus energy and to show the distribution between the levelized costs of capital, O&M, and fuel. The grey bars show the LCOH2 in case no subsidies are claimed under the IRA iv
Figure 5 Comparison of the total LCOH2 between centralized and distributed production with PEM and SOEC. For the distributed production, the left bar represents production with a single NB and the right bar represents production with two NBs v
Figure 6 Box plots of the total LCOH2 difference between distributed and centralized production as determined from Monte Carlo simulations with consistent sampling. Centralized PEM/SOEC production is the reference for the differences, with the labels denoting what type of distributed production is used .. v
Figure 7 Comparison of the lowest LCOH2 estimates for centralized production with NOAK and FOAK NBs and different fuel types, the LCOH2 is broken up in two columns for each case to show share of the levelized cost of the electrolyzers versus energy and to show the distribution between the levelized costs of capital, O&M, and fuel. The grey bars show the LCOH2 in case no subsidies are claimed under the IRA v
Figure 8 Boxplots of the LCOH2 difference distributions resulting from coupled Monte Carlo simulations. For each boxplot, one assumption is changed compared to the reference, which is a community-scale PEM facility using UO_2-fueled NOAK NBs and claiming mixed subsidies vi
Figure 9 Boxplots of the LCOH2 difference distributions resulting from coupled Monte Carlo simulations. For each boxplot, one assumption is changed compared to the reference, which is on-site production using PEM electrolyzers with a single UO_2-fueled NOAK NB and claiming mixed subsidies vi
Figure 10 Visualization of the LANL's Megapower design [8] 1
Figure 11 Suggested locations for hydrogen production facilities of different technologies by 2030 in the low hydrogen demand scenario of [10]. Electrolyzer wind/solar refer to (centralized) electrolysis with wind/solar energy, thermochemical refers to facilities producing hydrogen from biomass from forests and agricultural residue, dairy facilities make hydrogen from anaerobic dairy digesters, food refers to hydrogen production from the residential waste stream, and SMR refers to steam methane reforming .. 5
Figure 12 The predicted hydrogen demand gap in CA in 2027 [3] 6
Figure 13 LCOH2 for community-scale PEM electrolysis with grid electricity 14
Figure 14 Tornado chart for the LCOH2 (in $/kg) in a community-scale PEM facility running on grid electricity 14
Figure 15 Comparison of the LCOH2 for PEM electrolysis using grid electricity when claiming different types of IRA subsidies, the LCOH2 is broken up in two columns for each case to show share of the levelized

cost of the electrolyzers versus energy and to show the distribution between the levelized costs of capital, O&M, and fuel 15
Figure 16 LCOH2 for distributed PEM electrolysis with grid electricity 16
Figure 17 LCOH2 for distributed PEM electrolysis with grid electricity when claiming PTCs under the IRA 16
Figure 18 NB capital cost scenarios reported in [34] 19
Figure 19 LCOE for electricity supplied by NOAK NBs without IRA subsidy 20
Figure 20 Tornado chart for the LCOE (in $/MWh) of electricity by NOAK NBs without IRA subsidy 20
Figure 21 LCOH2 for community-scale PEM electrolysis with electricity supplied by NOAK NBs without IRA subsidy 21
Figure 22 Tornado chart for the LCOH2 (in $/kg) in a community-scale PEM facility powered by NOAK NBs without IRA subsidy 21
Figure 23 LCOH2 for community-scale PEM electrolysis with electricity supplied by NOAK NBs claiming an IRA ITC 22
Figure 24 Tornado chart for the LCOH2 (in $/kg) in a community-scale PEM facility powered by NOAK NBs and claiming an IRA ITC 22
Figure 25 LCOH2 for community-scale PEM electrolysis with NOAK NBs subsidized by PTCs....23
Figure 26 Tornado chart for the LCOH2 (in $/kg) in a community-scale PEM facility powered by NBs claiming PTCs 23
Figure 27 LCOH2 for community-scale PEM electrolysis with electricity supplied by NOAK NBs with mixed IRA subsidies 24
Figure 28 Tornado chart for the LCOH2 (in $/kg) in a community-scale PEM facility powered by NOAK NBs with mixed IRA subsidies 24
Figure 29 Comparison of the LCOH2 for community-scale PEM electrolysis using NOAK NBs when claiming different types of IRA subsidies, the LCOH2 is broken up in two columns for each case to show share of the levelized cost of the electrolyzers versus energy and to show the distribution between the levelized costs of capital, O&M, and fuel 24
Figure 30 LCOE for community-scale production with FOAK NBs without IRA subsidy....25
Figure 31 Tornado chart for the LCOE (in $/MWh) for community-scale production with FOAK NBs without IRA subsidy....25
Figure 32 LCOH2 for community-scale PEM electrolysis with FOAK NB electricity without IRA subsidy ...25
Figure 33 LCOH2 for community-scale PEM electrolysis with electricity supplied by FOAK NBs with mixed IRA subsidy....25
Figure 34 Comparison of the LCOH2 for community-scale PEM electrolysis using FOAK NBs when claiming different types of IRA subsidies, the LCOH2 is broken up in two columns for each case to show share of the levelized cost of the electrolyzers versus energy and to show the distribution between the levelized costs of capital, O&M, and fuel 26
Figure 35 LCOE for electricity supplied by a single FOAK NB 28
Figure 36 Tornado chart for the LCOE (in $/MWh) of electricity by a single FOAK NB....28
Figure 37 Comparison of the LCOH2 for distributed PEM electrolysis using NOAK NBs when claiming different types of IRA subsidies, the LCOH2 is broken in two ways to show share of the levelized cost of the electrolyzers versus energy and to show the distribution between the levelized costs of capital, O&M, and fuel 29
Figure 38 LCOH2 for distributed PEM electrolysis with FOAK NBs without IRA subsidy 30

Figure 39 LCOH2 for distributed PEM electrolysis with FOAK NBs with mixed IRA subsidies 30
Figure 40 LCOH2 for community-scale SOEC electrolysis with electricity supplied by NOAK NBs without IRA subsidy 33
Figure 41 Tornado chart for the LCOH2 (in $/kg) in a community-scale SOEC facility powered by NOAK NBs without IRA subsidies 33
Figure 42 Comparison of the LCOH2 for community-scale SOEC electrolysis using NOAK NBs when claiming different types of IRA subsidies, the LCOH2 is broken up in two columns for each case to show share of the levelized cost of the electrolyzers versus energy and to show the distribution between the levelized costs of capital, O&M, and fuel 34
Figure 43 LCOH2 for community-scale SOEC electrolysis with electricity supplied by FOAK NBs without IRA subsidy 35
Figure 44 LCOH2 for community-scale SOEC electrolysis with electricity supplied by FOAK NBs with mixed IRA subsidies 35
Figure 45 LCOH2 for distributed SOEC electrolysis with electricity supplied by NOAK NBs without IRA subsidy 37
Figure 46 Tornado chart for the LCOH2 (in $/kg) for distributed SOEC electrolysis with electricity supplied by NOAK NBs without IRA subsidy.....37
Figure 47 LCOH2 for distributed SOEC electrolysis with electricity supplied by FOAK NBs without IRA subsidy 38
Figure 48 Tornado chart for the LCOH2 (in $/kg) for distributed SOEC facility powered by FOAK NBs without IRA subsidy 38
Figure 49 Schematic of PWR fuel assembly and fuel rods. Taken from Ref. [44] 39
Figure 50 Schematic representation of a TRISO particle. Taken from Ref. [45].....39
Figure 51 Tornado chart for the LCOH2 (in $/kg) in a centralized PEM facility powered by UO_2-fueled NBs with mixed IRA subsidies 41
Figure 52 Tornado chart for the LCOH2 (in $/kg) in a centralized PEM facility powered by TRISO-fueled NBs with mixed IRA subsidies 41
Figure 53 The evolution of the LCOE and LCOH2 as a function of the number of installed NBs in a centralized PEM model. The data labels represent the percentage decline compared to the previous data point and the grey line corresponds to the asymptote at infinite number of NBs.....42
Figure 54 Box plots with distribution overlay for the LCOH2 decline upon adding a second NB while claiming mixed subsidies in both cases. The box plot whiskers represent the 5^{th} and 95^{th} percentiles and the mean is represented by a diamond marker 42
Figure 55 The percentage decrease in the LCOE and LCOH2 upon adding a second NB as a function of the number of required on-site guards 43
Figure 56 2022 CAISO average wholesale electricity price in five-minute intervals. The threshold price between electricity and hydrogen production is 100 $/MWh in the figure 44
Figure 57 Revenue on per-MW basis associated with the sale of hydrogen and electricity of a coproducing PEM facility, the hydrogen only line corresponds to a facility that does not sell electricity to the grid 45
Figure 58 The LCOH2 impact of selling electricity to the grid as a function of the hydrogen price for both centralized and distributed production using PEM.....45
Figure 59 The annual number of hours in which hydrogen is produced instead of selling electricity to the grid as a function of the hydrogen price 45

Figure 60 2022 wholesale electricity price on the SOUTHBY_6_N001 node in Sacramento in five-minute intervals. The threshold price between electricity and hydrogen production is 100 $/MWh in the figure 46
Figure 61 Comparison of the LCOE for electricity production with NBs on a community-scale and for a single NB to the projected 2030 wholesale electricity price in CA (green) and retail price (grey) [5].....48
Figure 62 Comparison of the lowest LCOH2 estimates for community-scale production with different technologies, the LCOH2 is broken up in two columns for each case to show share of the levelized cost of the electrolyzers versus energy and to show the distribution between the levelized costs of capital, O&M, and fuel 49
Figure 63 Comparison of the lowest LCOH2 estimates for distributed production with different technologies, the LCOH2 is broken up in two columns for each case to show share of the levelized cost of the electrolyzers versus energy and to show the distribution between the levelized costs of capital, O&M, and fuel 49
Figure 64 Comparison of the lowest LCOH2 estimates for community-scale production with NOAK and FOAK NBs, the LCOH2 is broken up in two columns for each case to show share of the levelized cost of the electrolyzers versus energy and to show the distribution between the levelized costs of capital, O&M, and fuel 50
Figure 65 Boxplots of the LCOH2 difference distributions resulting from coupled Monte Carlo simulations. For each boxplot, one assumption is changed compared to the reference, which is a community-scale PEM facility using UO_2-fueled NOAK NBs and claiming mixed subsidies 52
Figure 66 Boxplots of the LCOH2 difference distributions resulting from coupled Monte Carlo simulations. For each boxplot, one assumption is changed compared to the reference, which is on-site production using PEM electrolyzers with a single UO_2-fueled NOAK NB and claiming mixed subsidies 52
Figure 67 Components of the hydrogen supply chain. Figure adapted from Ref. [2] to show the scope in this work 54
Figure 68 Components of a gaseous hydrogen refueling station. Figure adapted from Ref. [58] to show the scope in this work where greyed out items are not relevant to the type of refueling station and supply chain considered in this work and the red rectangles show which items are neglected in the cost difference modeling 55
Figure 69 Schematic representation of the distributed production model 57
Figure 70 Demand profile used in the sensitivity analyses of the transport and storage model with distributed production.....58
Figure 71 The model components in centralized production where a quarter of the production plant that supplies five separate stations is modeled.....59
Figure 72 Demand profiles used in the sensitivity analyses of the transport and storage model with centralized production.....61
Figure 73 The evolution of the binary values $xp\ j, i$ as a function of time over four days, a value of one indicates the truck is at the production plant 61
Figure 74 The evolution of the binary values $xs\ j, i$ as a function of time over four days, a value of zero indicates that the old trailer is being replaced with a new one and is hence unavailable 61
Figure 75 The mass of hydrogen stored in the station's tank as a function of time throughout the month when the station is subjected to the reference profile of used in sensitivity analyses 63
Figure 76 Component-wise pLCOH2 breakdown for distributed production resulting from a MC simulation with 5000 samples 64

Figure 77 Tornado chart for the pLCOH2 (in $/kg) of a station with on-site hydrogen production 64
Figure 78 The mass of hydrogen stored in the tanks as a function of time throughout a single week when the station is subjected to the reference profile of used in sensitivity analyses. The dashed line indicates which moments define the station tank capacity 67
Figure 79 Component-wise pLCOH2 breakdown for centralized production resulting from a MC simulation with 5000 samples 68
Figure 80 Logistical pLCOH2 breakdown for centralized production resulting from a MC simulation with 5000 samples 68
Figure 81 Tornado chart for the pLCOH2 (in $/kg) in a centralized production scheme 69
Figure 82 Component-wise pLCOH2 breakdown for distributed production resulting from a MC simulation with 5000 samples 70
Figure 83 Component-wise pLCOH2 breakdown for centralized production resulting from a MC simulation with 5000 samples 70
Figure 84 Comparison of the total LCOH2 between centralized and distributed production with PEM and SOEC. For the distributed production, the left bar represents production with a single NB and the right bar represents production with two NBs 71
Figure 85 Box plots of the total LCOH2 difference between centralized and distributed production as determined from Monte Carlo simulations with consistent sampling. Centralized PEM/SOEC production is the reference for the differences, with the labels denoting what type of distributed production is used 71
Figure 86 Tornado chart of the total cost (in $/kg) model for distributed PEM electrolysis with a single UO_2-fueled NOAK NB claiming mixed subsidies 72
Figure 87 Tornado chart of the total cost (in $/kg) model for centralized PEM electrolysis with UO_2-fueled NOAK NBs claiming mixed subsidies 72
Figure 88 Liquid metal and FLiBe core design of Shrivan et al. [33] A-2
Figure 89 Schematic of a CANDU disposal cask, taken from Ref. [73] A-2
Figure 90 Schematic showing the positions of the NB assemblies in the CANDU bundle slot, the radii of the blue and green circles match the radii of the NB assemblies and CANDU bundles A-2
Figure 91 Decay power as a function of time based on decay power calculations from Ref. [71] A-3
Figure 92 Rendering of the NUHOMS® EOS P37, taken from Ref. [74] A-3
Figure 93 Schematic showing the positions of the NB assemblies in the PWR assembly slot, taken from Ref. [74] A-3
Figure 94 The LCRF distribution resulting from a Monte Carlo simulation with an overlay of the approximate triangular distribution A-7
Figure 95 The cost breakdown of the LCRF resulting from Monte Carlo simulations with 50 000 samples A-7
Figure 96 Tornado chart of the LCRF (in $/NB) A-7
Figure 97 Comparison of the LCOH2 for community-scale PEM electrolysis using grid electricity when claiming different types of IRA subsidies, the LCOH2 is broken up in two columns for each case to show share of the levelized cost of the electrolyzers versus energy and to show the distribution between the levelized costs of capital, O&M, and fuel C-13
Figure 98 Comparison of the LCOH2 for distributed PEM electrolysis using grid electricity when claiming different types of IRA subsidies, the LCOH2 is broken up in two columns for each case to show share of the levelized cost of the electrolyzers versus energy and to show the distribution between the levelized costs of capital, O&M, and fuel C-14

Figure 99 Comparison of the LCOH2 for community-scale PEM electrolysis using NOAK UO_2-fueled NBs when claiming different types of IRA subsidies, the LCOH2 is broken in two ways to show share of the levelized cost of the electrolyzers versus energy and to show the distribution between the levelized costs of capital, O&M, and fuel C-15
Figure 100 Comparison of the LCOH2 for community-scale PEM electrolysis using FOAK UO_2-fueled NBs when claiming different types of IRA subsidies, the LCOH2 is broken in two ways to show share of the levelized cost of the electrolyzers versus energy and to show the distribution between the levelized costs of capital, O&M, and fuel C-16
Figure 101 Comparison of the LCOH2 for community-scale PEM electrolysis using NOAK TRISO-fueled NBs when claiming different types of IRA subsidies, the LCOH2 is broken in two ways to show share of the levelized cost of the electrolyzers versus energy and to show the distribution between the levelized costs of capital, O&M, and fuel C-17
Figure 102 Comparison of the LCOH2 for community-scale PEM electrolysis using FOAK TRISO-fueled NBs when claiming different types of IRA subsidies, the LCOH2 is broken in two ways to show share of the levelized cost of the electrolyzers versus energy and to show the distribution between the levelized costs of capital, O&M, and fuel C-17
Figure 103 Comparison of the LCOH2 for distributed PEM electrolysis using NOAK UO_2-fueled NBs when claiming different types of IRA subsidies, the LCOH2 is broken in two ways to show share of the levelized cost of the electrolyzers versus energy and to show the distribution between the levelized costs of capital, O&M, and fuel C-18
Figure 104 Comparison of the LCOH2 for distributed PEM electrolysis using FOAK UO_2-fueled NBs when claiming different types of IRA subsidies, the LCOH2 is broken in two ways to show share of the levelized cost of the electrolyzers versus energy and to show the distribution between the levelized costs of capital, O&M, and fuel C-19
Figure 105 Comparison of the LCOH2 for distributed PEM electrolysis using NOAK TRISO-fueled NBs when claiming different types of IRA subsidies, the LCOH2 is broken in two ways to show share of the levelized cost of the electrolyzers versus energy and to show the distribution between the levelized costs of capital, O&M, and fuel C-20
Figure 106 Comparison of the LCOH2 for distributed PEM electrolysis using FOAK TRISO-fueled NBs when claiming different types of IRA subsidies, the LCOH2 is broken in two ways to show share of the levelized cost of the electrolyzers versus energy and to show the distribution between the levelized costs of capital, O&M, and fuel C-20
Figure 107 Comparison of the LCOH2 for distributed PEM electrolysis using two NOAK UO_2-fueled NBs when claiming different types of IRA subsidies, the LCOH2 is broken in two ways to show share of the levelized cost of the electrolyzers versus energy and to show the distribution between the levelized costs of capital, O&M, and fuel C-21
Figure 108 Comparison of the LCOH2 for distributed PEM electrolysis using two FOAK UO_2-fueled NBs when claiming different types of IRA subsidies, the LCOH2 is broken in two ways to show share of the levelized cost of the electrolyzers versus energy and to show the distribution between the levelized costs of capital, O&M, and fuel C-22
Figure 109 Comparison of the LCOH2 for distributed PEM electrolysis using two NOAK TRISO-fueled NBs when claiming different types of IRA subsidies, the LCOH2 is broken in two ways to show share of the levelized cost of the electrolyzers versus energy and to show the distribution between the levelized costs of capital, O&M, and fuel C-23

Figure 110 Comparison of the LCOH2 for distributed PEM electrolysis using two FOAK TRISO-fueled NBs when claiming different types of IRA subsidies, the LCOH2 is broken in two ways to show share of the levelized cost of the electrolyzers versus energy and to show the distribution between the levelized costs of capital, O&M, and fuel C-23
Figure 111 Comparison of the LCOH2 for community-scale SOEC electrolysis using NOAK UO_2-fueled NBs when claiming different types of IRA subsidies, the LCOH2 is broken in two ways to show share of the levelized cost of the electrolyzers versus energy and to show the distribution between the levelized costs of capital, O&M, and fuel C-24
Figure 112 Comparison of the LCOH2 for community-scale SOEC electrolysis using FOAK UO_2-fueled NBs when claiming different types of IRA subsidies, the LCOH2 is broken in two ways to show share of the levelized cost of the electrolyzers versus energy and to show the distribution between the levelized costs of capital, O&M, and fuel C-25
Figure 113 Comparison of the LCOH2 for community-scale SOEC electrolysis using NOAK TRISO-fueled NBs when claiming different types of IRA subsidies, the LCOH2 is broken in two ways to show share of the levelized cost of the electrolyzers versus energy and to show the distribution between the levelized costs of capital, O&M, and fuel C-26
Figure 114 Comparison of the LCOH2 for community-scale SOEC electrolysis using FOAK TRISO-fueled NBs when claiming different types of IRA subsidies, the LCOH2 is broken in two ways to show share of the levelized cost of the electrolyzers versus energy and to show the distribution between the levelized costs of capital, O&M, and fuel C-26
Figure 115 Comparison of the LCOH2 for distributed SOEC electrolysis using NOAK UO_2-fueled NBs when claiming different types of IRA subsidies, the LCOH2 is broken in two ways to show share of the levelized cost of the electrolyzers versus energy and to show the distribution between the levelized costs of capital, O&M, and fuel C-27
Figure 116 Comparison of the LCOH2 for distributed SOEC electrolysis using FOAK UO_2-fueled NBs when claiming different types of IRA subsidies, the LCOH2 is broken in two ways to show share of the levelized cost of the electrolyzers versus energy and to show the distribution between the levelized costs of capital, O&M, and fuel C-28
Figure 117 Comparison of the LCOH2 for distributed SOEC electrolysis using NOAK TRISO-fueled NBs when claiming different types of IRA subsidies, the LCOH2 is broken in two ways to show share of the levelized cost of the electrolyzers versus energy and to show the distribution between the levelized costs of capital, O&M, and fuel C-29
Figure 118 Comparison of the LCOH2 for distributed SOEC electrolysis using FOAK TRISO-fueled NBs when claiming different types of IRA subsidies, the LCOH2 is broken in two ways to show share of the levelized cost of the electrolyzers versus energy and to show the distribution between the levelized costs of capital, O&M, and fuel C-29
Figure 119 Comparison of the LCOH2 for distributed SOEC electrolysis using two NOAK UO_2-fueled NBs when claiming different types of IRA subsidies, the LCOH2 is broken in two ways to show share of the levelized cost of the electrolyzers versus energy and to show the distribution between the levelized costs of capital, O&M, and fuel C-30
Figure 120 Comparison of the LCOH2 for distributed SOEC electrolysis using two FOAK UO_2-fueled NBs when claiming different types of IRA subsidies, the LCOH2 is broken in two ways to show share of the levelized cost of the electrolyzers versus energy and to show the distribution between the levelized costs of capital, O&M, and fuel C-31

Figure 121 Comparison of the LCOH2 for distributed SOEC electrolysis using two NOAK TRISO-fueled NBs when claiming different types of IRA subsidies, the LCOH2 is broken in two ways to show share of the levelized cost of the electrolyzers versus energy and to show the distribution between the levelized costs of capital, O&M, and fuel C-32
Figure 122 Comparison of the LCOH2 for distributed SOEC electrolysis using two FOAK TRISO-fueled NBs when claiming different types of IRA subsidies, the LCOH2 is broken in two ways to show share of the levelized cost of the electrolyzers versus energy and to show the distribution between the levelized costs of capital, O&M, and fuel C-32

1. Introduction

The levelized cost of hydrogen transport and dispensing in 2017 was 14.4-15.6 $/kg (in 2022$) [1]. These enormous costs limit the growth of the hydrogen economy. Herein lies an opportunity for nuclear batteries (NBs) to provide cost savings to the hydrogen fuel cycle by collocation of the hydrogen production with the demand clusters, thereby limiting or even negating the need for storage and distribution.

Nuclear batteries are meant to be a class of portable microreactors with a thermal power below 30 MWth and an electrical power below 10 MWe. A conceptualization of the Los Alamos National Lab's (LANL) Megapower reactor is shown in Figure 10. These compact reactors – the size of one or multiple shipping containers – would be factory-built and brought on-site with minimal site preparation allowing for rapid deployment (on the order of days to weeks). In addition, the reactors are being designed to operate autonomously for several years without refueling [7].

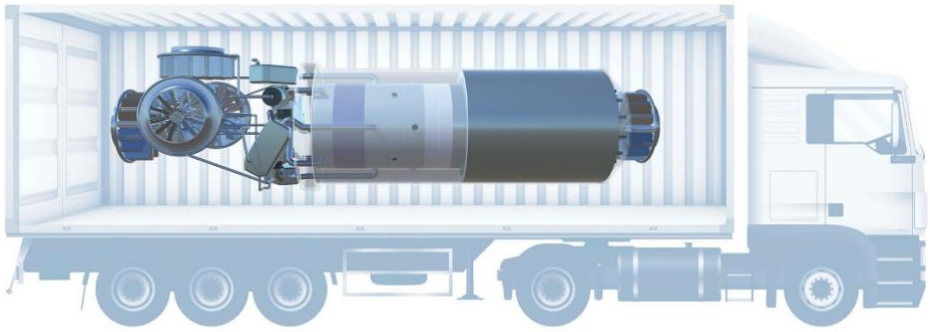

Figure 10 Visualization of the LANL's Megapower design [8]

The purpose of this study is to evaluate the technological and economic feasibility of using nuclear batteries for decentralized hydrogen production, both at community scale and with individual NBs – referred to as 'centralized' and 'distributed' production, respectively. First, a set of functional, operational, and economic requirements are identified, which are discussed in Section 2. Then in Section 3, representative case studies are developed based on a review of hydrogen demand projections. An economic model is made for each case in two parts: the production costs are discussed in Section 4 and the hydrogen storage and transport costs are estimated in Section 5. Finally, the conclusion and future work are given in Section 6. Results that are not shown in the main text of the report can be found in Appendix B and Appendix C.

2. Nuclear battery requirements

One of the objectives of this study is to develop the economic, functional, operational, and regulatory requirements for the NBs in the context of hydrogen production. While these requirements have been identified, their detailed and quantitative treatment is still a work in progress. However, some insights can already be gained from a qualitative discussion. The requirements and a qualitative measure of their importance/applicability are shown in Table 2. Here, the use of nuclear batteries for offshore power generation is also discussed because this application is part of the research project and the contrast between the requirements of both adds to the discussion. A more detailed explanation of the requirements follows.

Of course, the (levelized) costs of services provided by the NB are crucial to the viability of a NB hydrogen production project but less so for offshore applications. On offshore platforms, the complete NB package must adhere to strict weight/size limits and be able to tolerate acceleration due to wave motion. In contrast, no such limitations or nominal acceleration are present when producing hydrogen on land.

Table 2 Qualitative assessment of the requirements for the NBs when used in hydrogen production and offshore power generation: green indicates the requirement is highly relevant to the application, yellow indicates moderate relevance, and orange means the requirement is either not strict or not applicable

	Hydrogen	Offshore
Economic targets		
Levelized cost of electricity		
Levelized cost of heat		
Levelized cost of hydrogen		
System requirements		
Maximum weight, volume, area		
Tolerable acceleration		
Maintenance/refueling		
Minimum refueling interval		
Maximum duration of refueling outage		
Complete loss of power allowed during refueling?		
Load characteristics		
Thermal/electrical power		
Target temperature for heat delivery		

Load following	
Minimum power slow-down rate	
Maximum power ramp-up rate	
Black start capabilities	
Required availability/reliability	
Heat storage	
Grid supporting functionalities	
Characteristics of produced electricity	
Transportation	
Possible modes of transportation	
Maximum weight, volume, acceleration	
Safety and security	
Passive decay heat removal	
Extension of the EPZ beyond site boundary	
Number of independent shutdown modes	
Core damage frequency	
Large early release frequency	
Armed guards required	

The time between refueling the NBs and the time it takes to do so should be matched to the turnaround schedule of the offshore platforms, and a certain level of power should remain available during the turnaround. For the hydrogen production facilities, synchronizing the refueling of the NBs to the maintenance of the balance of plant is beneficial and preferred but less crucial. Also, unless the plant is in a remote location without access to the grid, power can be drawn from the grid during maintenance, so all NBs are allowed to be down at the same time. However, as also noted by Pham et al. [9], decentralized hydrogen production is most valuable where the grid is congested. So, if a sizeable portion of total power is needed during the outage, it might be prohibitively expensive to draw it from the grid. In that case, some of the NBs will need to remain online, which is easily achieved by using a staggered maintenance schedule.

Clearly, nuclear batteries must be able to meet both applications' electrical and thermal demands and deliver heat at the required temperatures. In addition, the NBs must also be able to follow the process loads on the offshore platform. Having some extent of load following is also preferred when producing

hydrogen, as it allows for greater operating flexibility. Yet, the NBs should run as much as possible at full capacity for optimal economic performance. Thus, the ability to change the operating power is less essential for hydrogen production than it is on offshore platforms. Note that the NBs can still be operated flexibly under base load conditions, e.g., selling electricity to the grid when prices are high and producing hydrogen when electricity prices are low. The ability to change the operating power alone is not sufficient. The NBs must be able to ramp up/down at the same rates with which the process demands change. However, the requirement on ramping up is more relaxed when producing hydrogen, as one could draw surge power from the grid.

Black start capabilities are not required in either case, as emergency diesel engines are available on the offshore platform and the hydrogen facility is connected to the grid. Still, one would prefer an easy start-up procedure after blackouts on a platform. Luckily, NBs are easy to start up on small backup generators because only one NB needs to be kickstarted with external power, after which this single NB can be used to spin up the others. In addition, electricity producers with black start capabilities are eligible for compensation from the grid operator, so it may be worthwhile to have a backup generator available on land to allow for black starts of the facility.

For hydrogen production, reliability/availability must be high to ensure the smooth and continuous operation of the plant. Yet, these requirements are more relaxed than on offshore platforms, where it is essential to maintain power at all times. An energy (heat) storage system may be of help here, ensuring power supply during short disruptions and coping process demand surges.

If the NBs of the hydrogen production facility also supply power to the grid, then some grid-supporting functionalities will be required of them. Of course, these requirements do not apply to offshore platforms where no grid exists. The flip side is that there are stricter margins for the voltage and frequency of the electricity on offshore platforms to ensure the stability of the microgrid.

The transport of the NBs from the factory where they are fabricated and the central facility where they are refueled to the hydrogen production plant will likely take place via road, rail, barge, or a combination thereof. Similarly, the transport of the NB to the offshore platform will consist of a combination of these transport modes to get to a harbor from where it is brought to the platform by ship. For the purpose of this study, it can be assumed that the transport is limited to these conventional methods – e.g., no air transport needed – and that access to proper roads and infrastructure is available – e.g., no transport to remote communities needed. Nevertheless, the conventional modes of transport will limit the system's weight and size and require the NB to tolerate dynamic loads resulting from transport.

Most of the safety and security considerations are applicable to both the hydrogen production and offshore platform, but some differences exist. For example, passive decay heat removal is not strictly required on the offshore platform, but is strongly preferred for enhanced safety, as this minimizes required operator action in an emergency. As another example, there is no need for an Emergency Planning Zone (EPZ) around the platform because no one lives around it. Note that these safety/security entries are listed to give an appreciation for the safety and security concerns and how these might be case specific, a detailed safety/security review is outside the scope of this first report.

3. Case studies

A location and project start date must be chosen to provide a consistent set of assumptions and projections. Our study will assume projects in California (CA) because some hydrogen infrastructure has already been built there. As a result, hydrogen development projections and hydrogen station data are readily available. The project start date is chosen to be 2030, as a trade-off between having sufficient hydrogen demand and being able to use more near-term (and thus more accurate) cost and hydrogen demand projections.

In the 2020 report by the CA Energy Commission on the buildout of the hydrogen economy in CA [10], a siting study is included, which aims to find the optimal hydrogen production locations in CA considering the local terrain, proximity to expected demand clusters, water supply, etc. Figure 11 shows the resulting recommendations for 2030 in their low hydrogen demand scenario.

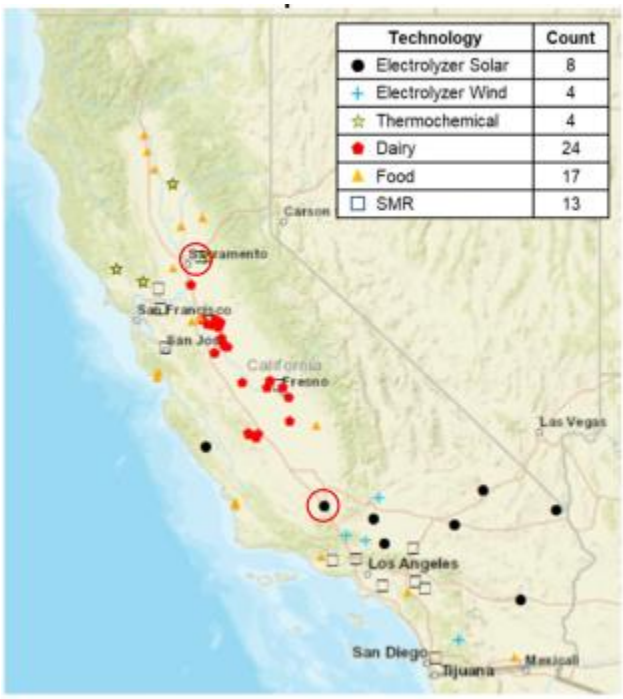

Figure 11 Suggested locations for hydrogen production facilities of different technologies by 2030 in the low hydrogen demand scenario of [10]. Electrolyzer wind/solar refer to (centralized) electrolysis with wind/solar energy, thermochemical refers to facilities producing hydrogen from biomass from forests and agricultural residue, dairy facilities make hydrogen from anaerobic dairy digesters, food refers to hydrogen production from the residential waste stream, and SMR refers to steam methane reforming

Two project sites are chosen (indicated by red circles on the figure), the first near Sacramento and the second on the I5 near Bakersfield, because these are hotspots in the projected hydrogen demand (Figure 12) [3], [11]. The facility near Sacramento produces at a community scale and supplies several customers. On the other hand, the project in Bakersfield produces hydrogen for a single fueling station with a single NB, thereby negating the need for hydrogen distribution.

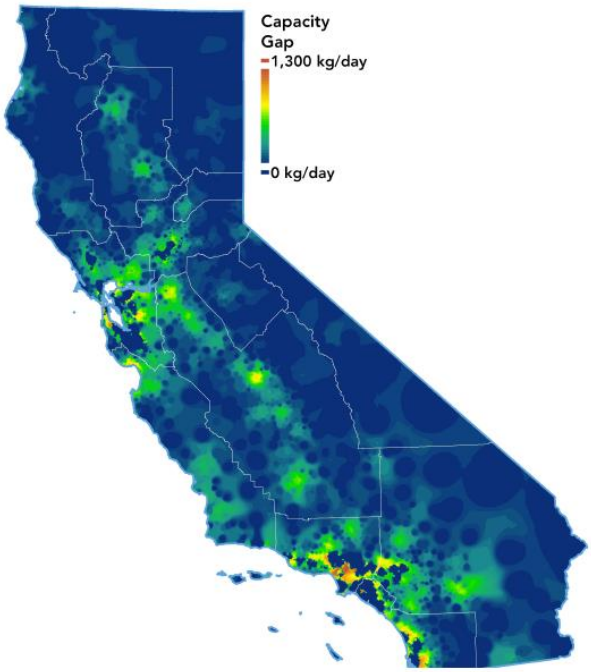

Figure 12 The predicted hydrogen demand gap in CA in 2027 [3]

The demand in Sacramento is assumed to be entirely due to light-duty vehicles (LDV) and heavy-duty vehicles (HDV), consistent with the low renewable hydrogen demand scenario of the CA Energy Commission report [10]. This scenario assumes a fleet of 250 000 fuel cell electric vehicles in CA by 2030, 2.72% of which (6800 vehicles) are assumed to be in Sacramento based on the projections of the CA Air Resource Board [10]. Further, assuming a fuel economy of 83.75 mpge for hydrogen fuel cell vehicles [10] and an average of 12 000 mi/y per vehicle [12], this results in an LDV demand of 993 ton H2/y. To simplify calculations, the HDV demand is assumed to equal the LDV demand, resulting in a total demand of 1987 ton H2/y or 5440 kg H2/d. An electrical input of roughly 12 MW is needed to meet such a hydrogen demand at constant operation using a Polymer Electrolyte Membrane (PEM) electrolyzer that requires 52 kWh/kg H2, which is feasible using multiple nuclear batteries.

The hydrogen demand estimation here aims not to provide accurate demand projections but to check whether the power demands are reasonable for nuclear batteries. In addition, the above demand estimates are conservative. So, to minimize the diseconomies of scale, a higher demand of 25 000 kg/d is assumed for the community-scale facility, which could represent, e.g., a facility located between San Francisco and Sacramento.

Furthermore, the demand of the standalone hydrogen fueling station in the distributed hydrogen production model is assumed to be 1600 kg/d – the capacity of the largest hydrogen fueling station currently operating in CA [3]. The electrical demand the electrolyzers corresponds to about 4 MWe, which can be delivered by a single Westinghouse eVinci NB.

Table 3 The cases considered in the economic analysis

Paradigm	Method	Capacity	Transportation method
Community-scale/centralized	Grid + PEM	25 000	Truck delivery
	NB + PEM	25 000	Truck delivery
	NB + SOEC	25 000	Truck delivery
Distributed	Grid + PEM	1600	None
	NB + PEM	1600	None
	NB + SOEC	1600	None

At this stage, three hydrogen production technologies are considered in this study: PEM electrolysis, and electrolysis in Solid Oxide Electrolyzer Cells (SOEC), where the energy for electrolysis is either supplied by the grid or NBs. Although they are not the direct subject of this study, solar-powered PEM electrolysis and steam methane reforming (SMR) cost estimates can be added later to evaluate competing technologies on an apples-to-apples basis. The different cases are summarized in Table 3.

As mentioned before, there is no need for hydrogen transport and distribution in the distributed production paradigm, while some hydrogen transport will be needed under community-scale production. Only truck transport will be considered, as it is the most economical mode of transport for such small capacities and distances [13]. Note that throughout the report, 'community-scale' and 'centralized' will be used interchangeably, even though the community-scale facility feeds into the hydrogen distribution network and is thus a 'semi-centralized' facility according to the nomenclature used by Reddi et al. [2] – as will be discussed in greater detail in Section 5.1

4. Hydrogen production cost analysis

Tang et al. [14] conducted a review of hydrogen cost studies and conclude that the levelized cost of hydrogen depends strongly on the setting of production (centralized vs. distributed), grid integration, government subsidies, and the inclusion of distribution cost. Thus, in this section on the cost of hydrogen production with NBs, all but the latter will be examined, with the distribution costs being treated in Section 5.

First, the cost model and simulation setup are discussed in Section 4.1, followed by a discussion of the Inflation Reduction Act (IRA) subsidies in Section 4.2. Section 4.3 details the cost of producing hydrogen using grid electricity in CA and serves as a reference for the costs discussed in further Sections 4.4 and 4.5, which assume hydrogen production using NBs. The NB models are further investigated in Sections 4.6, 4.7, and 4.8 which look at the use of TRISO fuels, the effect of increasing facility capacity and participating in the electricity market, respectively. Finally, Section 4.9 compares the results of Sections 4.3 through 4.8 and provides further discussion.

4.1. Cost modeling methodology

In this section, simple levelized cost models for each of the production methods of Table 3 are developed. The levelized cost of hydrogen (LCOH2) is split into the levelized electrolyzer cost and the levelized energy cost, with the former being subdivided into a capital cost and operations and maintenance (O&M) cost:

$$LCOH2 = LCOH2_{Electr.\ cap} + LCOH2_{Electr.\ O\&M} + LCOH2_{Energy} \quad (1)$$

To calculate the levelized electrolyzer capital cost, the initial capital cost (ICC) is annualized using a capital cost recovery factor (CRF):

$$CRF = \frac{r \cdot (1+r)^{t_{ec}}}{(1+r)^{t_{ec}} - 1} \quad (2)$$

Where r is the real discount rate and t_{ec} is the economic lifetime of the project. For a plant of annual capacity c and operating cycles of length t_{op} with subsequent outages of length t_{out}, the levelized capital cost is found as:

$$LCOH2_{Electr.\ cap} = \frac{ICC \cdot CRF}{c} \cdot \frac{t_{op} + t_{out}}{t_{op}} \quad (3)$$

In calculating the levelized cost of O&M, the fixed O&M and variable O&M components are treated separately, because the fixed O&M costs are paid regardless of the operating time and must thus be corrected by the capacity factor – similar to the capital costs.

$$LCOH2_{Electr.\ O\&M} = \frac{O\&M_{Fixed}}{c} \cdot \frac{t_{op} + t_{out}}{t_{op}} + \frac{O\&M_{Variable}}{c} \quad (4)$$

The levelized cost of energy is calculated from the levelized costs of electricity (LCOE) and heat (LCOH) together with the electrical intensity (E_{Elec} in kWh/kg H2) and thermal intensity (E_{Th} in kWh/kg H2) of the process:

$$LCOH2_{Energy} = LCOE \cdot E_{Elec} + LCOH \cdot E_{Th} \tag{5}$$

For PEM electrolysis, the thermal energy intensity is assumed to be zero so $LCOH2_{energy}$ only follows from the LCOE. The LCOE is simply the retail price of electricity bought from the grid when using grid electricity. When using NBs, the LCOE is the cost of the NBs normalized over the total yearly electricity production (P) and is further subdivided into a levelized capital cost, O&M cost, and fuel cost:

$$LCOE = LCOE_{Capital} + LCOE_{O\&M} + LCOE_{Fuel} \tag{6}$$

Where the $LCOE_{O\&M}$ is calculated similarly to Equation (4). The levelized capital cost now also contains the cost of decommissioning (COD), which is annualized using a sinking fund factor (SFF):

$$SFF = \frac{r}{(1+r)^{t_{ec}} - 1} \tag{7}$$

$$LCOE_{Capital} = \frac{ICC \cdot CRF + COD \cdot SFF}{P} \cdot \frac{t_{op} + t_{out}}{t_{op}} \tag{8}$$

Finally, there is the calculation of the levelized cost of fuel, which is more subtle because the nuclear fuel cost (F_{Nucl}) is paid in whole at the start of a multiyear cycle. The nuclear fuel cost is annualized using the fuel capital recovery factor (FCRF):

$$FCRF = \frac{r \cdot (1+r)^{t_{op}}}{(1+r)^{t_{op}} - 1} \tag{9}$$

The cost of refueling (F_{RF}) is only incurred at the end of the fuel cycle, and the cost of waste disposal (F_W) is incurred even later, because the spent fuel spends a certain time (t_{sfp}) in the spent fuel pool. Both costs are thus annualized with respective sinking fund factors $RFSFF$ and $WSFF$ given by:

$$RFSFF = \frac{r}{(1+r)^{t_{op}} - 1} \tag{10}$$

$$WSFF = \frac{r}{(1+r)^{t_{op}} - 1} \cdot \frac{1}{(1+r)^{t_{sfp}}} \tag{11}$$

The levelized cost of fuel is then:

$$LCOE_{Fuel} = \frac{F_{Nucl} \cdot FCRF + F_{RF} \cdot RFSFF + F_W \cdot WSFF}{P} \tag{12}$$

In SOEC electrolysis, the heat produced by the NBs is used both for electricity production and in the electrolysis process itself. In that case, an LCOH is calculated in the same way as the LCOE is calculated form Equations (4), (6), (8), and (12). Using the thermal efficiency of the NBs (η) the LCOE is then obtained from the LCOH as $LCOE = LCOH/\eta$.

The plant design capacity will be varied in the models. So, no fixed capital and O&M cost estimates can be used. Hence, normalized costs are used and the economy of scale is accounted for using scaling exponents:

$$Cost = Cost_{ref}\left(\frac{c}{c_{ref}}\right)^{n} \tag{13}$$

Where c is the capacity and n is a scaling exponent smaller than unity. However, as electrolyzer costs are typically reported in a normalized way ($/kW), Equation (13) is adapted as follows:

$$Cost = c\left[\frac{Cost_{ref}}{c_{ref}}\left(\frac{c}{c_{ref}}\right)^{n-1}\right] \tag{14}$$

To account for the uncertainty in the model parameters, Monte Carlo (MC) simulations and sensitivity analyses are carried out for each model. In a Monte Carlo simulation, a probability distribution is assigned to each parameter, rather than assigning a fixed value. Here, only triangular and uniform distributions are used. The code then runs many (50 000) versions of the economic model, each time randomly picking parameter values according to their distributions. The result is a distribution of levelized costs, which represents the uncertainty of the model and the average of which represents the expected levelized cost. *In this report, the average (μ), standard deviation (σ), minimum (m) and maximum cost (M) are reported as $\mu \pm \sigma\ [m, M]$.*

In a sensitivity analysis, on the other hand, all parameters are fixed (to the expected value of the MC distributions), while one parameter is varied between specified ranges. In this study, the parameters will be changed by ± 30% of their original value with the exception of the capacity factor because of the 100% upper limit.

A sensitivity analysis thus shows the impact of a single parameter on the outcome of the model, while a MC simulation takes into account the uncertainty of all parameters simultaneously. Importantly, when comparing the cost difference between two scenarios with shared cost parameters, the Monte Carlo simulations must be performed such that the shared parameters are sampled consistently between both models. The cost differences can thus not simply be determined based on the outcome of separate simulations, as this would grossly overestimate the uncertainty on the estimate.

Again, note that no hydrogen storage or transport costs are included in this section. These are treated in Section 5.

Finally, the cost estimates from external sources are adjusted for inflation using the US Bureau of Economic Analysis implicit price deflators for gross domestic product [15]. Thus, all costs reported here are given in Q2 2022 USD.

4.2. The Inflation Reduction Act subsidies

The Inflation Reduction Act (IRA) of 2022 allows low-carbon power sources, such as nuclear energy, to claim tax credits in order to boost their development and reach the climate goals. The credits phase out in 2032 (or when the US emissions are less than 25% of the 2022 levels, whichever is earlier) [16], and are thus not relevant to Nth-of-a-kind (NOAK) NBs. However, it is not unlikely that there will be future bills to stimulate low-carbon technologies and/or that the IRA is extended. Thus, the IRA is used as benchmark/proxy for future stimulus to low-carbon technologies and treated as if it does not phase out.

Under the IRA amendment to Section 45Y of the Internal Revenue Code (IRC), the NBs would be eligible to claim a clean electricity PTC of 3 $/MWh, which can be quintupled to 15 $/MWh if wage and apprenticeship requirements are met [16]–[19]. Given the high wages and the extensive training programs for employees in the nuclear industry, it is assumed that the wage and apprenticeship standards are met. The PTC can be increased by a further 10% if domestic content standards are met regarding the iron, steel and manufactured products used in the facility [17], [18]. Once again, in the context of NBs, it seems likely that these standards will be met, so a PTC of 16.5 $/MWh will be used in this report. Note that the PTC can be increased by yet another 10% is the power source is located in an 'energy community'. However, this bonus is case-specific and will hence not be considered.

Similar to the clean electricity PTC of Section 45Y, a clean hydrogen PTC is available in the new IRC Section 45V, which can be claimed alongside the clean electricity PTC granted that the hydrogen is produced in the U.S. (but the hydrogen may be transported to other countries) [17], [18]. The base credit is 0.60 $/kg and is multiplied by a percentage between 20% and 100% based on the emissions associated with the hydrogen production, Table 4 [17], [20].

For the purpose of the IRA, life-cycle greenhouse gas (GHG) emissions are the same as in the section of the Clean Air Act that deals with renewable fuel standards and only emissions up to the point of hydrogen production (well-to-gate) are considered [21]. The Greenhouse gases, Regulated Emissions, and Energy use in Technology (GREET) model will be used for emissions accounting, but at the time of writing, there is still a lot of uncertainty as to which emissions the regulator will account for and how.

Only upstream emissions associated with fuel production are accounted for in the GREET model, emissions related to e.g., construction of an installation are not. As a result, the scope 3 GHG emissions associated with solar and wind energy are identically zero in the GREET model. Nuclear is clearly disadvantaged compared to other low-carbon technologies under this accounting method, as most of its lifecycle emissions occur in the front-end fuel production, whereas most of the emission of, e.g., solar are associated with construction [22]. Still, neglecting construction emissions results in lower default GREET emissions for hydrogen produced with nuclear (0.2 – 0.4 kg CO2e/kg H2) than values found in the literature – e.g., 0.47 – 2.13 kg CO2e/kg H2 [23]. For the purpose of this study, it is assumed that the regulator will account emissions in the same way as the GREET model.

Using the assumptions of the GREET model for the front-end carbon intensity of the nuclear fuel cycle, the GHG emissions per kilogram of hydrogen are estimated for both PEM and SOEC electrolysis. The GHG footprint of the hydrogen is most sensitive to the discharge burnup of the fuel – i.e., the amount of energy extracted per initial kilogram of uranium in the fuel. In further Monte Carlo calculations, the fuel burnup will be picked randomly from its distribution. So, instead of finding the GHG emissions for each randomly-

Table 4 The base clean hydrogen credit under the IRA as a function of the hydrogen production emissions

Emissions [kg CO2e/kg H2]	**Base credit [$/kg]**
< 0.45	0.60
0.45 – 1.50	0.20
1.50 – 2.50	0.15
2.50 – 4.00	0.12

picked burnup value, a threshold value is determined below which the GHG emissions are too high to claim the highest level of clean hydrogen PTCs. The threshold value of 0.45 kg CO2e/kg H2 or higher is reached for burnups below 9.7 MWd/kg HM and 7.2 MWd/kg HM for PEM and SOEC, respectively. For a fuel burnup below this value, the base credit is thus 0.2 $/kg. Note that the threshold value for the burnup is lower for SOEC because of the higher overall energy efficiency of SOEC compared to PEM, which results in less fuel need. Once again, it is assumed that the apprenticeship and wage standards are met, so the hydrogen PTC is increased fivefold to 3.0 $/kg or 1.0 $/kg depending on the fuel burnup. Note that there is no domestic content bonus for clean hydrogen PTCs [17], [18], [20].

Finally, there is also the possibility for claiming ITCs under Section 48E, instead of PTCs under Section 45. The base credit is 6% of the investment for a qualified hydrogen production and/or storage facility [17], [18], [20]. Once more, this credit can be quintupled to 30% if wage and apprenticeship standards are met and if domestic content standards are met, the credit is further increased by 10% (i.e., multiplying by 1.1 to give 33%, not adding 10% to give 40%) [17]–[19]. The ITC assumed in this work is thus 33%.

Although a single tax payer cannot claim both a PTC and ITC, different tax payers can. A project in which the NBs are and electrolyzers are owned by different tax payers could thus claim an ITC on the NBs and still claim a clean hydrogen PTC. Later in the report, this is referred to as ‘mixed’ subsidies.

When claiming an ITC, the initial capital cost of the NBs and electrolyzers is lowered by 33%, but other than that, all equations discussed in Section 4.1 still apply. The effect of the ITC on the amortization is thus neglected. When claiming both the hydrogen PTC (PTC_{H_2}) and the clean electricity PTC (PTC_{e^-}), the LCOH2 becomes:

$$LCOH2 = LCOH2_{Electrolyzers} + (LCOE - PTC_{e^-}) \cdot E_{Elec} + LCOH \cdot E_{Th} - PTC_{H_2} \quad (15)$$

In calculations with mixed subsidies, only the capital cost of the NBs is lowered by 33% and the clean hydrogen PTC is applied.

4.3. PEM electrolysis with grid electricity

4.3.1. Community-scale production

This case considers community-scale hydrogen production using PEM electrolysis at a community scale (25 000 kg/d) with electricity bought from the grid. The assumptions used in the cost model are listed in Table 5. Note that when only a mode (i.e., the 50th percentile) is given, the parameter is fixed, when the minimum and maximum are given, these correspond to the range of a uniform distribution, and when the minimum, maximum, and mode are given, these describe a triangular distribution.

The current lifetime of PEM electrolyzers (20y [24]) is chosen as a minimum for the future project. Similarly, the capacity factor of the NREL's H2A model for current PEM electrolysis is taken as the lower limit for our 2030 electrolyzers [25]. The mode of the capacity factor distribution is taken from the capacity factor used in the H2A model for future electrolysis [26].

Furthermore, the modes of the capital and the O&M costs are taken at a reference capacity of 25 773 kg/d, corresponding to an average annual production of 25 000 kg/d at a capacity factor of 97%. The capital cost scaling exponent is adopted from the H2A models directly, whereas the scaling exponent for the O&M costs follows from a logarithmic interpolation between the O&M costs calculated in the H2A model at 25 773 kg/d and 50 000 kg/d.

Table 5 Model assumptions for a community-scale PEM facility with electricity bought from the grid

Parameter	Unit	Min	Mode	Max	Source
Real discount rate	%	2	6	12	
Economic lifetime	y	20		25	[24]
Capacity factor	%	86	97	98	[25], [26]
Electrolyzer capital cost	$/kWe	454	567	998	[26]
Reference capacity	kg/d		25 773		
Scaling exponent	-		0.6		[26]
Electrolyzer fixed O&M cost	($/y)/kWe	27	41	91	[26]
Reference capacity	kg/d		25 773		
Scaling exponent	-		0.56		[26]
Industrial retail electricity price in CA	$/MWh	162	184	200	[5]
Electrical energy intensity	kWh/kg		51.3		[26]

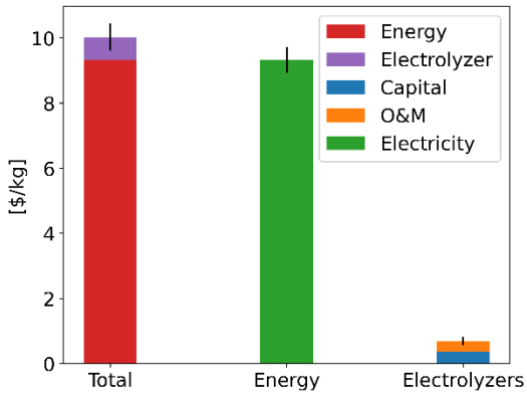

Figure 13 LCOH2 for community-scale PEM electrolysis with grid electricity

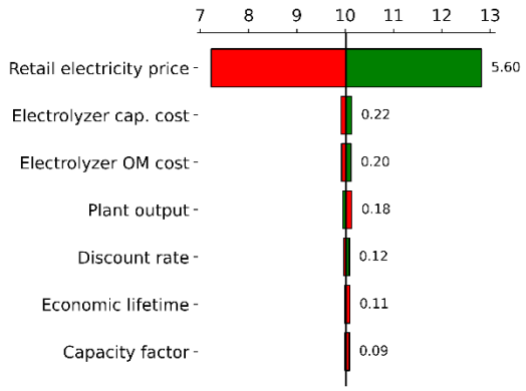

Figure 14 Tornado chart for the LCOH2 (in $/kg) in a community-scale PEM facility running on grid electricity

Finally, the retail electricity price is taken from 2030 price projections by the CA Energy Commission, and the energy intensity of the electrolysis is taken to be the default value used in the H2A model for future PEM electrolysis.

The expected LCOH2 resulting from the MC simulations is 10.03 ± 0.42 [8.80, 11.41] $/kg, with the cost breakdown shown in Figure 13. The total cost is dominated by the cost of electricity, which results in a cost of 9.34 $/kg, whereas the electrolyzer capital and O&M cost only making up 0.36 $/kg and 0.33 $/kg, respectively. A similar distribution of the electricity, capital, and O&M costs is seen in the results of Lee et al. and Peterson et al. [27], [28] Unsurprisingly, the levelized cost is by far the most sensitive to the retail electricity price, Figure 14.

At first glance, an LCOH2 of 10.03 $/kg might seem unreasonable, but it is a direct result of the high retail electricity prices in CA. Indeed, in 2021, the average industrial retail prices in CA were 148 $/MWh, twice the US average of 73 $/MWh [29]. At electricity prices similar to the national average (73 – 79 $/MWh), Peterson et al. report a far lower LCOH2 of 4.5 – 5 $/kg [28]. By contrast, in the OECD report on the role of nuclear power in the hydrogen economy [30], an LCOH2 of 7.5 $/kg is reported at 150 $/MWh and for similar assumptions regarding the electrolyzer efficiency, which aligns with the LCOH2 reported here after accounting for the difference in retail electricity prices and the electrolyzer costs – which were neglected in the OECD report. Finally, it should be noted that while the retail electricity prices in CA are high, CA is not an outlier, as there are states with higher rates still, e.g., Hawaii.

As discussed in Section 4.2, production tax credits (PTCs) or investment tax credits (ITCs) are available under the IRA for clean hydrogen production, granted that the emissions associated with its production are below 4 kg CO2e/kg H2 [17], [18]. The 2022 greenhouse gas emissions report of the CA Air Resource Board reports an average emission of 0.21 kg CO2e/kWh for electricity production in CA [31], which, combined with the assumed PEM energy intensity of 51.3 kWh/kg H2, leads to 10.8 kg CO2e/kg H2. Therefore, this rough estimate shows that the hydrogen produced in this facility will not be eligible for the clean hydrogen PTCs if lifecycle emissions of grid electricity are based on the average carbon intensity of the generators.

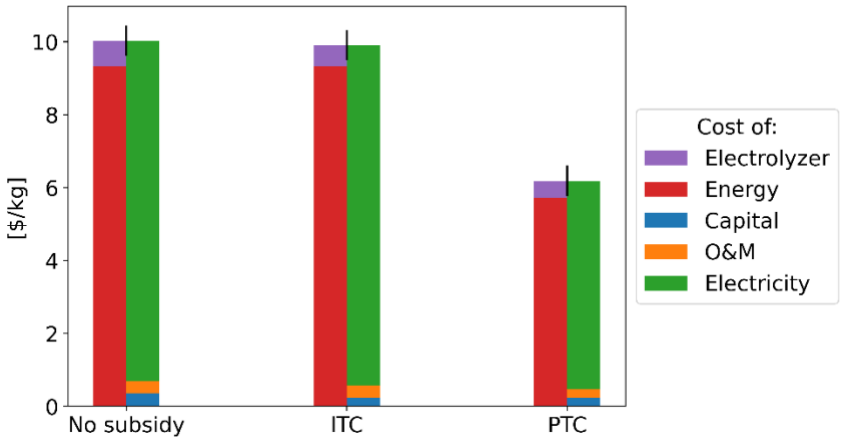

Figure 15 Comparison of the LCOH2 for PEM electrolysis using grid electricity when claiming different types of IRA subsidies, the LCOH2 is broken up in two columns for each case to show share of the levelized cost of the electrolyzers versus energy and to show the distribution between the levelized costs of capital, O&M, and fuel

However, it is not yet certain how the regulator will allocate the emissions associated with grid electricity [21]. For example, a hydrogen producer taking electricity from the grid might be able to enter in a power purchase agreement with a renewable producer to lower the GHG emissions associated with its hydrogen, thereby making it eligible for the clean hydrogen PTCs. In that case, the LCOH2 is lowered significantly to 6.18 ± 0.42 [4.96, 7.40] $/kg under the assumption that the highest PTC of 3.0 $/kg can be claimed. One could instead opt to claim an ITC, but given the low capital cost of the electrolyzers, the LCOH2 is only decreased to 9.90 ± 0.41 [8.73, 11.08] $/kg, see Figure 15.

4.3.2. Distributed production

Here, we consider distributed production using PEM electrolysis with electricity from the grid supplying a single hydrogen station at 1600 kg/d (for CF = 1). The assumptions used in the cost model are listed in Table 6. Note that when only the mode is given, the parameter is fixed, when the minimum and maximum are given, these correspond to the range of a uniform distribution, and when the minimum, maximum, and mode are given, these describe a triangular distribution.

The electrolyzer capital and O&M costs are calculated using the H2A model for distributed PEM electrolysis [32] at a reference capacity of 1650 kg/d, corresponding to an average annual production of 1600 kg/d at a capacity factor of 97%. Once again, the capital cost scaling exponent is adopted from the H2A models directly. In contrast, the scaling exponent for the O&M costs follows from a logarithmic interpolation between the O&M costs calculated in the H2A model at 1300 kg/d and 2000 kg/d. All other parameters are equal to those used in the model of the community-scale facility in Section 4.3.1.

Now, the LCOH2 is 10.11 ± 0.42 [8.83, 11.51] $/kg, which is only 0.10 $/kg higher than in the community-scale case. The small difference between the two cases is a result of the LCOH2 being dominated by the electricity cost, rather than the electrolyzer cost, Figure 16.

Again, the LCOH2 is lowered significantly to 6.27 ± 0.42 [4.98, 7.66] $/kg, if the project can claim clean hydrogen and electricity PTCs. As can be seen on Figure 17, the main contributor here is the clean hydrogen PTC of 3.0 $/kg, with the clean electricity PTC only contributing 0.85 $/kg.

Table 6 Model assumptions for distributed PEM electrolysis with electricity bought from the grid

Parameter	Unit	Min	Mode	Max	Source
Real discount rate	%	2	6	12	
Economic lifetime	y	20		25	[24]
Capacity factor	%	86	97	98	[25], [26]
Electrolyzer capital cost	$/kWe	553	691	1216	[32]
Reference capacity	kg/d		1650		
Scaling exponent	-		0.6		[32]
Electrolyzer fixed O&M cost	($/y)/kWe	28	42	93	[32]
Reference capacity	kg/d		1650		
Scaling exponent	-		0.955		[32]
Industrial retail electricity price in CA	$/MWh	162	184	200	[5]
Electrical energy intensity	kWh/kg		51.3		[26]

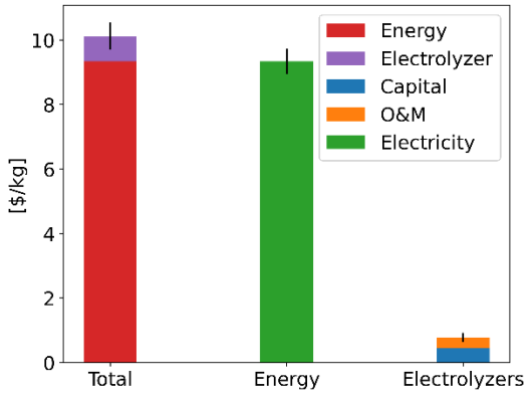

Figure 16 LCOH2 for distributed PEM electrolysis with grid electricity

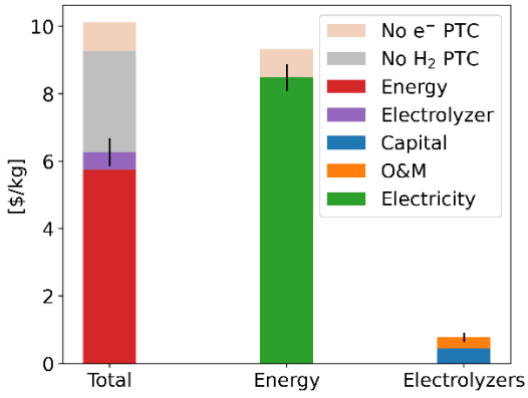

Figure 17 LCOH2 for distributed PEM electrolysis with grid electricity when claiming PTCs under the IRA

4.4. PEM electrolysis with nuclear batteries

4.4.1. Community-scale production

Here, hydrogen is produced at a community scale using PEM electrolysis with electricity provided by NBs. The plant is sized to have an average daily output of 25 000 kg/d and the NBs only supply energy to the electrolyzers, no excess heat or electricity is produced/sold. The assumptions used in the cost model are listed in Table 7. Note that when only the mode is given, the parameter is fixed, when the minimum and maximum are given, these correspond to the range of a uniform distribution, and when the minimum, maximum, and mode are given, these describe a triangular distribution.

The thermal power of 15 MWth results in an electrical power of about 4 to 5 MWe, which is average for NBs and comparable to Westinghouse's eVinci design or BWXT's Pele design. Most commercial NB designs are high-temperature helium-cooled reactors, for which a burnup of 15 MWd/kg HM is a reasonable upper limit. Some designs use heat pipes to cool the core, in which case the expected burnup is lowered to about 5 MWd/kg HM. Note that these burnup values are far lower than what is expected for traditional large-scale light-water reactors, where the burnup is over 50 MWd/kg HM.

Table 7 NOAK model assumptions for a community-scale PEM facility with electricity produced by NBs, FOAK NB capital costs are shown in red

Parameter	Unit	Min	Mode	Max	Source
Real discount rate	%	2	6	12	
Economic lifetime	y	20		25	
Thermal power	MW/unit		15		
Capacity factor	%	80	90	95	
Thermal efficiency	%	25		35	
Discharge burnup	MWd/kg HM	5	15	15	
Yellow cake cost	$/kg HM		111		[7]
Cost of conversion	$/kg HM		6		[7]
Cost of enrichment	$/SWU		171		[7]
Cost of UO_2 fabrication	$/kg HM	250		500	
Refueling cost	M$/NB	0.84	1.09	1.45	
Waste disposal cost	k$/NB	50		400	
NB capital cost	$/kWe	3000 10 000	6000 15 000	10 000 20 000	[7]

Decommissioning cost	$/MWhe	10		50	
Fixed NB O&M cost	M$/y/unit	0.45	0.5	0.55	
FTE compensation	k$/y	160		300	
FTEs needed	FTEs/site	2	10	15	
Electrolyzer capital cost	$/kWe	454	567	998	[26]
Reference capacity	kg/d		25 773		
Scaling exponent	-		0.6		[26]
Electrolyzer fixed O&M cost	($/y)/kWe	27	41	91	[26]
Reference capacity	kg/d		25 773		
Scaling exponent	-		0.56		[26]
Electrical energy intensity	kWh/kg		51.3		[26]

Most NB designs use TRISO fuels. Yet, designs with 5 wt% enriched uranium oxide (UO_2) fuel are considered the most promising [33] and are thus treated as the base case for further analysis. TRISO fuels will be covered in Section 4.6. While UO_2 is the traditional fuel type, the fuel assemblies will be non-traditional, yet fuel production costs are taken in the same range as regular nuclear reactor fuel.

After all fuel is used, the NBs will be transported to a central facility to be refueled and serviced. So, unlike traditional reactors (in the US), the spent fuel is not stored on site, but at the central facility. The cost of the refueling and waste storage are estimated in Appendix A. In addition, a higher-than-usual decommissioning cost is assumed to account for the additional activation of the reactor materials due to the increased neutron leakage from the small core.

Changes in the capacity factor change the required power and electrolyzer design capacity because the annual hydrogen production in this model is fixed. To accommodate the change in power demand, the number of NBs is varied, while their power output remains fixed at 15 MWth. A fractional number of units is used to match the installed capacity exactly to the electrolysis power demand to avoid cogeneration of electricity and hydrogen at this stage. Obviously, fractional units do not exist in reality, but this can be thought of as an approximate cost allocation.

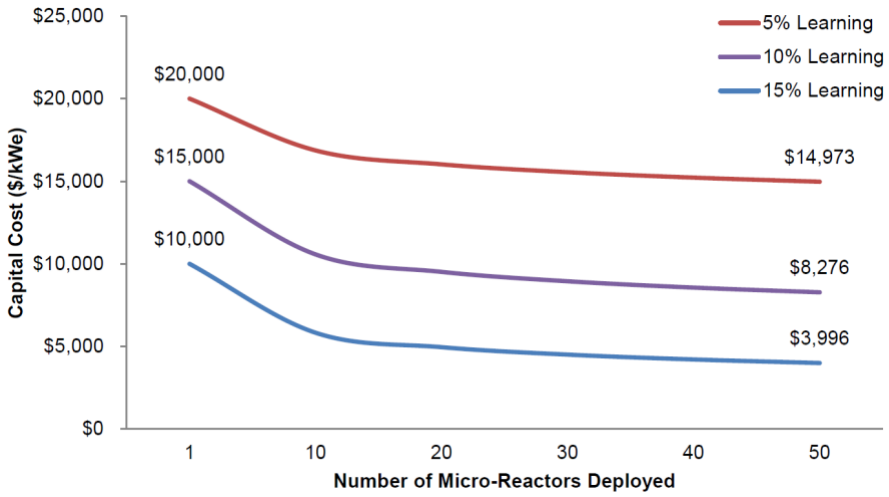

Figure 18 NB capital cost scenarios reported in [34]

Again, the economic lifetime of the project is capped at 25 years, which is conservative for nuclear power generation and the lifetime of NB will likely far exceed this. For example, the Nuclear Energy Institute assumes a lifetime of 40 years in their economic assessment of NBs [34].

It is expected that the regulator will require armed guards on site at least initially, even though the NB will be monitored remotely and will operate autonomously, hence the needed full-time employees (FTEs). These guards will be on-site regardless of the operating state of the reactor and are thus modeled as fixed O&M costs.

The NB capital cost ranges are taken for an Nth-of-a-kind (NOAK) NB, which, admittedly, is not consistent with the assumed project start date of 2030. Figure 18 shows three NB capital cost scenarios of the 2019 Nuclear Energy Institute (NEI) report on microreactors [34]. The learning rate of only 5% in their high first-of-a-kind (FOAK) capital cost scenario seems overly conservative for a standardized, factory-built NB. Instead, using a learning rate of 10% leads to a capital cost of roughly 11 000 $/kWe for the 50th unit. In our model, slightly more optimistic capital cost ranges are used, which are more in line with the previous work of Buongiorno et al. [7] Note that these capital costs cover more than just the cost of the NB, but also include site preparation, installation, etc.

A recent study by Abou-Jaoude et al. [6] takes a detailed look at the mass manufacturing of the INL's MARVEL reactor. They identify a near-term NB production scenario with minimal regulatory risk, where the NBs are produced in a non-nuclear factory with fuel placement, testing, refueling, maintenance and spent fuel storage happening on site – much like the case for traditional reactors. Even in this suboptimal NB production paradigm for a reactor that is not designed for commercial use, they estimate learning rates of 15% to be feasible with a 70% unit cost decline. Thus, our assumed NOAK cost declines compared to the FOAK estimates of the NEI [34] do not seem overly optimistic.

Finally, the electrolyzer capital and O&M costs are estimated as in Section 4.3.1.

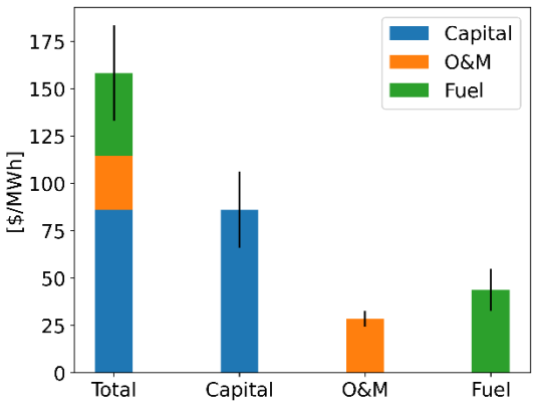

Figure 19 LCOE for electricity supplied by NOAK NBs without IRA subsidy

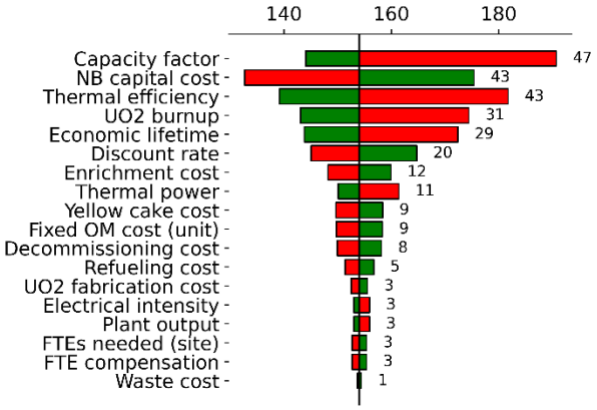

Figure 20 Tornado chart for the LCOE (in $/MWh) of electricity by NOAK NBs without IRA subsidy

NOAK NBs without IRA subsidies

Figure 19 shows that the LCOE of the NBs is 158 ± 25 [88, 297] $/MWh, with the levelized capital cost being the main contributor (86 $/MWh), as per usual for nuclear energy. Unlike in traditional nuclear power plants, though, the levelized cost of fuel is the second most important factor at 44 $/MWh as a result of the low fuel burnup for NBs.

The results of the sensitivity analysis for the LCOE are shown in Figure 20. Due to the high share of fixed costs – the levelized capital cost and fixed O&M costs make up 114 $/MWh of the 158 $/MWh – the operator is heavily penalized for not making full use of the installed capacity, resulting in the significant effect of lowering the capacity factor. Also, due to the high capital cost of the NBs, the LCOE has a significant sensitivity to this parameter. High sensitivities to the capacity factor and NB capital cost are also found in the literature [7], [34]. On a similar note, the high sensitivity to the economic lifetime and discount rate are also related to the large share of the capital cost. Increasing the reactor economic lifetime to 40 years (similar to the assumption of the Nuclear Energy Institute [34]) can thus significantly improve economics.

Lowering the thermal efficiency increases the cost dramatically, as more thermal power is needed to produce the same amount of electricity. As a result, far more fuel is needed, which increases fuel cost, and more units are needed, which leads to more (fixed) O&M costs. Note that there is no impact on the capital cost because the NB capital cost is normalized to the electrical power.

In addition, the sizable share of the fuel costs results in a high sensitivity to the UO_2 burnup, as a decrease in burnup yields an increase in the fuel need for a given amount of energy produced. The enrichment cost is the most impactful out of all front-end fuel cycle parameters, followed by the yellowcake (i.e., uranium input) cost and finally, the fabrication cost– which is unsurprising given that UO_2 pellets are easy to manufacture. Overall, the yellowcake cost has a small impact on the LCOE, making the system resilient to uranium price upsets. Furthermore, the refueling and servicing cost has a small influence, which is good given that the estimation of this cost is highly uncertain. Finally, the waste cost is minimal at about 1 $/MWh – which is a typical figure for nuclear power.

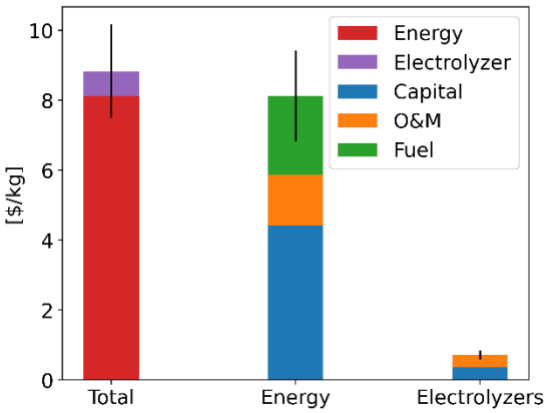

Figure 21 LCOH2 for community-scale PEM electrolysis with electricity supplied by NOAK NBs without IRA subsidy

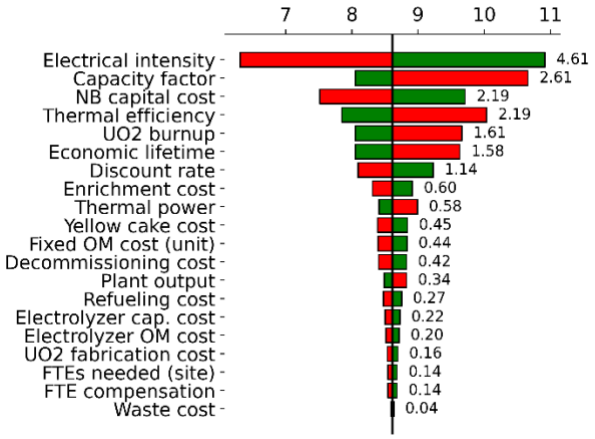

Figure 22 Tornado chart for the LCOH2 (in $/kg) in a community-scale PEM facility powered by NOAK NBs without IRA subsidy

Moreover, changing the thermal power impacts the O&M costs due to the per-unit fixed O&M costs becoming increasingly important as the number of units rises. Similarly, a small portion of the impact of a lower capacity factor is also due to the increased number of units needed at lower capacity factors, driving up the O&M costs. Note that while changing the number of units at fixed capacity affects the LCOE significantly, changing the number of units due to a change in total plant output does not – as can be seen in the small effect of changing the plant output. Finally, also note that the influence of the (electrolysis) electrical intensity influences the required power because the hydrogen output is fixed in our model. Hence, changing the intensity results in a change in electrical power and so, the electrical intensity shows up in the LCOE sensitivities.

The LCOE of 158 $/MWh is below the projected retail industrial electricity prices for CA in 2030 [5] and is consistent with cost estimates found in the literature. The Nuclear Energy Institute reports an LCOE for microreactors between 100 – 400 $/MWh, with the lower end of the range corresponding to their optimistic NOAK scenario, and the upper end corresponding to their pessimistic FOAK scenario [34]. Our LCOE is on the lower end of this range, as expected given the more optimistic capital cost ranges used here. Also, most cost estimates in the sensitivity analysis of Buongiorno et al. [7], lie in the range of 100 – 160 $/MWh, which agrees with our results. Their base case, however, reports a lower LCOE of 80 $/MWh due to their more optimistic assumptions regarding the NB capital and decommissioning costs, number of required FTEs and their compensation, capacity factor, and SNF fees.

The use of NBs lowers the LCOH2 compared to using grid electricity, from 10.03 $\pm$ 0.42 $/kg to 8.83 ± 1.34 [5.14, 15.89] $/kg. The energy cost makes up the lion share of the LCOH2 at 92%, see Figure 21, with the remaining cost being split relatively evenly between the electrolyzer capital and O&M costs. Because the LCOH2 is almost entirely driven by the energy cost, a change in the electrical intensity of the electrolysis is translated almost one-to-one in a change in LCOH2. Hence, the electrical intensity shows up at the most influential parameter, Figure 22. The tornado chart also shows the small influence of the electrolyzers, as expected given their small (8%) share in the LCOH2. Note that the plant output now has a bit more effect on the levelized cost, due to the economy of scale in the electrolyzer cost calculations via Equation (14). All other parameters show similar effects as discussed for the LCOE.

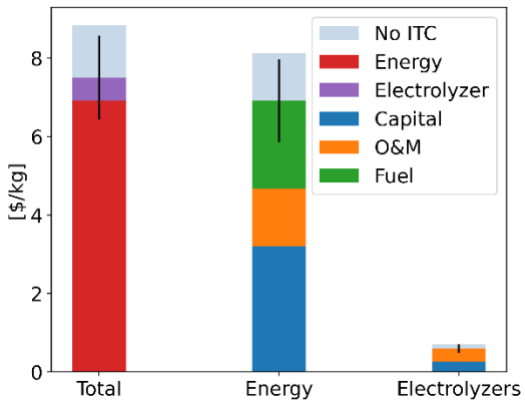

Figure 23 LCOH2 for community-scale PEM electrolysis with electricity supplied by NOAK NBs claiming an IRA ITC

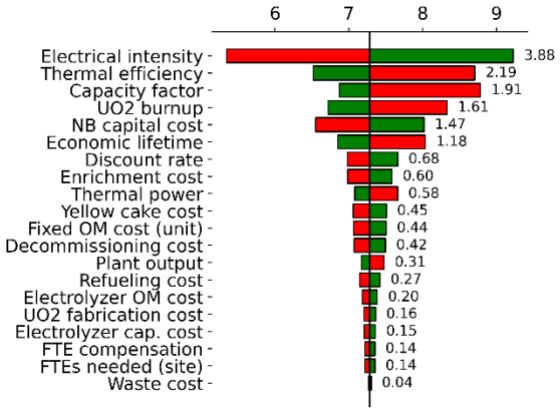

Figure 24 Tornado chart for the LCOH2 (in $/kg) in a community-scale PEM facility powered by NOAK NBs and claiming an IRA ITC

These hydrogen costs are far higher than what is typically reported for 'nuclear hydrogen'. First off, traditional nuclear power plants have lower levelized costs than can be expected from NBs due to the economy of scale. The Nuclear Energy Agency (NEA) reports LCOE estimates for traditional plants in the range of 50 – 100 $/MWh and capital costs between 2400 and 7700 $/kWe [35] and in the US, the existing nuclear fleet has an even lower LCOE between 30 – 50 $/MWh [36]. As an example in this range, the NEA reports an LCOH2 of 3.4 $/kg, assuming a capital cost of 4850 $/kWe and operational costs of 24.2 $/MWh (our operational costs are closer to 72 $/MWh) [26]. In very optimistic studies about the evolution of nuclear technology, even lower capital cost can be found. For example, LucidCatalyst uses capital costs as low as 700 $/kWe in their most optimistic 2050 scenario, resulting in a < 1 $/kg LCOH2 [37].

A second reason for low reported costs of nuclear hydrogen is the use of amortized reactors, such as Diablo Canyon in CA, for which the reported LCOH2 is 2.00 – 2.50 $/kg [38]. These reactors have low LCOEs (e.g., 43 $/MWh [38]) and need minimal investment for repurposing the plant towards hydrogen production (only some 550 $/kWe according to the NEA estimates [30]). A final reason is the use of more exotic hydrogen production techniques that can utilize more of the high-temperature heat of nuclear energy, such as the S-I and Cu-Cl cycles for which Parkinson et al. give an LCOH2 of 1.69 – 3.12 $/kg [23].

NOAK NBs with IRA subsidies

Claiming an ITC under the IRA reduces the LCOH2 from 8.83 $/kg without subsidy to 7.49 ± 1.06 [4.47, 12.80] $/kg. The major cost savings, of course, come from the NBs, as the electrolyzer capital cost only accounts for 0.38 $/kg in the unsubsidized LCOH2 to begin with, see Figure 23.

As expected, the LCOH2 has become less sensitive to parameters that relate to the levelized capital cost – i.e., the NB capital cost, the economic lifetime, capacity factor, and discount rate, Figure 24. Parameters that influence the O&M and fuel costs – e.g., thermal power, thermal efficiency, UO_2 discharge burnup – are unaffected by the ITC and have thus gained more importance.

If instead of claiming the ITC, the PTCs are claimed, then, the LCOH2 drops from 8.83 $/kg to 5.42 ± 1.83 [1.11, 13.56] $/kg. The cost breakdown in Figure 25 shows that the clean hydrogen PTC results in a larger saving than the clean energy PTC – the clean energy PTC lowers the LCOH2 by 0.85 $/kg, while the clean hydrogen PTC is close to 3.0 $/kg. Note that in about 22% of the cases, the fuel burnup is below the

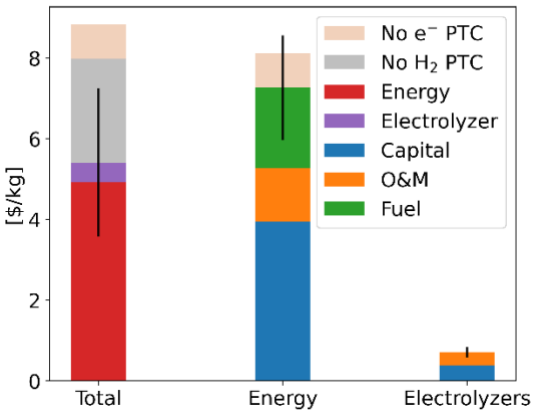

Figure 25 LCOH2 for community-scale PEM electrolysis with NOAK NBs subsidized by PTCs

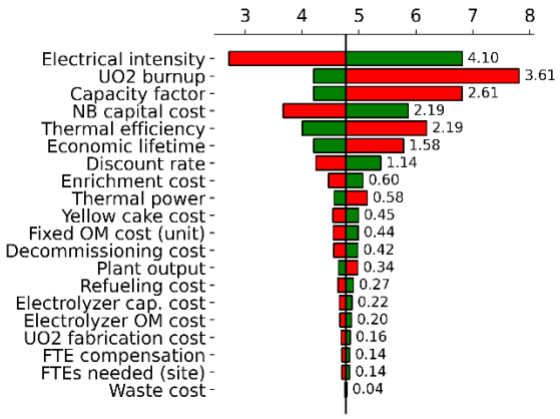

Figure 26 Tornado chart for the LCOH2 (in $/kg) in a community-scale PEM facility powered by NBs claiming PTCs

threshold value of 9.69 MWd/kg HM derived in Section 4.2. This means the hydrogen lifecycle emissions are too high for the 3.0 $/kg credit, and a 1.0 $/kg credit applies instead. As a result, the average effect of the clean hydrogen PTC is 2.56 $/kg.

Figure 26 shows the sensitivity analysis when claiming the PTCs. The UO_2 burnup now has a larger influence on the LCOH2 because besides affecting fuel costs, it also affects the lifecycle emissions and by extension, the clean hydrogen credits. If the burnup becomes sufficiently low, the credit is reduced from3.0 $/kg to 1.0 $/kg as discussed above. Other than that, the PTCs only change the sensitivity to the electrical intensity. For all other parameters, the PTCs merely result in a translation of the base value compared to the original case without IRA credits in Figure 22. The clean hydrogen PTCs are deducted from the cost at the very end and do not interact with the cost structure, nor any of the model parameters – besides the UO_2 burnup. So, it is easy to see how this would not impact the sensitivities or any parameter but the UO_2 burnup. If the electrical intensity remains fixed – as it does under the sensitivity analysis of any other parameter – the clean electricity PTC results into a fixed credit per unit hydrogen produced (i.e., 0.0165 $/kWh · 51.3 kWh/kg = 0.846 $/kg). Thus under the same reasoning as before, it does not affect the sensitivities of any parameters.

Due to the high capital cost of the NBs, the impact of the ITC on the levelized cost of energy is larger than the impact of the clean energy PTC. It is thus more beneficial to claim 'mixed' credits, where an ITC is claimed by the tax payer operating the NBs and a clean hydrogen PTC is claimed by the (different) tax payer operating the electrolyzers. Indeed, the LCOH2 is lowest in this case at 5.05 ± 1.66 [1.55, 12.63] $/kg, see Figure 27. The model sensitivities under mixed credits show traits of both the ITC and PTC cases, Figure 28. The UO_2 burnup again has an enlarged impact due to it lowering the clean hydrogen PTCs and the parameters related to the NB capital cost have a smaller influence on the cost due to their lower overall share in the LCOH2.

Figure 29 compares the LCOH2 breakdowns for the different subsidy options. The mixed subsidies will be the lowest-cost choice for all cases powered by NBs, so the other subsidy options will not be discussed again in further sections.

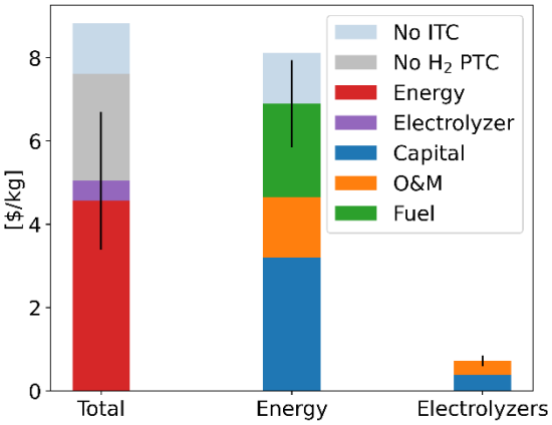

Figure 27 LCOH2 for community-scale PEM electrolysis with electricity supplied by NOAK NBs with mixed IRA subsidies

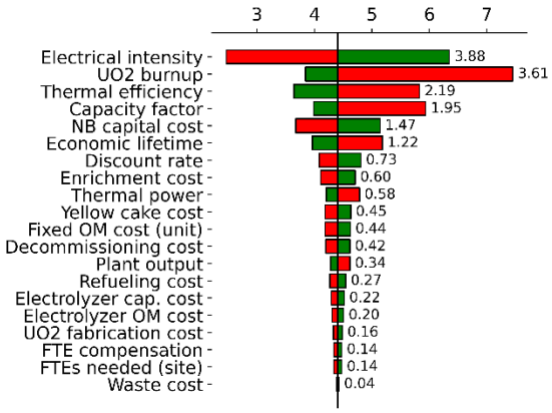

Figure 28 Tornado chart for the LCOH2 (in $/kg) in a community-scale PEM facility powered by NOAK NBs with mixed IRA subsidies

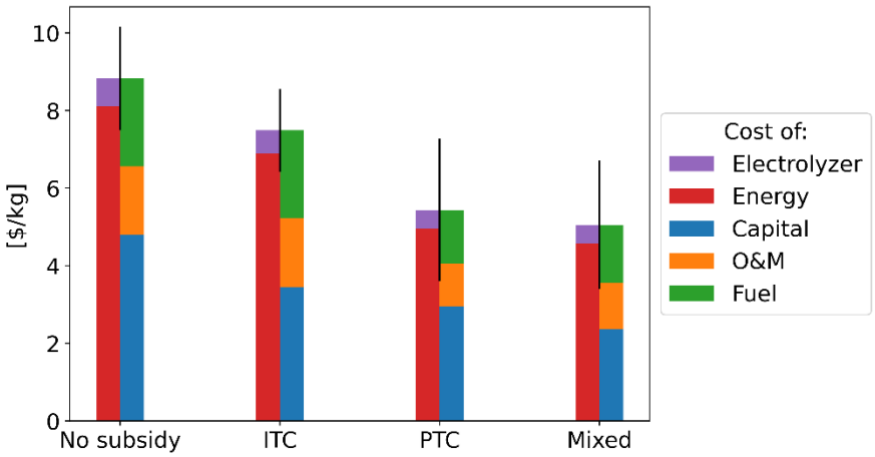

Figure 29 Comparison of the LCOH2 for community-scale PEM electrolysis using NOAK NBs when claiming different types of IRA subsidies, the LCOH2 is broken up in two columns for each case to show share of the levelized cost of the electrolyzers versus energy and to show the distribution between the levelized costs of capital, O&M, and fuel

FOAK NBs with and without IRA subsidies

So far, all calculations were performed assuming NOAK NBs. In the remainder of this section, the economics of a first-of-a-kind (FOAK) NB. The capital costs distribution for the FOAK NB is inspired by the Nuclear Energy Institute's report on nuclear microreactors [34], Figure 18. The resulting distribution is triangular with a minimum capital cost of 10 000 $/kWe, a mode of 15 000 $/kWe, and a maximum of 20 000 $/kWe. All other costs are taken to equal those of the NOAK calculations, meaning that learning effects in O&M and fuel fabrication/disposal are thus neglected here.

The LCOE of a FOAK NB is 257 ± 40 [145, 445] $/MWh, which is about 1.6 times higher than the NOAK LCOE of 158 $/MWh, Figure 30. The rise in LCOE is entirely due to an increase in levelized capital cost from 86 $/MWh to 185 $/MWh (factor 2.1). The levelized costs of O&M and fuel have not changed compared to the NOAK scenario, they thus remain at 28 $/MWh and 44 $/MWh, respectively. The dominance of the NB is thus larger than before. This is also reflected in the sensitivity analysis, with the NB capital cost,

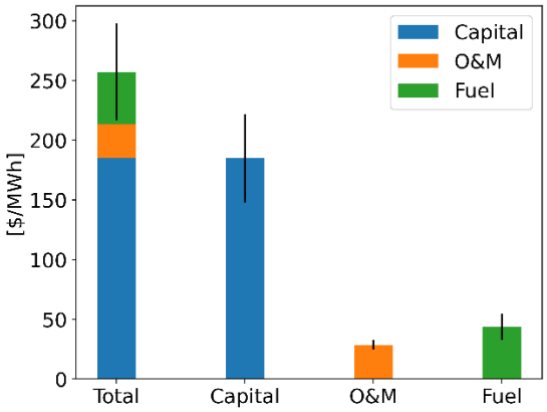

Figure 30 LCOE for community-scale production with FOAK NBs without IRA subsidy

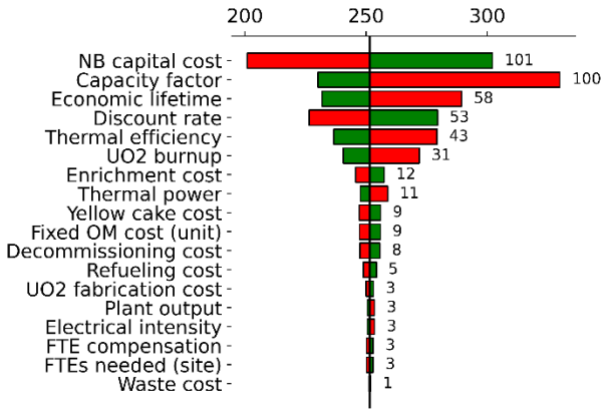

Figure 31 Tornado chart for the LCOE (in $/MWh) for community-scale production with FOAK NBs without IRA subsidy

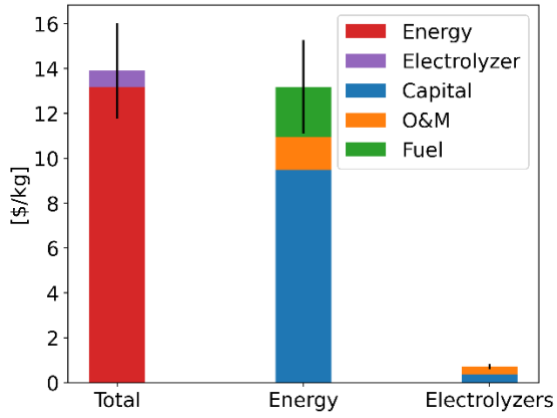

Figure 32 LCOH2 for community-scale PEM electrolysis with FOAK NB electricity without IRA subsidy

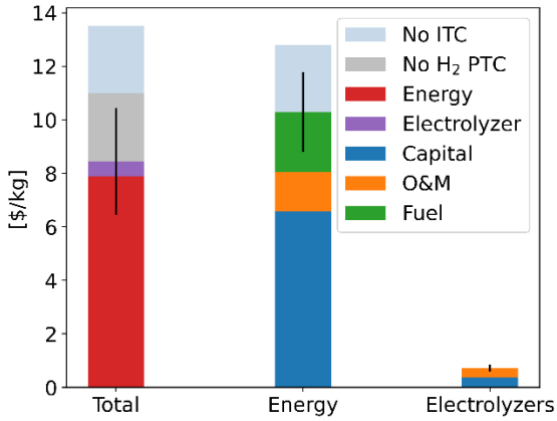

Figure 33 LCOH2 for community-scale PEM electrolysis with electricity supplied by FOAK NBs with mixed IRA subsidy

economic lifetime, capacity factor, and discount rate becoming the most influential parameters, Figure 31.

In their 2019 report, the Nuclear Energy Institute estimates the LCOE of an investor-owned FOAK NB to be 210 – 400 $/MWh [34]. Our LCOE is thus on the lower end of their range, which is to be expected given the lower (NOAK) O&M costs used here. In addition, the upper end of their range is for the most pessimistic (20 000 $/kWe) scenario. Obviously, the higher NB capital cost is also translated into a higher LCOH2, with a rise from 8.83 $/kg in the unsubsidized NOAK scenario to 13.89 ± 2.13 [8.09, 23.67] $/kg in the unsubsidized FOAK scenario, see Figure 32 The increase is entirely due to the higher cost of energy (13.17 $/kg instead of 8.11 $/kg), which itself is increased solely due to the increase in NB capital cost. The sensitivity analysis of the LCOH2 shows the same order for the most influential parameters as the sensitivity analysis of the LCOE (Figure 31). The tornado and bar charts of the LCOH2 in the FOAK scenario can be found in Appendix B and Appendix C, but are not shown here for sake of brevity.

Again, claiming mixed credits under the IRA is most beneficial and can reduce the LCOH2 significantly from 13.89 $/kg to 8.44 ± 1.99 [3.53, 18.27] $/kg, see Figure 34. Due to the higher NB capital cost, the ITC now has a larger impact, as can be seen in Figure 33. The sensitivity analyses can be found in Appendix B and Appendix C.

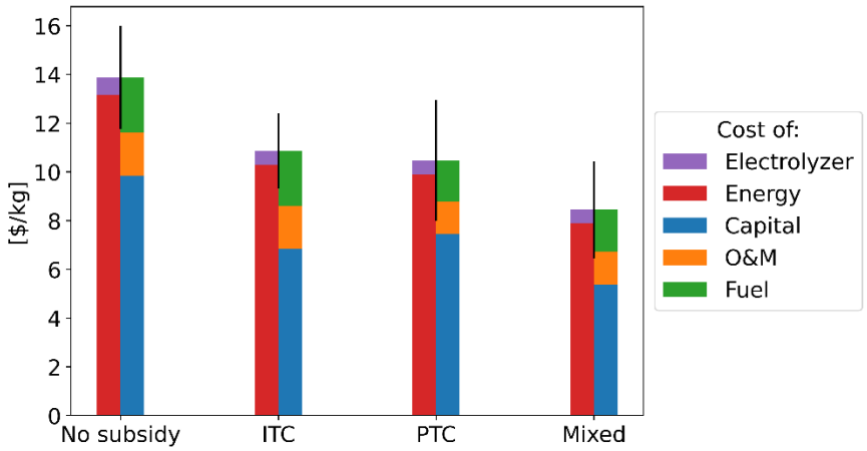

Figure 34 Comparison of the LCOH2 for community-scale PEM electrolysis using FOAK NBs when claiming different types of IRA subsidies, the LCOH2 is broken up in two columns for each case to show share of the levelized cost of the electrolyzers versus energy and to show the distribution between the levelized costs of capital, O&M, and fuel

4.4.2. Distributed production

Here, a project is considered in which hydrogen is produced using PEM electrolysis and a NB with an average plant output of 1600 kg/d on the site of the customer. Once again, the NB only supplies energy to the electrolyzers, no excess heat or electricity is produced/sold. The assumptions used in the cost model are listed in Table 8. Note that when only the mode is given, the parameter is fixed, when the minimum and maximum are given, these correspond to the range of a uniform distribution, and when the minimum, maximum, and mode are given, these describe a triangular distribution.

Table 8 NOAK model assumptions for distributed PEM electrolysis with electricity produced by NBs, FOAK capital costs are shown in red

Parameter	Unit	Min	Mode	Max	Source
Real discount rate	%	2	6	12	
Economic lifetime	y	20		25	
Capacity factor	%	70	85	90	
Thermal efficiency	%	25		35	
Discharge burnup	MWd/kg HM	5	15	15	
Yellow cake cost	$/kg HM		111		[7]
Cost of conversion	$/kg HM		6		[7]
Cost of enrichment	$/SWU		171		[7]
Cost of UO_2 fabrication	$/kg HM	250		500	

Refueling cost	M$/NB	0.84	1.09	1.45	
Waste disposal cost	k$/NB	50		400	
NB capital cost	$/kWe	3000 10 000	6000 15 000	10 000 20 000	[7]
Decommissioning cost	$/MWhe	10		50	
Fixed NB O&M cost	M$/y/unit	0.45	0.5	0.55	
FTE compensation	k$/y	160		300	
FTEs needed	FTEs/site	2	10	15	
Electrolyzer capital cost	$/kWe	553	691	1216	[32]
Reference capacity	kg/d		1650		
Scaling exponent	-		0.6		[32]
Electrolyzer fixed O&M cost	($/y)/kWe	28	42	93	[32]
Reference capacity	kg/d		1650		
Scaling exponent	-		0.955		[32]
Electrical energy intensity	kWh/kg		51.3		[26]

Again, the annual hydrogen production is fixed, which results in a change in the electrolyzer design capacity and the power demand when the capacity factor changes. But in contrast to the model for a community-scale facility, there is only one unit with varying thermal power rather than a varying number of units at fixed power.

The capacity factor is lowered compared to community-scale production to account for the possibility of, e.g., periods of lowered hydrogen demand. In addition, the uptime of one NB will be lower than that of multiple NBs, for which maintenance and refueling can be staggered to increase reliability.

All other model assumptions regarding the NB are equal to those discussed in Section 4.4.1, and the electrolyzers are modeled as in Section 4.3.1.

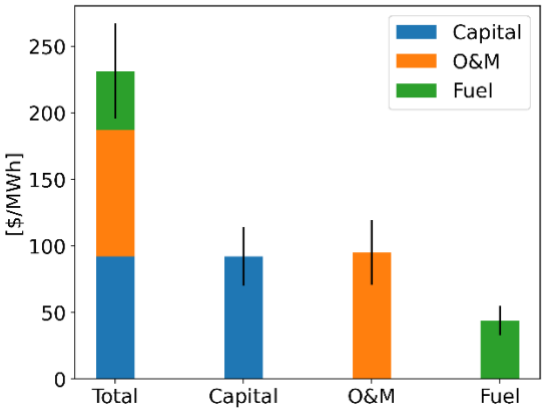

Figure 35 LCOE for electricity supplied by a single FOAK NB

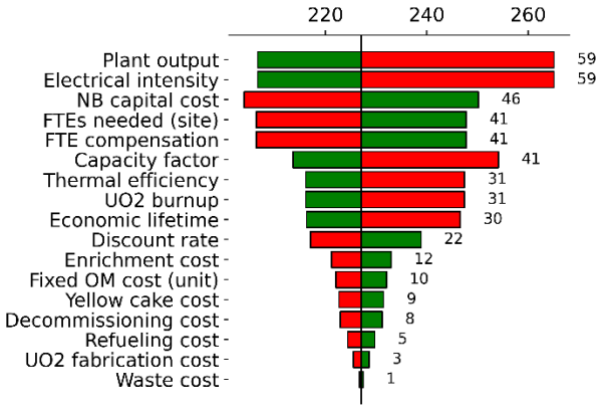

Figure 36 Tornado chart for the LCOE (in $/MWh) of electricity by a single FOAK NB

NOAK NBs with and without IRA subsidies

Note that the O&M costs of the NBs do not scale with reactor power because security requirement do not scale with the output power, nor do the fixed NB O&M costs (which include costs such as NRC operating fees, NRC inspections, insurance premiums, etc.). Consequently, the levelized O&M cost for the single low-power NB is much higher at 95 $/MWh compared to 28 $/MWh for the community-scale case with multiple units, and it is mainly driven by the cost of the on-site armed guards (80%). The increase in the O&M costs is the culprit behind the LCOE rise from 158 $/MWh to 231 ± 36 [120, 411] $/MWh, see Figure 35. Although, the levelized capital cost is also slightly higher than for the community-scale facility (at 92 $/MWh compared to 86 $/MWh), because the average capacity factor is lower for the distributed production.

The LCOE of the low-power NB is much higher than the retail electricity price in CA, thus, the unsubsidized distributed production will not be economical. Only in outlier contexts, such as Hawaii, the state with the highest average retail electricity prices (270 $/MWh [29]), will the low-power NB be competitive. Yet, it must be noted that our estimates for the low-power NB are far more pessimistic than those found in the literature. The INL estimates an LCOE of 155 $/MWh for an NOAK NB at a similar total number of NBs produced [39]. Comparing their NOAK estimate to ours directly is not straightforward, as they have used different learning rates for different cost elements. A more meaningful comparison is thus between the FOAK cases, which will be given further in this section.

Figure 36 shows the results of the LCOE sensitivity analysis. The plant output – which is directly related to the thermal power of the single unit – is most influential because it spreads the O&M costs over more or less electricity production. It does not affect the levelized capital cost, though, because the normalized capital cost is fixed. Furthermore, the fourth and fifth most influential parameters are the number of required FTEs and their compensation, due to the large share of O&M costs in the LCOE. Note also that the fixed O&M costs of NB have become more important than for the community-scale production. The impacts of the other parameters can be understood as before, with the NB capital cost, capacity factor, economic lifetime, and discount rate all relating back to the sizeable share of the capital cost in the LCOE – about a third of the LCOE is due to capital cost – and with the thermal efficiency and UO_2 discharge burnup relating to the fuel costs.

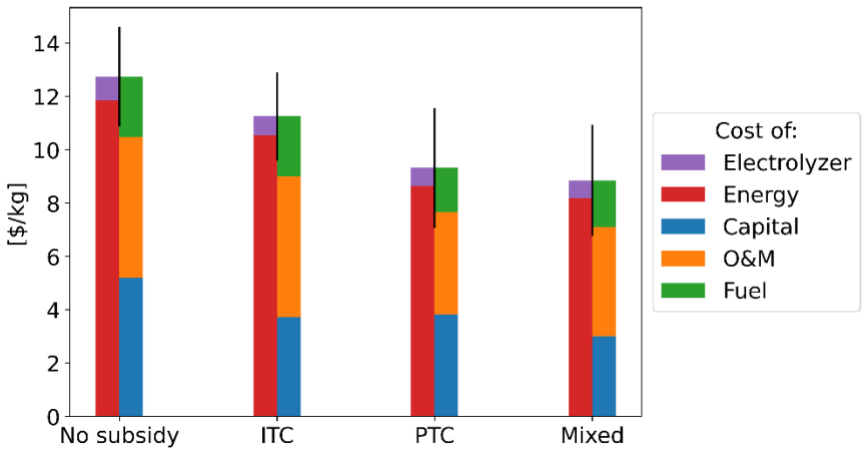

Figure 37 Comparison of the LCOH2 for distributed PEM electrolysis using NOAK NBs when claiming different types of IRA subsidies, the LCOH2 is broken in two ways to show share of the levelized cost of the electrolyzers versus energy and to show the distribution between the levelized costs of capital, O&M, and fuel

Note that the fixed hydrogen output with the needed electricity delivered by a single NB makes a change in the electrical intensity with fixed hydrogen output equal to a change of hydrogen output at fixed electrical intensity, with both effectively being a change of the reactor power. Similarly, this setup makes changes in the UO_2 burnup and thermal efficiency equivalent.

Unsurprisingly given the high LCOE of the low-power NB, the LCOH2 in the distributed production is high at 12.73 ± 1.87 [6.77, 22.19] $/kg, with 93% attributed to the energy (NB) cost. The sensitivity analysis of the LCOH2 shows a similar order and impact for the most influential parameters. Figures for the LCOH2 are not shown here for sake of brevity, but can be found in 0.

The distributed production facility is eligible to claim tax credits under the IRA and claiming the mixed credits is most beneficial. These lower the LCOH2 from 12.73 $/kg to 8.85 ± 2.08 [3.13, 17.49] $/kg. Unfortunately, the credits do little to combat the large O&M costs, so the LCOH2 remains high, see Figure 37. With the IRA subsidies, the use of NBs for distributed production becomes more economical than using unsubsidized grid electricity. If IRA subsidies can be claimed for the grid electricity, however, the latter is more economical. The cost breakdowns and sensitivity analyses when claiming tax credits can be found in Appendix B and Appendix C.

FOAK NBs with and without IRA subsidies

As was the case in Section 4.4.1, the FOAK calculations are performed by increasing the NB capital cost, while keeping all other costs and parameters fixed, thereby neglecting any learning effect in the O&M and fuel costs. Consequently, the levelized capital cost increases from 92 $/MWh to 199 $/MWh, raising the LCOE to 338 ± 50 [188, 583] $/MWh. As a result, the LCOH2 for the distributed production using FOAK NBs is 18.21 ± 2.61 [10.22, 31.06] $/kg. The cost breakdown is shown in Figure 38.

For their (economically optimized) FOAK unit, the INL estimates an LCOE of 363 $/MWh [39]. The lion share of the LCOE comes from the investment/capital costs at 241 $/MWh, which is similar to our levelized capital cost of 199 $/MWh. The second largest cost driver in their design is the fuel, with a levelized cost of 83 $/MWh. Their fuel cost is about 70% higher than our fuel cost of 44 $/MWh, which is not unsurprising since low-enriched (5 wt%) UO_2 fuel is used in this study, whereas they assume a higher enrichment of

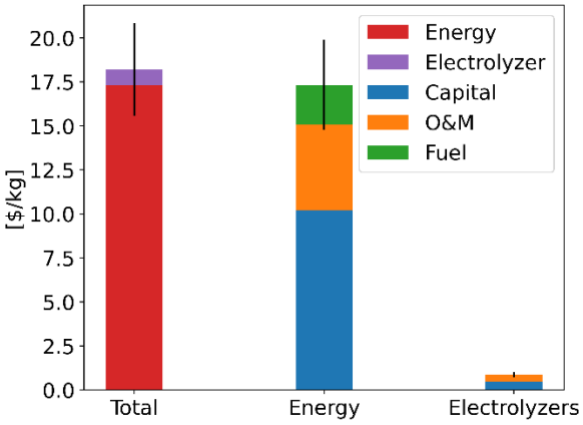

Figure 38 LCOH2 for distributed PEM electrolysis with FOAK NBs without IRA subsidy

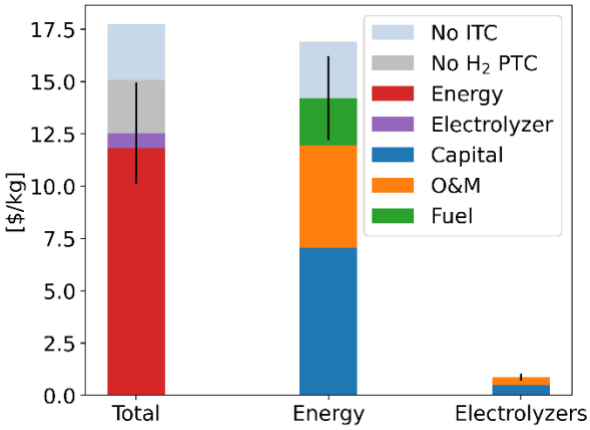

Figure 39 LCOH2 for distributed PEM electrolysis with FOAK NBs with mixed IRA subsidies

the fuel (19.7 wt%) – for which higher costs are to be expected. Finally, the INL estimates a levelized O&M cost of about 40 $/MWh [39], a half of the 95 $/MWh estimated here. For one, according to the INL operations can be streamlined to only 5 FTEs and they assume a lower compensation of FTEs – e.g., they estimate the compensation of a security guards to be 70 000 $/y, whereas all FTEs in our model are compensated between 160 000 and 300 000 $/y. Also, due to differences in cost structure, O&M costs in the INL report do not include items from our definition of fixed NB O&M costs – i.e., insurance premiums, NRC operating fee, etc.

The IRA subsidies can substantially lower the LCOH2 from 18.21 $/kg to 12.51 ± 2.42 [5.34, 24.86] $/kg – the cost breakdown is shown in Figure 39. However, this is not sufficient to make the FOAK NBs competitive compared to distributed hydrogen production using grid electricity. Once more, figures for all calculations can be found in Appendix B and Appendix C.

4.5. SOEC electrolysis with nuclear batteries

4.5.1. Community-scale production

This section studies a community-scale SOEC plant in which NBs provide electricity and heat. The plant is sized to have an average daily output of 25 000 kg/d, and the NBs only supply energy to the electrolyzers; no excess heat or electricity is produced/sold. The assumptions used in the cost model are listed in Table 9. Note that when only the mode is given, the parameter is fixed, when the minimum and maximum are given, these correspond to the range of a uniform distribution, and when the minimum, maximum, and mode are given, these describe a triangular distribution.

Table 9 NOAK model assumptions for a community-scale SOEC facility with electricity and heat provided by NBs, FOAK capital costs are shown in red

Parameter	Unit	Min	Mode	Max	Source
Real discount rate	%	2	6	12	
Economic lifetime	y	20		25	
Thermal power	MW/unit		15		
Capacity factor	%	80	90	95	
Thermal efficiency	%	25		35	
Discharge burnup	MWd/kg HM	5	15	15	
Yellow cake cost	$/kg HM		111		[7]
Cost of conversion	$/kg HM		6		[7]
Cost of enrichment	$/SWU		171		[7]
Cost of UO_2 fabrication	$/kg HM	250		500	
Refueling cost	M$/NB	0.84	1.09	1.45	
Waste disposal	k$/NB	50		400	
NB capital cost	$/kWe	3000 10 000	6000 15 000	10 000 20 000	[7]
Decommissioning cost	$/MWhe	10		50	
Fixed NB O&M cost	M$/y/unit	0.45	0.5	0.55	
FTE compensation	k$/y	160		300	

FTEs needed	FTEs/site	2	10	15	
Electrolyzer capital cost	$/kWe	1257	1561	1728	[40]
Reference capacity	kg/d		25 000		
Scaling exponent	-		0.6		[40]
Electrolyzer fixed O&M cost	($/y)/kWe	72	96	119	[40]
Reference capacity	kg/d		25 000		
Scaling exponent	-		0.755		[40]
Operating temperature	°C		650		[41]
Thermal energy intensity	kWh/kg		7.0		[41]
Electrical energy intensity	kWh/kg		38.2		[41]

The plant is modeled much the same way as in Section 4.4.1, i.e., the number of NBs is varied while the power remains fixed. In addition, the same assumptions regarding the NBs are used. Here, however, a part of the thermal output of the NBs is used to heat the SOEC electrolyzers directly.

The electrolyzer cell's operating temperature is 650 °C in accordance with the NREL's H2A model on future SOEC electrolysis [41]. This temperature is well within the range achievable with NBs. Moreover, this H2A model is also used to estimate the mode of the electrolyzer costs and the energy intensities. In determining the cost range around the modes, the same ratio of mode to minimum/maximum cost is used as for the PEM electrolysis discussed in Section 4.4.1.

NOAK NBs with and without IRA subsidies

As mentioned in Section 4.1, the LCOE of the NBs used for SOEC cannot be calculated directly due to the cogeneration of heat and electricity and it is instead derived from the LCOH as $LCOE = LCOH/\eta$. Seeing as none of the NB parameters have changed, the resulting LCOE should be the same here as it was in Section 4.4. There are, however, very slight differences on the order of 1% because the total number of NBs needed for the more efficient SOEC electrolysis is different than for PEM electrolysis. As a result, the impact of the fixed FTE cost per site is different. Given the small difference of the LCOE with those reported in Section 4.4, they will not be discussed further in the main text. However, all LCOE results are given in Appendix B.

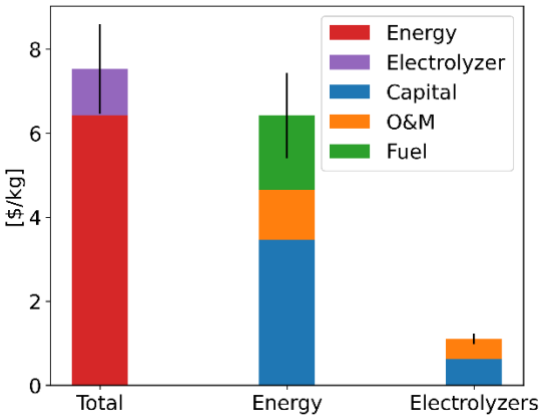

Figure 40 LCOH2 for community-scale SOEC electrolysis with electricity supplied by NOAK NBs without IRA subsidy

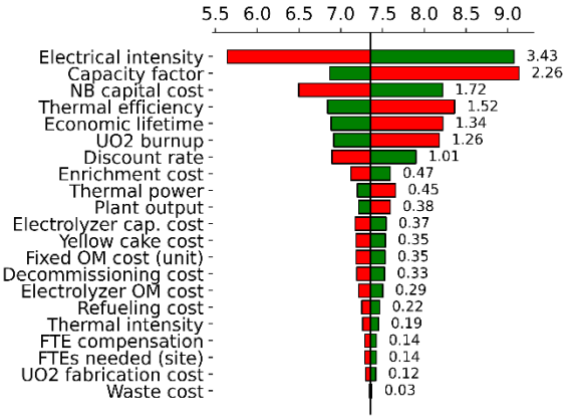

Figure 41 Tornado chart for the LCOH2 (in $/kg) in a community-scale SOEC facility powered by NOAK NBs without IRA subsidies

Using part of the high-temperature heat directly in the electrolysis, rather than first converting it to electricity in roughly a 3:1 or 4:1 ratio, lowers the total energy demand. Consequently, about a fifth less NBs are needed, thereby reducing the energy cost from 8.11 $/kg for unsubsidized PEM to 6.41 $/kg for unsubsidized SOEC. However, this cost reduction is partially offset by the increased cost of the SOEC electrolyzers (1.11 $/kg) compared to PEM electrolyzers (0.71 $/kg). As a result, the LCOH2 is only lowered from 8.62 $/kg when using PEM to 7.52 ± 1.06 [4.44, 13.63] $/kg when using SOEC, with the cost breakdown shown in Figure 40.

Again, the levelized capital cost is the main contributor to the LCOH2. The levelized fuel cost is lowered compared to PEM electrolysis due to the higher energy efficiency of the SOEC electrolysis. The levelized O&M cost also decreases slightly due to the lowered number of units needed per amount of hydrogen produced, which results in less fixed NB O&M costs per unit hydrogen produced.

Comparing the LCOH2 sensitivity analysis (shown in Figure 41) to the LCOH2 sensitivity analysis for unsubsidized, community-scale PEM electrolysis (Figure 21) shows that, overall, the cost drivers are similar in SOEC and PEM electrolysis with NBs. Although, the thermal efficiency of the NBs has become slightly less impactful due to the higher overall energy efficiency of SOEC and the electrolyzers costs have a larger impact now. Still, the LCOH2 remains relatively insensitive to the electrolyzer costs, which is good as cost projections for SOEC electrolyzers in the literature vary greatly. Note that while the electrical intensity still has the largest influence, the thermal efficiency has a limited impact. This is a result of the rather low thermal demand (7 kWh/kg vs. 38 kWh/kg) and the fact that heat is produced in a 3:1 or 4:1 ratio to electricity.

Similar to the results for PEM electrolysis, the LCOH2 for SOEC reported here is higher than what can typically be found in the literature for nuclear-powered SOEC because the large-scale plants benefit from the economy of scale. The NEA estimates the LCOH2 for newly built reactors between 2.1 – 2.9 $/kg [30] and Pinsky et al. give an LCOH2 range of 2.53 – 4.21 $/kg [42]. An exception is the work of Lee et al. who investigate the coupling of a high-temperature small modular reactor to an SOEC stack. They report LCOH2s in the range of 5 – 7.6 $/kg [27], which agrees with our result. The reason for their higher LCOH2 lies in the fact that they assume an LCOE of 140 – 184 $/MWh – the LCOE of the NBs is 158 $/MWh. This range is significantly higher than what is typically assumed for large scale plants – e.g., the NEA assumes an LCOE of 42 – 65 $/MWh for their SOEC estimates [30].

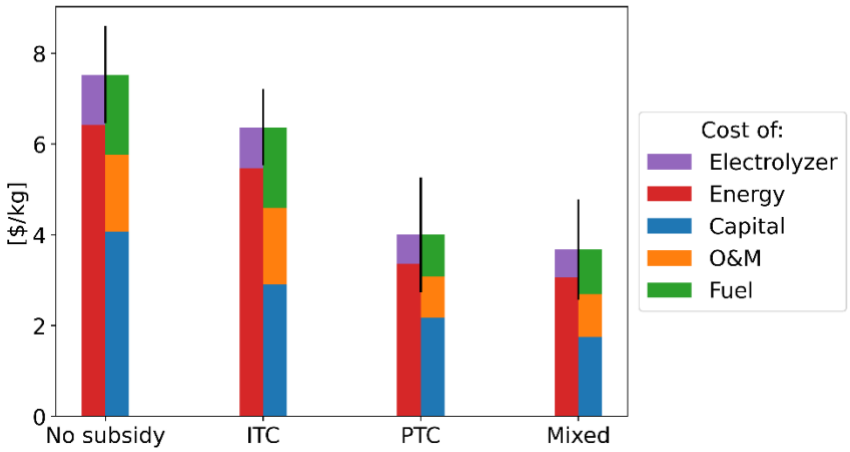

Figure 42 Comparison of the LCOH2 for community-scale SOEC electrolysis using NOAK NBs when claiming different types of IRA subsidies, the LCOH2 is broken up in two columns for each case to show share of the levelized cost of the electrolyzers versus energy and to show the distribution between the levelized costs of capital, O&M, and fuel

Because of the higher overall energy efficiency of SOEC compared to PEM, the emissions associated with hydrogen production are lower for the SOEC plant than for the PEM plant given the same assumptions regarding the NBs. As a result, the lower hydrogen PTC of 1.0 $/kg is only sampled about 5% of the time compared to 22% for PEM, resulting in a larger impact of the hydrogen PTC subsidies. Once more, the mixed subsidies are most beneficial, lowering the LCOH2 from 7.52 $/kg without subsidy to 3.67 ± 1.11 [0.95, 10.13] $/kg, see Figure 42. The cost breakdown and sensitivity analyses for the subsidized cases are given in Appendix B and Appendix C.

FOAK NBs with and without IRA subsidies

For the FOAK NBs, the capital cost is again increased while leaving all other parameters untouched, resulting in a LCOH2 increase from 7.52 $/kg to 11.51 ± 1.71 [6.88, 19.48] $/kg. Figure 44 shows that the LCOH2 is most sensitive to parameters that relate to the capital cost – the NB capital cost, economic lifetime, capacity factor, and discount rate – which is not unexpected given the 66% share of the capital cost in the LCOH2.

Making use of the mixed IRA tax credits, the FOAK NB SOEC plant can reach an LCOH2 of 6.32 ± 1.41 [2.65, 15.25] $/kg (cost breakdown in Figure 44). This is comparable to the cost of subsidized PEM with grid electricity in CA, for which the LCOH2 is 6.18 $/kg. The cost breakdown and sensitivity analyses for the ITC and PTC cases are given in Appendix B and Appendix C.

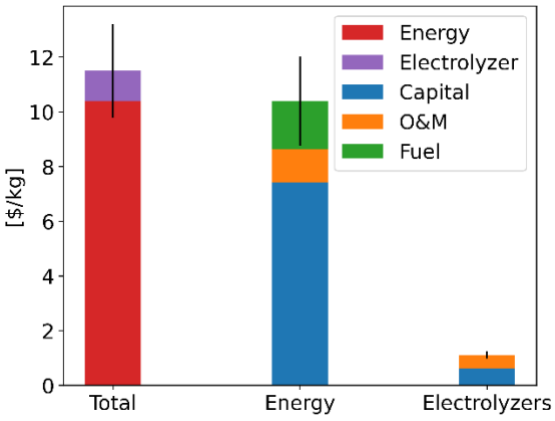

Figure 43 LCOH2 for community-scale SOEC electrolysis with electricity supplied by FOAK NBs without IRA subsidy

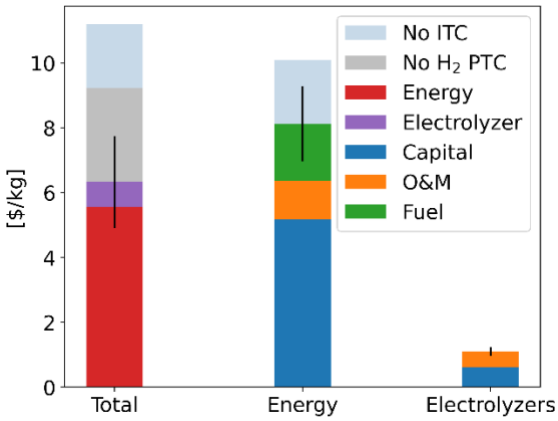

Figure 44 LCOH2 for community-scale SOEC electrolysis with electricity supplied by FOAK NBs with mixed IRA subsidies

4.5.2. Distributed production

This case considers a project in which hydrogen is produced on the site of the customer using SOEC electrolysis and a NB with an average plant output of 1600 kg/d. Again, the NB only supplies energy to the electrolyzers; no excess heat or electricity is produced/sold. The assumptions used in the cost model are listed in Table 10. Note that when only the mode is given, the parameter is fixed, when the minimum and maximum are given, these correspond to the range of a uniform distribution, and when the minimum, maximum and mode are given, these describe a triangular distribution.

Table 10 NOAK model assumptions for distributed PEM electrolysis with electricity and heat provided by NBs, FOAK capital costs are shown in red

Parameter	Unit	Min	Mode	Max	Source
Real discount rate	%	2	6	12	
Economic lifetime	y	20		25	
Capacity factor	%	70	85	90	
Thermal efficiency	%	25		35	
Discharge burnup	MWd/kg HM	5	15	15	
Yellow cake cost	$/kg HM		111		[7]
Cost of conversion	$/kg HM		6		[7]
Cost of enrichment	$/SWU		171		[7]
Cost of UO_2 fabrication	$/kg HM	250		500	
Refueling cost	M$/NB	0.84	1.09	1.45	

Waste disposal	k$/NB	50		400	
NB capital cost	$/kWe	3000 10 000	6000 15 000	10 000 20 000	[7]
Decommissioning cost	$/MWhe	10		50	
Fixed NB O&M cost	M$/y/unit	0.45	0.5	0.55	
FTE compensation	k$/y	160		300	
FTEs needed	FTEs/site	2	10	15	
Electrolyzer capital cost	$/kWe	1531	1902	2106	[36]
Reference capacity	kg/d		1650		
Scaling exponent	-		0.6		[36]
Electrolyzer fixed O&M cost	($/y)/kWe	77	103	129	[36]
Reference capacity	kg/d		1650		
Scaling exponent	-		0.955		[36]
Operating temperature	°C		650		[37]
Thermal energy intensity	kWh/kg		7.0		[37]
Electrical energy intensity	kWh/kg		38.2		[37]

Analogously to the treatment of the distributed PEM facility of Section 4.4.2, there is only one NB with varying thermal power to meet the energy demands. Other than that, the plant is modeled with the same parameters as the community-scale SOEC facility of Section 4.5.1, except for the electrolyzers. The energy intensities are again taken from the H2A model for future SOEC electrolysis. Unfortunately, the design capacity under consideration falls outside the limits of the capital cost correlations in the H2A model. So, the capital and O&M costs are roughly estimated by scaling the electrolyzer costs for the community-scale SOEC facility by the same ratio as there is between the electrolyzer costs in the community-scale and distributed PEM cases. In addition, the same scaling exponents as in the distributed PEM cases.

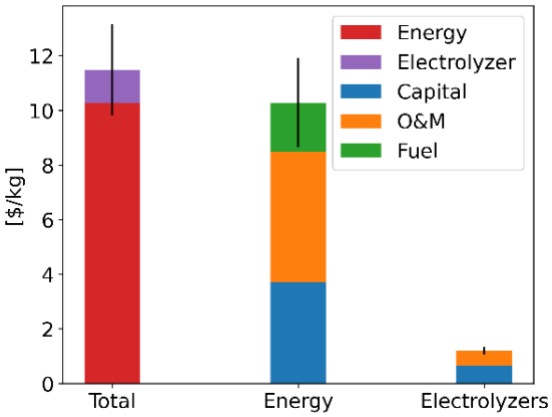

Figure 45 LCOH2 for distributed SOEC electrolysis with electricity supplied by NOAK NBs without IRA subsidy

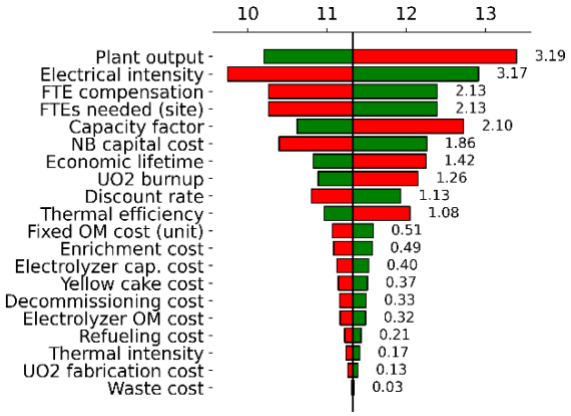

Figure 46 Tornado chart for the LCOH2 (in $/kg) for distributed SOEC electrolysis with electricity supplied by NOAK NBs without IRA subsidy

NOAK NBs with and without IRA subsidies

For the distributed production, there is a larger difference in the LCOE calculated for the PEM electrolysis and the LCOE calculated for the SOEC electrolysis because the total power of the single NB is lower in the SOEC context. As a result, the fixed O&M costs carry more weight and the LCOE is 6 – 10% higher than in Section 4.4.2. Other than that, all conclusions relating to the LCOE are similar, and the LCOE results are not repeated here for sake of brevity, but they can be found in Appendix B.

Like for the distributed PEM hydrogen production, there is a high levelized O&M cost due to the lack of scaling of the fixed NB O&M costs and security requirements with the NB power, Figure 45. The levelized capital and fuel costs remain similar to their values in the community-scale SOEC production. Due to the dominance of the power-insensitive O&M costs, the LCOH2 difference between distributed SOEC and PEM remains limited, with a cost decrease from 12.73 $/kg for PEM to 11.50 ± 1.69 [6.53, 20.35] $/kg.

The sensitivity analysis (Figure 46) shows similar trends as the LCOE sensitivity of the distributed PEM case (Figure 36). The plant output and electrical intensity are again the most influential, but no longer have the exact same sensitivity (as was the case in distributed PEM electrolysis) because the partial thermal demand makes an increase in hydrogen output no longer a one-to-one increase in electrical demand.

As expected, FTE parameters are among the most influential parameters due to the large share of the O&M costs in the LCOH2. In terms of sensitivity, these parameters are followed by parameters that relate to the capital cost – economic lifetime, capacity factor, etc. The LCOH2 has become more sensitive to the electrolyzer costs compared to the PEM cases, but overall, the effect of electrolyzer costs remains limited. Thus, the crude estimation these costs will not have a large impact on the LCOH2.

The mixed credits under the IRA can reduce the cost of hydrogen to 7.56 ± 1.68 [2.78, 16.89] $/kg, which is below the unsubsidized production using grid electricity (at 10.12 $/kg). The cost breakdown and sensitivity analyses for the ITC, PTC, and mixed cases are given in in Appendix B and Appendix C.

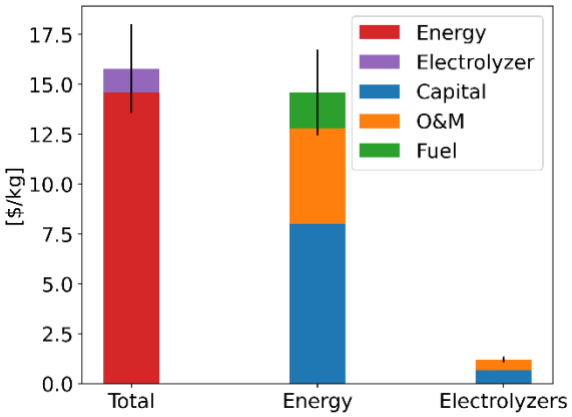

Figure 47 LCOH2 for distributed SOEC electrolysis with electricity supplied by FOAK NBs without IRA subsidy

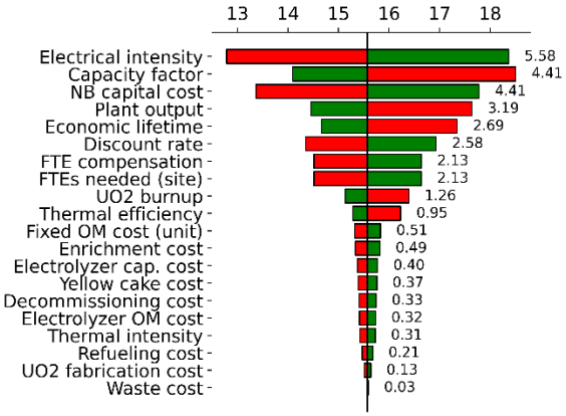

Figure 48 Tornado chart for the LCOH2 (in $/kg) for distributed SOEC facility powered by FOAK NBs without IRA subsidy

FOAK NBs with and without IRA subsidies

Once more, the FOAK calculations are performed by increasing the NB capital cost, while keeping all other costs and parameters fixed, thereby neglecting any learning effect in the O&M and fuel costs. Consequently, the LCOH2 increases to 15.81 ± 2.24 [8.20, 25.85] $/kg, with a larger share of the NB capital cost, Figure 47. Also as a result of the higher NB capital cost, the capacity factor and normalized NBs capital cost have now become the second and third most influential parameters for the LCOH2 closely followed by the plant output, Figure 48. The main takeaway of the sensitivity analysis remains the same as for the NOAK case, though, the LCOH2 remains especially sensitive to the O&M costs and NB capital cost.

The mixed IRA tax credits result in a cost of 10.44 ± 1.95 [4.39, 21.35] $/kg comparable to that of unsubsidized distributed PEM with electricity bought from the grid (10.12 $/kg). The cost breakdown and sensitivity analyses for the ITC and PTC cases are given in in Appendix B and Appendix C.

4.6. TRISO fuel

Traditional reactor fuel consists of fuel pellets stacked into fuel rods with a cylindrical cladding that are collected into larger assemblies, Figure 49. In contrast, TRISO fuels are small particles with a spherical fuel kernel surrounded by multiple shells, Figure 50. The silicon carbide (SiC) layer is the most important and acts as a cladding, trapping the fission products inside. Additionally, there is a porous buffer that accommodates expansion of the fuel kernel as well as the buildup of fission gasses. Finally, there are the pyrolytic carbon layers that protect the silicon carbide layer from chemical attack [43].

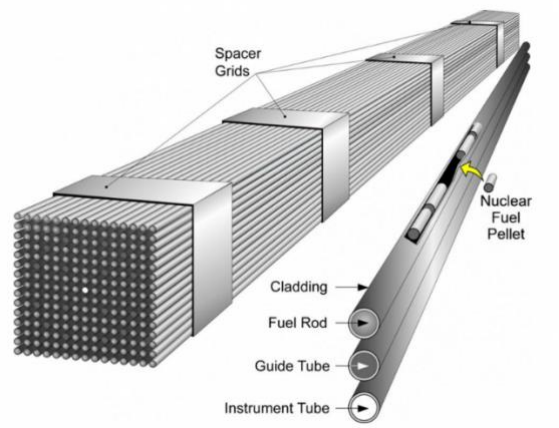

Figure 49 Schematic of PWR fuel assembly and fuel rods. Taken from Ref. [44]

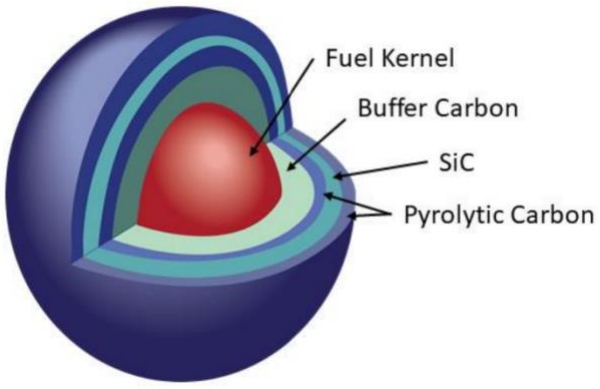

Figure 50 Schematic representation of a TRISO particle. Taken from Ref. [45]

TRISO fuels offer enhanced safety features due to the robust trapping of the fission products in the TRISO particles as well as high burnup and the possibility to operate at high temperature. Hence, it is not surprising that many of the NB designs currently being developed aim to use these fuels, Table 11.

The more complex structure of the fuel results in far higher fuel fabrication costs, with the INL estimating the TRISO fabrication cost at about 15 000 $/kg HM for their nominal estimates [46]. Based on their estimate and our judgement, we use a fabrication cost range of 10 000 – 20 000 $/kg HM.

In addition, TRISO fuel has a far higher enrichment to counteract the fact that the uranium mass goes down when substituting a volume of UO_2 with a volume of TRISO particles due to the less efficient packing of fuel in the volume. Typically, such a substitution would result in less than 10% of the original fuel volume being taken up by TRISO fuel kernels. Hence, TRISO fuel particles need a higher enrichment to maintain a sufficient fissile inventory. The increase in enrichment leads to an increase in cost. However, the enrichment cost increase is overshadowed by the increase in fabrication cost compared to traditional UO_2 fuel. Hence, our analysis is based on a design that uses maximum enrichment (19.75 wt%) to minimize the fuel loading.

The higher burnup of TRISO fuels results in less overall fuel being needed. However, the fuel itself is more expensive as mentioned above. The latter is seen to be more important, as using TRISO fuel adds 14 $/MWh to the levelized fuel cost, thereby increase it to 57 $/MWh. This is mainly a result of the high fabrication cost, which would have to come down to 8150 $/MWh to reach the same levelized fuel cost as UO_2 in our model.

Table 11 A list of NB designs that are being developed

Name	Company	Fuel	Coolant	Power [MWe]
Pele	BWXT	HALEU TRISO	Helium	3 – 5
eVinci	Westinghouse	HALEU TRISO	Na	5
XENITH	X-Energy	HALEU TRISO	Helium	7
Kaleidos	Radiant Nuclear	HALEU TRISO	Helium	1
MARVEL	INL	HALEU TRIGA	NaK	< 0.1
ARC	Alpha Tech Research Corp	LEU	Fluoride salt	12
HOLOS	HolosGen	HALEU TRISO	Helium	< 13
Nugen Engine	NuGen	HALEU TRISO	Helium	1 – 3
PWR-20	Last Energy	LEU UO_2	H_2O	20

As a result of the higher energy cost, the LCOH2 rises 0.63 $/kg in PEM electrolysis. However, the cost increase is lower – only 0.18 $/kg – when claiming clean hydrogen PTCs because the higher TRISO burnup leads to lower lifecycle emissions, thereby allowing the owner to always claim the full 3 $/kg PTC. The LCOH2 for centralized production is 9.46 ± 1.36 [5.38, 15.80] $/kg without IRA subsidy and 5.24 ± 1.10 [1.74, 10.11] $/kg when claiming mixed subsidies. For distributed production, the LCOH2 is 13.36 ± 1.89 [7.26, 21.88] $/kg without claiming subsidies and 9.05 ± 1.68 [3.45, 15.98] $/kg with mixed subsidies.

For SOEC, the 14 $/MWh LCOE increase only translates to a 0.5 $/kg increase in LCOH2, or 0.39 $/kg when claiming the PTCs. The difference is now smaller because, for SOEC, the burnup threshold for the lower PTCs is smaller, as explained in Section 4.2. In unsubsidized centralized production, the LCOH2 is 8.02 ± 1.09 [4.44, 13.63] $/kg. When claiming the mixed credits, it is lowered to 4.07 ± 0.88 [1.26, 8.23] $/kg. For unsubsidized distributed production, the LCOH2 is 12.00 ± 1.69 [6.76, 19.41] $/kg, which is lowered to 7.98 ± 1.54 [3.15, 14.93] $/kg with mixed subsidies. All other permutations of subsidies and the resulting LCOE and LCOH2 values are given in Appendix B and Appendix C.

Figure 51 Figure 52 compare the sensitivity analyses for centralized production with mixed subsidies when using UO_2 and TRISO fuels. A first thing to note is the lower impact of the TRISO burnup compared to the UO_2 burnup. This is a result of the drop in clean hydrogen PTC at low UO_2 burnup, which does not occur for lower TRISO burnups, as they are still above the burnup threshold discussed in Section 4.2.

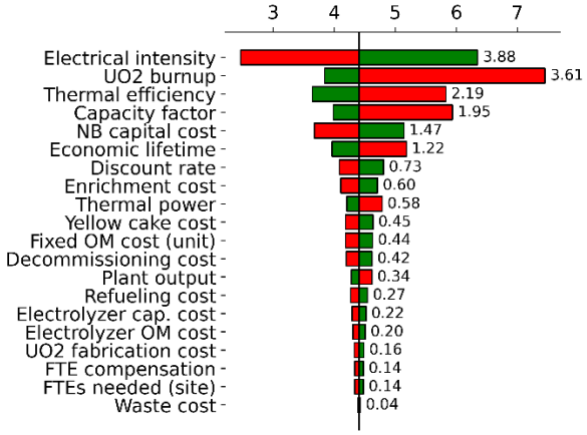

Figure 51 Tornado chart for the LCOH2 (in $/kg) in a centralized PEM facility powered by UO_2-fueled NBs with mixed IRA subsidies

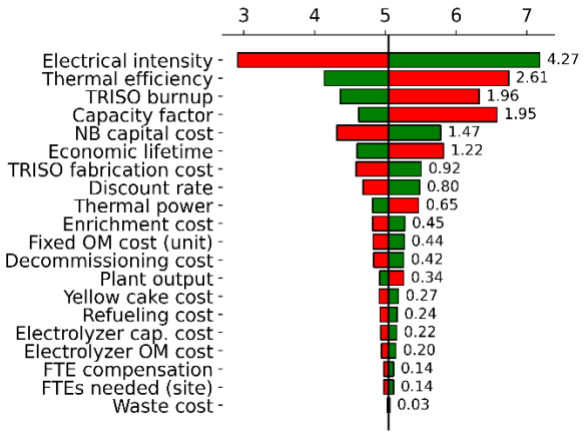

Figure 52 Tornado chart for the LCOH2 (in $/kg) in a centralized PEM facility powered by TRISO-fueled NBs with mixed IRA subsidies

In addition, the relative impact of the fuel cycle costs have shifted. For UO_2 fuels, the order of cost impact is: enrichment > uranium > fabrication, whereas it is fabrication > enrichment > uranium due to the immense fabrication cost of TRISO fuels. Note that the impact of yellow cake (uranium) cost is lower for TRISO fuels due to the lower overall uranium mass needed, thereby making the TRISO-fueled NBs even more resilient to uranium price upsets.

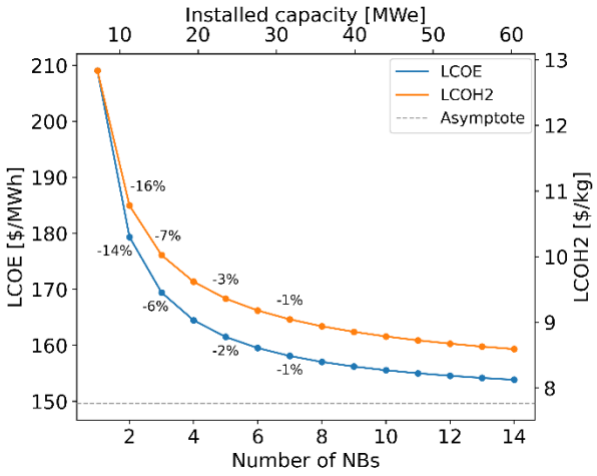

Figure 53 The evolution of the LCOE and LCOH2 as a function of the number of installed NBs in a centralized PEM model. The data labels represent the percentage decline compared to the previous data point and the grey line corresponds to the asymptote at infinite number of NBs

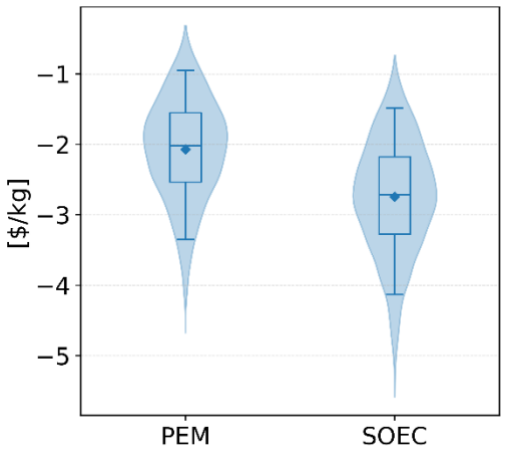

Figure 54 Box plots with distribution overlay for the LCOH2 decline upon adding a second NB while claiming mixed subsidies in both cases. The box plot whiskers represent the 5th and 95th percentiles and the mean is represented by a diamond marker

4.7. Effect of facility sizing

The cost of on-site armed guards is the main driver for the cost increase between centralized and distributed production, as it is site-specific and independent of the power output. Increasing the facility size is an obvious solution to combat the increase in levelized cost due to the fixed guard cost. However, increasing the plant output has diminishing returns. So, in this section, we look at the evolution of cost as a function of the number of NBs to get an idea of the optimal range of NBs.

To that end, the number of NBs is varied in the centralized cost model with all parameters normalized to the expected value of their cost distributions given in Sections 4.4 and 4.5. No Monte Carlo simulations are run for the sweep. So, the data shown in Figure 53 Figure 55 is the result of single calculations with normalized parameters. The electrolyzer cost function is used outside of its intended range during the sweep. However, this does not affect the overall trends observed due to the small influence of the electrolyzer costs in the LCOH2. By contrast, the cost differences of Figure 54 are based on Monte Carlo simulations in which the distributed model is used and in which the model parameters are sampled consistently between the one-NB and two-NB cases to avoid overestimating the spread on the cost difference – as will be explained in more detail in Section 4.9.

Clearly, the costs fall significantly upon installation of a second (and third) NB, Figure 53. On average, the addition of a second NB in unsubsidized distributed production leads to a 38 $/MWh decrease in the LCOE and a 2.08 $/kg decrease in the LCOH2. Again, note that these values do not perfectly match those of Figure 53 because they result from Monte Carlo simulations of the distributed model, whereas the figure is created with single calculations starting from the centralized production model. Also note that both the LCOE and LCOH2 approach the same asymptote, but at different rates due to the presence of the electrolyzer costs.

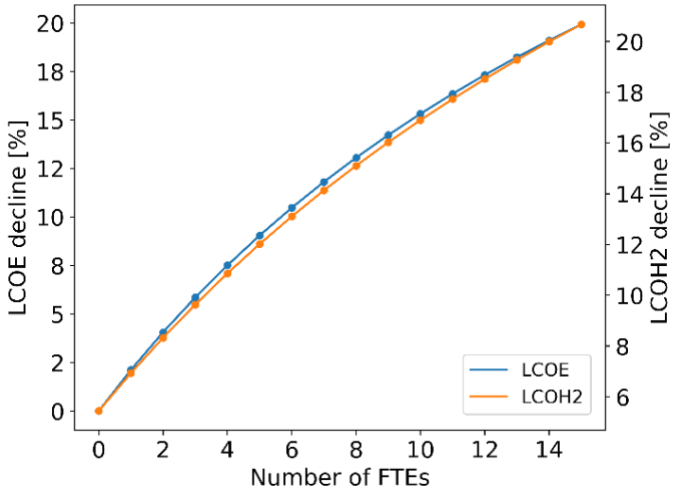

Figure 55 The percentage decrease in the LCOE and LCOH2 upon adding a second NB as a function of the number of required on-site guards

For PEM, the LCOH2 after adding a second NB is 6.79 ± 1.85 [2.13, 16.93] $/kg with mixed IRA subsidies, which is about 2.07 ± 0.72 [0.31, 4.67] $/kg lower than when using a single NB, Figure 54. When using subsidized SOEC with two NBs, the LCOH2 is 4.81 ± 1.26 [1.65, 13.01] $/kg; again, lower than the LCOH2 when using a single NB by 2.74 ± 0.80 [0.74, 5.59] $/kg. There is thus clearly a heavy penalty to using only one NB. A double NB station would have too large of a capacity, but projects with two large, coupled stations are conceivable – e.g., two stations on either side of an interstate. Note that the LCOE and LCOH2 for other subsidy and fuel permutations with two NBs are also given in Appendix B and Appendix C.

While there is a clear benefit to adding NBs at low capacity, the diminishing returns quickly show up – e.g., adding a fifth or seventh NB only decreases the LCOE by 2% or 1%, respectively. Indeed the 6.79 $/kg LCOH2 when using two NBs is already close to the 5.05 $/kg LCOH2 for centralized production with PEM – 4.81 $/kg versus 3.67 $/kg for SOEC. In addition, NBs suffer from diseconomies of scale compared to technologies with a higher generation capacity (e.g., small modular reactors). So, it is unlikely that adding many NBs will be the lowest cost option and the upper bound on a reasonable number of NBs will be determined by the nearest high-power competing technology. Overall, it appears that the optimal number of NBs will be a handful – e.g., four.

Figure 55 shows the percentage decline in the LCOE/LCOH2 when increasing the number of NBs from one to two as a function of the number of on-site FTEs. It is no surprise that if there are less on-site guards, the levelized costs will be less capacity dependent because the benefit of increasing the facility capacity stems from diluting the site-specific and power-independent cost of on-site guards over a larger production. There is still an effect of doubling the capacity on the LCOH2 without any on-site guards because of the lower electrolyzer cost. With guards present, the percentage decrease in LCOE/LCOH2 increases sublinearly with an increase in the number of FTEs, reaching about a 20% drop for the maximum number of 15 FTEs.

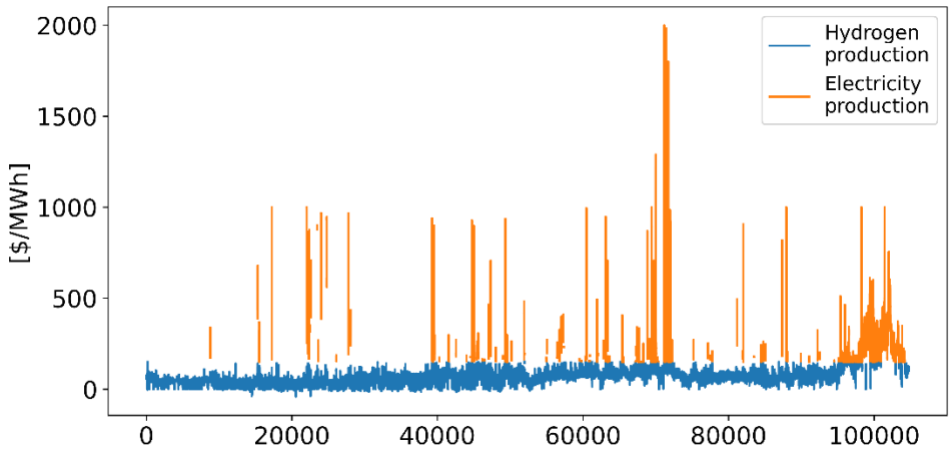

Figure 56 2022 CAISO average wholesale electricity price in five-minute intervals. The threshold price between electricity and hydrogen production is 100 $/MWh in the figure

4.8. Revenue from grid participation

Grid participation has the potential to boost the profitability of a NB project by allowing to capitalize on the price dynamics and ancillary service payments. While we primarily focus on selling electricity during high-demand periods and securing resource adequacy payments, the impact of purchasing electricity during low-price periods will also be briefly discussed.

Capacity payments

In order to ensure that supply can meet demand (i.e., resource adequacy) at all times, some electricity markets have capacity payments to attract investment in new generation capacity as well as to incentivize generators to be online in times of need. CAISO also has capacity payments in the form of a monthly payment based on the Qualifying Capacity of a dispatchable generator, which is determined based on periodic maximum power tests. The payment depending on the location and time of year to more efficiently incentivize generation in places and times of need [47].

The average resource adequacy payment in 2021 was 7.40 2022$/kW/month. Assuming a 100% capacity factor, such a payment equates to a welcome 10 $/MWh discount in the LCOE, which results in a 0.52 $/kg discount in the LCOH2 for PEM and a 0.38 $/kg discount for SOEC. The 85th percentile payment is 9.61 2022$/kW/month, which is a 13.2 $/MWh, which is a 0.67 $/kg discount for PEM.

Electricity sales revenue

From Sections 4.3 through 4.5, it is clear that the electricity cost by far dominates the cost of hydrogen. In the extreme case that the electricity cost is the only cost – i.e., we neglect the electrolyzer cost – the cost of hydrogen can be linked to an equivalent cost of electricity. Assuming an intensity of 50 kWh/kg for PEM, 20 $/MWh electricity will result in a 1 $/kg LCOH2. Of course, the same reasoning holds for prices and we can use the equivalence to optimize the NB project between selling electricity to the grid or producing hydrogen. If hydrogen is priced at 3 $/kg, one should produce hydrogen so long as electricity prices are below the equivalent hydrogen price of 60 $/MWh and sell electricity to the grid otherwise. This principle is shown in Figure 56 with a threshold price of 100 $/MWh.

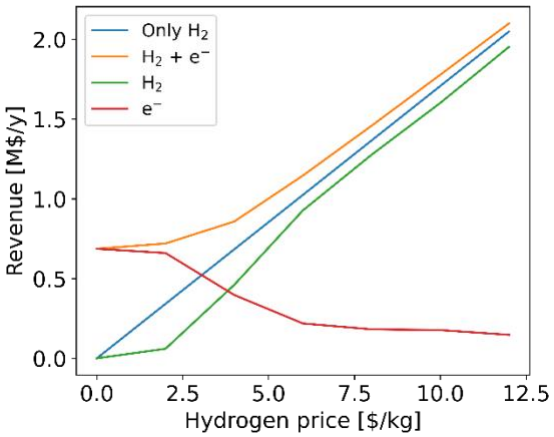

Figure 57 Revenue on per-MW basis associated with the sale of hydrogen and electricity of a coproducing PEM facility, the hydrogen only line corresponds to a facility that does not sell electricity to the grid

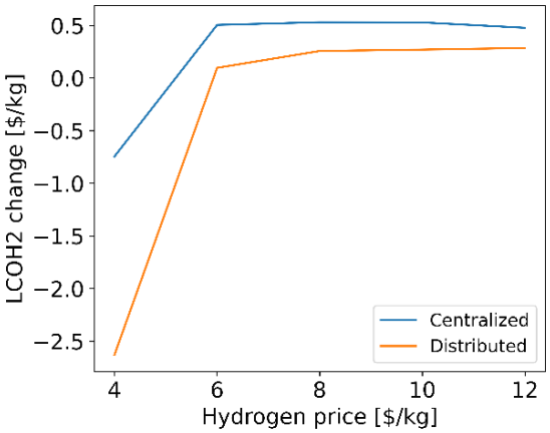

Figure 58 The LCOH2 impact of selling electricity to the grid as a function of the hydrogen price for both centralized and distributed production using PEM

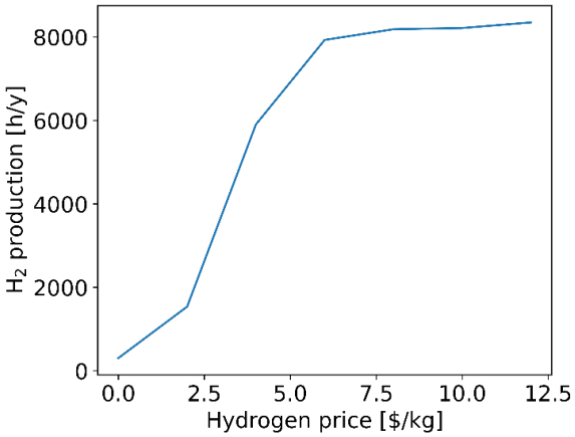

Figure 59 The annual number of hours in which hydrogen is produced instead of selling electricity to the grid as a function of the hydrogen price

In reality, one cannot switch between producing hydrogen and selling electricity immediately, as the PEM electrolyzers take some time to ramp up and down. This must be taken into account to avoid overestimating the benefit of switching production for short-duration price spikes. For this ramping time we assume 5 min, in line with assumptions of Buttler et al. [24] and Nguyen et al. [48]. Note also that in all calculations the PEM intensity is assumed to be 51.3 kWh/kg rather than 50 kWh/kg in line with the value assumed in our economic models.

First we optimize the electricity sales versus hydrogen production of the NB project retrospectively, using the average 2022 wholesale electricity price in 5 minute intervals – this is the dataset used to make Figure 56. The revenue streams per MW of capacity are shown in Figure 57. At low hydrogen prices, almost all revenue comes from electricity production and there is an obvious incentive for selling electricity to the grid. At higher hydrogen prices, the effect of selling electricity is more limited and electricity is sold to the grid only in very high price events.

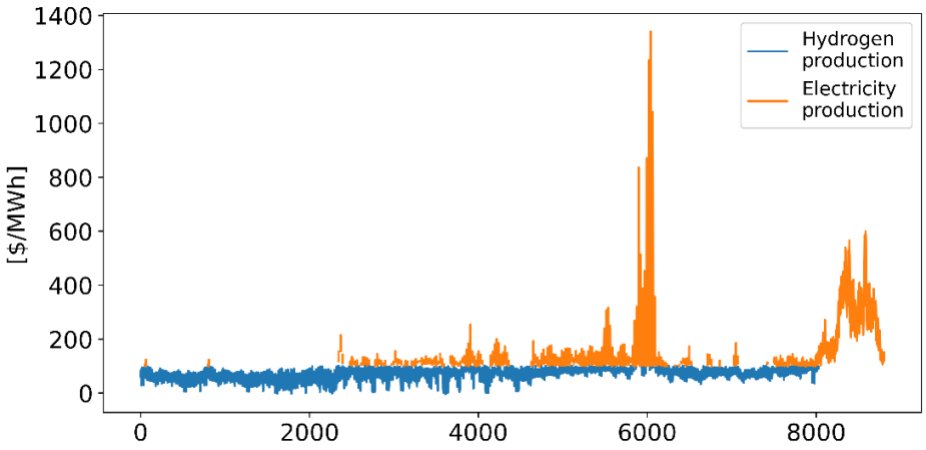

Figure 60 2022 wholesale electricity price on the SOUTHBY_6_N001 node in Sacramento in five-minute intervals. The threshold price between electricity and hydrogen production is 100 $/MWh in the figure

While electricity sales increase the project revenue, they decrease the hydrogen output. If the loss of hydrogen production is sufficiently high, this can lead to an increase in the LCOH2 (Figure 58 Figure 59) is insufficient to counteract spreading the costs over a lower hydrogen output. Note that this lowering of the LCOH2 is an artifact of the cost allocation – or rather, lack thereof – between the hydrogen production and electricity sales. Importantly, the analysis here does not take into account the possibility of increasing the facility size to maintain the annual hydrogen output. Allowing for an increase in capacity would boost the economics of the project significantly, as was discussed in Sections 4.4 and 4.5.

The LCOH2s of centralized PEM production with NBs are 5 $/kg and 9 $/kg. So, a more relevant range of hydrogen prices for such a project is, e.g., 6 $/kg to 10 $/kg. In this range, selling electricity to the grid increases revenue by 11.8 % to 4.1% and the revenue of electricity sales per MW of capacity is 12 – 80 k$/y, respectively. The resulting LCOH2 discount is pretty stable for centralized production around 0.5 $/kg and varies between 0.1 and 0.3 $/kg for distributed production.

Of course, the benefit of electricity sales depends on the specific behavior of the electricity prices, which is varies across time and location. For example, repeating the above exercise with the 2022 LMP data of the SOUTHBY_6_N001 node in Sacramento (shown in Figure 60) sees almost no benefit of electricity sales with an impact on the LCOH2 on the order of 0.01 $/kg.

There are two reasons why there is no gain to selling electricity to the grid when using the Cambium data set. For one, the energy prices (marginal costs) in the dataset are 1.7 to 8.3 times lower than the historical 2022 prices. Second, there are no high price events like we see in the real price data. This lack of extreme volatility is a well-known shortcoming of the Cambium dataset [49], [45]. The problem is exacerbated by the fact that we can expect an increase in price volatility with the increasing renewable penetration, as was already seen in recent years [51]. As such, using the Cambium dataset underestimates the revenue stream possible from selling electricity to the grid.

Yet, the little to no gain from electricity sales is not the only reason that grid participation is not worth it for NBs. So far, only electricity sales were considered, but under grid participation, one should also buy electricity in times of low prices – with low prices being prices below the marginal cost of electricity production of the NBs. Then it is only economical to operate the NBs when prices are above its marginal

cost – producing hydrogen when prices are lower the equivalent hydrogen price and selling electricity to the grid otherwise.

The marginal cost of productions for the NBs can be approximated by the levelized cost of fuel, which is about 45 $/MWh when using UO_2 fuel and 57 $/MWh when using TRISO fuels. Both are relatively high, with the average 2022 CAISO prices being lower in 28% to 42% of the time, respectively, and the Cambium average monthly price being lower for all months. As a result, the NBs would not operate often, and infrequent operation is detrimental to the economics of such a high capital cost asset. Thus, the use of NBs is likely not economical when connected to the grid, and they should instead be considered for off-grid application.

It is, of course, too early to write off NB use in grid applications based on the rudimentary analysis presented here. For one, the power prices vary significantly between different grids and different locations within the grid – under locational marginal pricing, at least. For example, in Sacramento, the 2022 price series only showed lower power prices than the NB marginal cost in 12% and 26% of the intervals for UO_2 and TRISO fuels, respectively. Second, not all types of grid revenue have been considered, e.g., the NBs can likely also claim black start payments and Kopp et al. [52] found that participating in the control reserve market was most profitable for a power-to-gas plant in Germany. Finally, no calculations have been made regarding the effect of buying electricity, the cost of a connection, the impact of electrolyzer switching on degradation, etc.

Finally, note that we have not considered any grid participation revenue for electrolysis with grid electricity. Such a project could, e.g., participate in demand response programs and minimize electricity costs by avoiding operation in times of high prices. The latter option was investigated by Nguyen et al. [48] and was found to lower electricity costs by up to 30% in CA.

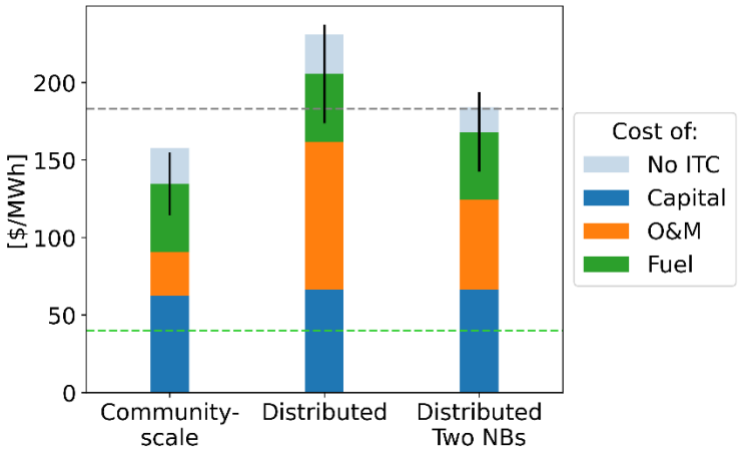

Figure 61 Comparison of the LCOE for electricity production with NBs on a community-scale and for a single NB to the projected 2030 wholesale electricity price in CA (green) and retail price (grey) [5]

4.9. Production cost comparison and discussion

Figure 61 shows the LCOE of the NBs used in a community-scale facility (of roughly 60 MWe) and the LCOE of a NBs used for distributed energy generation as well as the projected wholesale and retail electricity prices in CA by 2030. Clearly, the LCOE of the NBs is far higher than the wholesale electricity price. However, by avoiding the bulk of the transmission and distribution costs through colocation, the NBs are able to provide electricity at a competitive price (i.e., below the average retail price) in the community-scale facility as well as for the two-NB distributed project – although only with IRA subsidies.

Thus, using NBs to supply the energy for electrolysis is cheaper than buying electricity from the grid for community-scale production, as is also reflected in the lower LCOH2 when using NBs, Figure 62. In addition, Vicker et al. estimate the cost of hydrogen produced using solar in CA to be 6.18 – 6.79 $/kg [4]. Adjusted for IRA subsidies, the LCOH2 with solar is then 3.2 – 3.8 $/kg, which is similar to our cost estimate for community-scale SOEC electrolysis with NBs (3.67 $/kg). However, the costs remain higher than those of traditional nuclear power plants or steam methane reforming (plus carbon capture), whose cost is estimated at 1.50 – 2.50 $/kg in the literature [27], [30], [42], [53]–[55]. The NBs can thus provide hydrogen at a competitive cost compared to other decentralized assets but not compared to large-scale assets.

The economics of distributed production are worse, though, due to the lack of scaling of the NB O&M costs with the NB power resulting in a higher cost compared to using grid electricity, Figure 63. The NB capital and fuel costs, on the other hand, remain insensitive to the scale at which power is produced – which is a direct result from using normalized capital and fuel costs in the model.

A higher production capacity helps to reduce the large share of the fixed cost significantly: the addition of a second NB results in a similar LCOH2 compared to using grid electricity for PEM and a lower LCOH2 for SOEC, Figure 63. Such a capacity would be too high for a single station, but is conceivable for coupled stations or by coproducing hydrogen/electricity for other means. As discussed in Section 4.7, however, the benefit of adding more NBs plateaus rather quickly and at high capacity it is likely that larger-scale

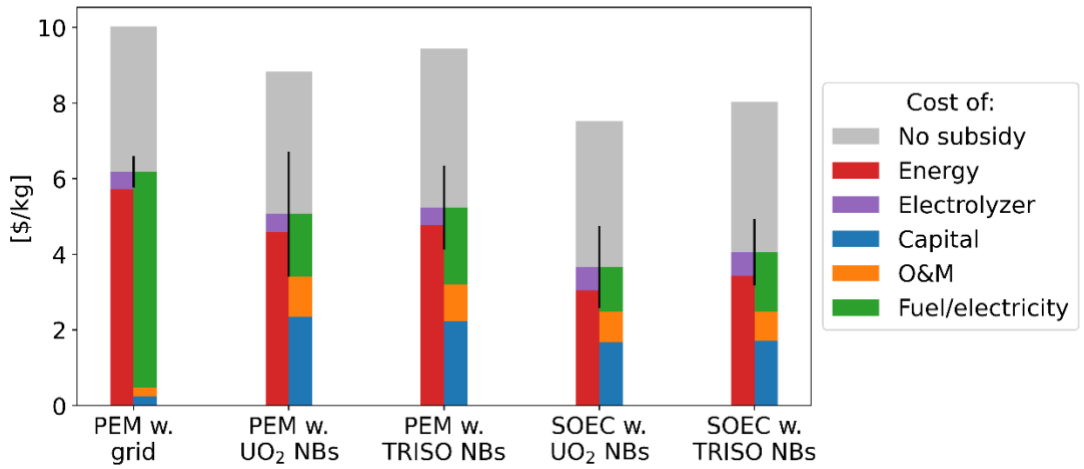

Figure 62 Comparison of the lowest LCOH2 estimates for community-scale production with different technologies, the LCOH2 is broken up in two columns for each case to show share of the levelized cost of the electrolyzers versus energy and to show the distribution between the levelized costs of capital, O&M, and fuel

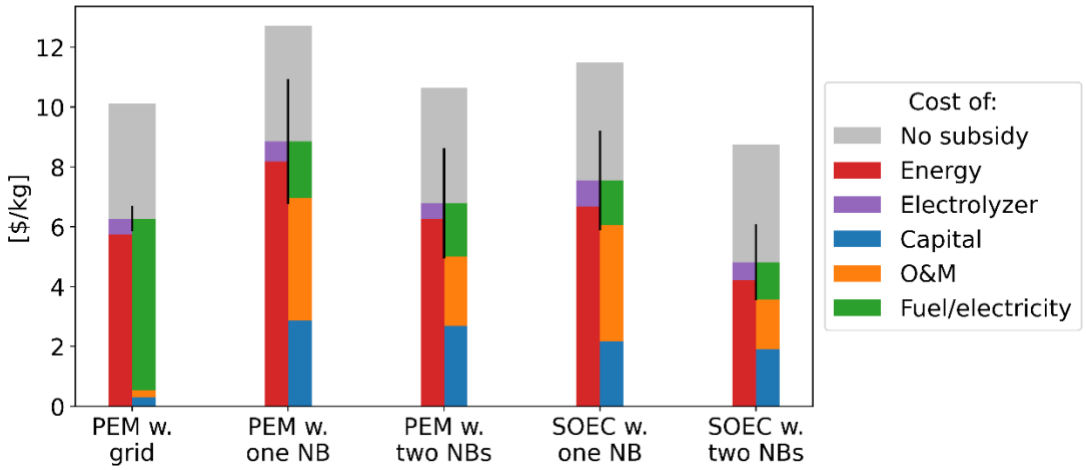

Figure 63 Comparison of the lowest LCOH2 estimates for distributed production with different technologies, the LCOH2 is broken up in two columns for each case to show share of the levelized cost of the electrolyzers versus energy and to show the distribution between the levelized costs of capital, O&M, and fuel

technologies will be more cost effective due to economies of scale. So, the optimal number of NBs is expected to be only a handful.

Still, our results for distributed production paint a more pessimistic picture for NBs than the work of Pham et al. [9], who find that small modular reactors and NBs can result in substantial cost savings over using grid electricity with centralized energy production. A first reason for the discrepancy is the optimistic assumed cost of their decentralized nuclear assets, which is around 2600 $/kWe. At capital costs that are more representative for NBs (i.e., 5200 $/kWe), they no longer see such widespread use of decentralized nuclear power. Also, the availability of such cheap nuclear power is not taken into account in their competing scenario – i.e., using grid electricity. Both of these assumptions make the use of NBs more attractive. On the other hand, in our study, the advantage of being able to use NBs in areas with a congested grid or in remote locations is not utilized, which makes the use of NBs look worse.

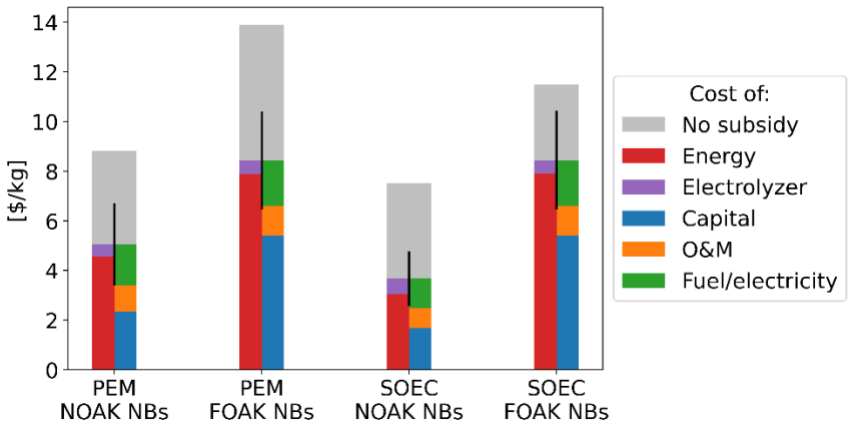

Figure 64 Comparison of the lowest LCOH2 estimates for community-scale production with NOAK and FOAK NBs, the LCOH2 is broken up in two columns for each case to show share of the levelized cost of the electrolyzers versus energy and to show the distribution between the levelized costs of capital, O&M, and fuel

Much like the benefit of colocation resulted in a competitive electricity cost compared to the retail price, it must be investigated whether the on-site hydrogen production with NBs results in more attractive at-the-pump hydrogen costs – especially in light of the immense hydrogen transport and dispensing costs (14.4 – 15.6 $/kg in 2017 [1]). The large spread in hydrogen transport and storage cost estimates – e.g., 2.4 – 12.5 $/kg depending on market volume and technology [55] – shows that these costs should be estimated on a case-by-case basis. To this end, we develop a hydrogen storage and transport cost model in Section 5.

Participation of the NBs in the electricity market was partly examined and does not seem worthwhile based on our rudimentary analysis. Due to the relatively high marginal cost of electricity for the NBs, it will often be more economical to buy electricity from the grid leading to less frequent NB operation, which drives up the levelized costs. It is expected – but not calculated – that the revenue from the capacity payments or electricity sales will be insufficient to counteract the lowered capacity factor of the NBs due to buying electricity at low prices.

However, one has to keep in mind that there are other potential revenue streams resulting from grid participation that were not examined – e.g., black start payments or participating in the reserve market. In addition, the optimization of hydrogen production versus electricity selling was basic and did not include an analysis of buying electricity. More detailed analyses with appropriate cost allocation might find different conclusions. So, one cannot yet decisively rule out the benefit of grid participation based on our analysis.

The high levelized O&M costs in distributed production are mainly driven by the cost of on-site armed guards and as a result, the on-site guard requirement determines the extent to which the facility size affects the LCOE/LCOH2, as shown in Section 4.7. For now, it remains uncertain how many guards the regulator will demand – if any. What is clear, though, is that this regulation will greatly impact the economics of distributed production using NBs. For example, both the number of personnel present and their compensation has been estimated higher in this study than in the economic analysis of the INL [39], which result in a twice-as-large levelized O&M cost. Note other site-specific costs – e.g., a part of the licensing cost – will have similar effects.

Another way in which policy will significantly impact the economics of using NBs, is in the IRA subsidies – or similar low-carbon technology stimulation bills. The IRA subsidies can lower the LCOH2 by roughly 30 – 50% (Figure 62 and Figure 63), with the clean hydrogen PTC being most influential. The emissions accounting for these PTCs will thus have a large impact on the competitiveness of the NBs with other technologies. In particular the competitiveness with solar and wind, who get a clear advantage in the default emissions accounting of the GREET model. One of the many grey areas in this sense is the emissions accounting of grid electricity, and by extension, the eligibility of electrolysis using grid electricity for hydrogen PTCs. In case such projects are not eligible, the distributed hydrogen production using NBs is the lower cost option, Figure 63.

Most NB designs under commercial development use TRISO fuels, which offer advantages like enhanced safety and higher burnup – which reduces fuel consumption. On the flipside, the fuel is more expensive and increases the LCOE by 14 $/MWh. The increase in LCOE is partially offset by the ability to claim the full hydrogen PTC in all cases, as the higher burnup and lower fuel need results in less overall lifecycle emissions. TRISO fuel makes the project's cost more sensitive to fabrication costs (needing a significant reduction for cost parity with UO_2) but less sensitive to enrichment and uranium costs, enhancing resilience against uranium price fluctuations. The 0.2 – 0.6 $/kg cost increase when using TRISO fuels is small enough to leave all conclusions so far unchanged, as can be seen in Figure 62.

While using some of the high-temperature heat of the NBs in SOEC electrolysis offers cost savings, it's partly offset by the higher electrolyzer cost. A more attractive option is using NBs solely for high-temperature heat in processes like SMR – or in a hydrogen, electricity, and heat polygeneration system as envisioned by Genovese et al. [56]. However, with McKinsey's projection of natural gas prices remaining below $2.8 per MMBTU ($9.56/MWh) until 2030 [57], the NBs with an LCOH of around $45/MWh may struggle to compete. Yet, it is crucial to remember that much of the value in NBs comes from emission reduction, price stability, and standalone operation in remote areas.

Finally, due their higher capital cost, hydrogen produced with FOAK NBs has a far higher cost, Figure 64. In community-scale facilities using the better-suited SOEC electrolysis, the LCOH2 with NBs can become comparable to the grid electricity benchmark. Still, it remains likely that NBs will see their first application in situations with less economic pressure than hydrogen production, e.g., powering military bases or mining sites. However, these results show the crucial importance of the economics of multiples in determining the competitiveness of NBs.

Figure 62 Figure 64 show the lowest cost outcomes of Monte Carlo simulations of many different scenarios. The standard deviation is given alongside the averages to give an idea of the spread of the cost distributions that result from the Monte Carlo simulations. However, these standard deviations are misleading when estimating the LCOH2 differences. Simply comparing distributed PEM electrolysis with one and two NBs in Figure 63 gives the impression that the difference between both is not at all statistically significant. Importantly, such a comparison wrongly assumes that both distributions are independent. Both cost models share the exact same cost structure and parameter input – they only differ in facility size. Thus, when sampling parameters in the Monte Carlo simulation, the same value should be used in both models, and only then should LCOH2 differences be determined. Such LCOH2 differences resulting from Monte Carlo simulations with consistent sampling of shared parameters are shown in Figure 65 Figure 66.

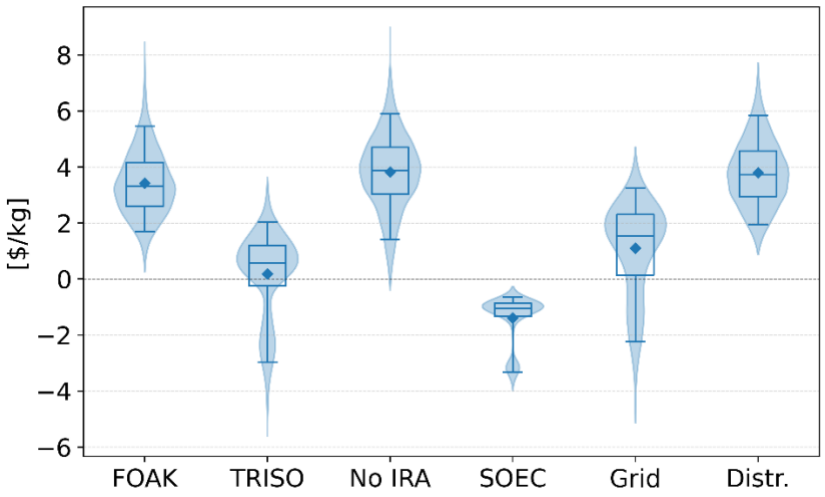

Figure 65 Boxplots of the LCOH2 difference distributions resulting from coupled Monte Carlo simulations. For each boxplot, one assumption is changed compared to the reference, which is a community-scale PEM facility using UO_2-fueled NOAK NBs and claiming mixed subsidies

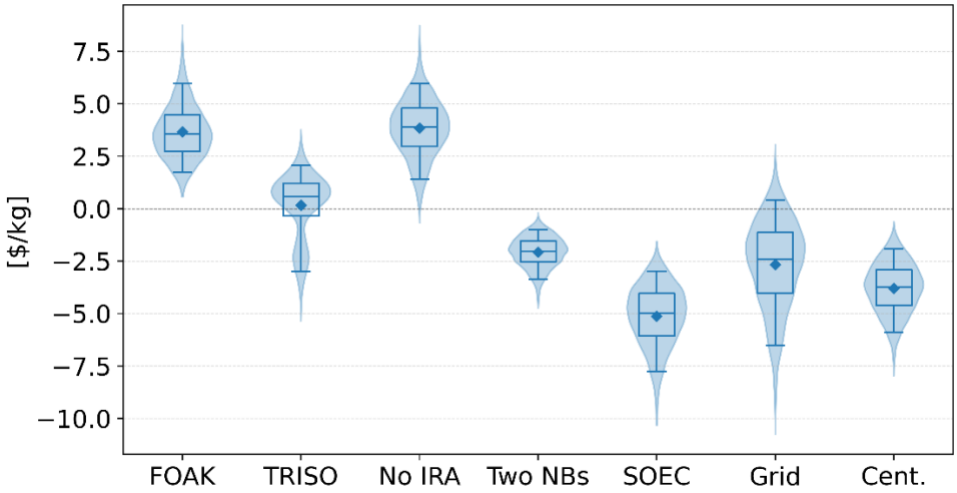

Figure 66 Boxplots of the LCOH2 difference distributions resulting from coupled Monte Carlo simulations. For each boxplot, one assumption is changed compared to the reference, which is on-site production using PEM electrolyzers with a single UO_2-fueled NOAK NB and claiming mixed subsidies

In addition to supporting all previous conclusions, Figure 65 Figure 66 give valuable insight into the spread of LCOH2 differences and the associated confidence. For example, TRISO fuels generally increase the LCOH2 by up to 2 $/kg. However, they can also lead to cost savings of about 2 $/kg compared to those cases where the UO_2-fueled NBs cannot claim the full clean hydrogen PTCs, hence the long downward tail of the LCOH2 difference distribution. Similarly, the downward tails in the LCOH2 differences when switching to SOEC or grid electricity stem from cases where the clean hydrogen PTCs cannot be claimed in full with UO_2-fueled NBs.

5. Partial hydrogen storage, distribution, and dispensing costs

As already mentioned a few times throughout the report, the hydrogen infrastructure adds an enormous cost that overshadows the production cost – e.g., transport and dispensing cost about 14.4 – 15.6 $/kg in 2017 [1]. So, comparing the costs of hydrogen production in the centralized and distributed fashion in Section 4 is not sufficient, the hydrogen supply costs should be considered also, which is the aim of this section. However, our goal is not to estimate the hydrogen supply cost for centralized and distributed production, but the hydrogen supply cost *difference* between both cases.

Section 5.1 gives a brief introduction about the hydrogen supply chain in the context of vehicle refueling and details what aspects are (not) included in the scope of the model. Section 5.2 describes the cost model structure and discusses the analysis method. Next, the rudimentary hydrogen delivery and storage model developed for the sizing of tanks is discussed in Section 5.3. The specific model input and results for distributed and centralized production are discussed in Sections 5.4 and 5.5, respectively. Finally, Section 5.6 gives a comparison between the total hydrogen cost for both cases.

5.1. Modeling scope

The hydrogen refueling infrastructure has many different steps with naming similar to those used for grid infrastructure, Figure 67. Much like electricity, hydrogen can be produced in a centralized or distributed fashion. The large-scale centralized production hubs are generally far away from demand centers and there is thus need for transport of large quantities of hydrogen over long distances. This step is referred to as transmission and is generally done via pipelines after passing through a packaging (compression) hub.

After transmission, the hydrogen arrives in a distribution terminal that is closer to the demand cluster (e.g., a city), where is it temporarily stored before being sent into the distribution grid. Whereas the transmission is always done via pipelines, distribution can occur through a smaller pipeline network or with trucks carrying trailers of high-pressure gaseous hydrogen or liquefied hydrogen. In addition, the storage in the distribution terminal can also be gaseous – in geological formations or pressure vessels – or liquefied in cryogenic tanks.

In our work, only gaseous delivery is considered because DOE's Hydrogen Strategy mentions it as the most economical for short distances [13] and we assume that the community-scale/centralized plant is close to the demand. However, Reddi et al. [2] find that gaseous delivery is not economical at station capacities above 500 kg/d [2]. Gaseous delivery may thus not be the most economical mode of distribution, which could make centralized production look unfairly worse.

Note that our use of 'centralized' or 'community-scale' production in this report corresponds to the 'semi-centralized' production in Figure 67 and would thus feed in at the distribution terminal. As a result, there are no transmission costs that need to be taken into account in our model.

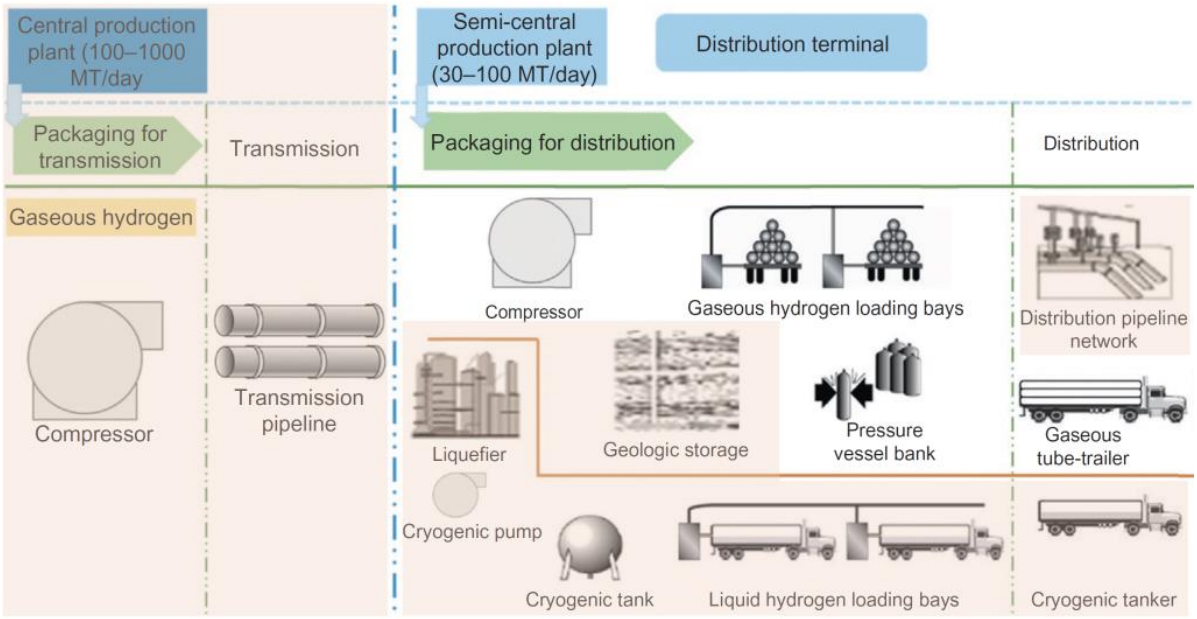

Figure 67 Components of the hydrogen supply chain. Figure adapted from Ref. [2] to show the scope in this work

There is a final step in the hydrogen refueling supply chain, namely the dispensing in the refueling stations. Figure 68 shows the layout of a gaseous 700 bar refueling station. Gaseous hydrogen is either produced on-site or delivered to the station by trucks – again, no liquefied hydrogen or pipeline delivery is considered. When a full trailer gets delivered, the empty trailer is taken back. As a result, the trailer itself acts as a storage tank for the station.

Next, the hydrogen pressurized to 950 bar in one step, or it is pressurized to 500 bar, after which it is compressed to 900 bar by a booster compressor. For simplicity, only the direct compression is considered in this work. After compression, the hydrogen must be precooled to -40 °C to avoid excessively high temperatures while filling the car's tank. This is done in a heat exchanger with an associated chiller unit. Finally, a dispenser unit regulates the flow when filling by applying a varying amount of back pressure.

A fair comparison between the attractiveness of the centralized versus distributed production must be based on the cost of hydrogen delivered to the car, i.e., after taking all supply chain costs into account. However, creating a cost model of the complete hydrogen delivery infrastructure is outside the scope of this work. So instead, our focus is on the components that change the most between on-site and centralized production in an effort to estimate the cost difference, rather than trying to estimate the cost itself accurately. For example, the chilling equipment and dispensers are not implemented in the model, as they are not changed between on-site or centralized production. Along the same reasoning, cost items such as site work, licensing, safety equipment, etc. are not taken into account.

In 2017, the cost of hydrogen production was between 2 – 3 2017$/kg [58] and the cost of hydrogen delivered to the refueling stations was 6 – 8 2017$/kg [58]. Thus, the cost saving potential for avoiding transmission and distribution through on-site production is in the range of 3 – 6 2017$/kg, or 3.5 – 7.1 $/kg adjusted for inflation – assuming that any modifications to the refueling station under on-site production do not affect the delivery cost significantly. The LCOH2 difference between centralized and distributed production, on the other hand, is about 3.8 $/kg for PEM, which lies within the range of

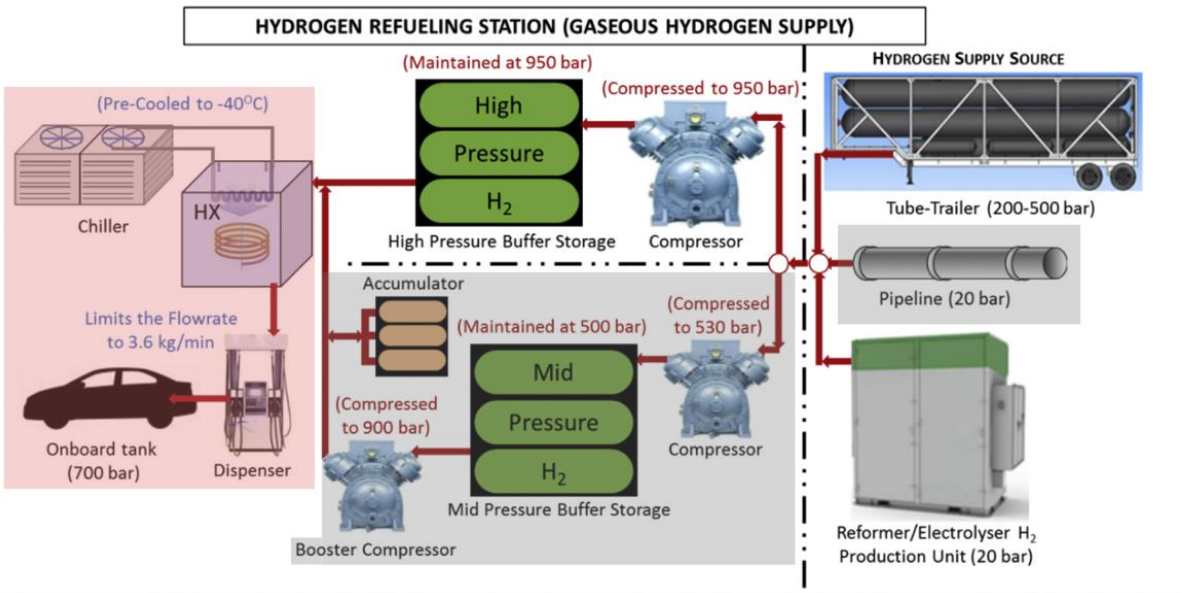

Figure 68 Components of a gaseous hydrogen refueling station. Figure adapted from Ref. [58] to show the scope in this work where greyed out items are not relevant to the type of refueling station and supply chain considered in this work and the red rectangles show which items are neglected in the cost difference modeling

possible cost savings. Although the 3.8 $/kg difference lies on the lower end of the cost saving range, it is important to acknowledge that the literature range contains transmission costs. So, it is not immediately clear whether distributed or centralized production is more economical.

To make matters worse, hydrogen storage and transport estimates vary greatly in the literature – e.g., 2.4 – 12.5 $/kg depending on market volume and technology [55] – with sometimes conflicting conclusions and about the cost drivers. For example, Monforti et al. [59] find centralized production to be most economical at low station capacities, whereas Brey et al. [60] mention that centralized production is the norm for high station capacities. Thus, a simple, but case-specific, cost model for hydrogen storage and delivery is developed in this work.

5.2. Cost modeling methodology

In this section, the cost models for the non-production costs associated with the cases of Table 3 are discussed. However, as mentioned in Section 5.1, the goal is not to model the cost of hydrogen distribution and dispensing, rather it is to estimate the cost difference between the distribution and dispensing costs for community-scale and on-site production. As a result, many cost items are not included in the model. To remind the reader, this section will refer to the calculated costs as *partial* levelized costs of hydrogen (pLCOH2).

Much like in Section 4.1, the pLCOH2 is split in different components, namely the levelized cost of storage, compression, and trucking:

$$pLCOH2 = pLCOH2_{Stor.} + pLCOH2_{Comp.} + pLCOH2_{Truck.} \quad (16)$$

Each of these components is further subdivided into capital, O&M, and fuel/energy components:

$$pLCOH2_X = pLCOH2_{X,cap} + pLCOH2_{X,O\&M} + pLCOH2_{X,fuel} \quad (17)$$

Initial capital costs (ICC) are again annualized using a capital recovery factor that is calculated based on the discount rate (r) and asset lifetime (t). However, no decommissioning costs (or revenues) are taken into account in the distribution cost model, so no sinking fund factors are needed. In addition, the stations and production plants are assumed to run full-time in the model. The levelized capital costs thus simply follow from multiplication of the capital cost with the capital recovery factor divided by the hydrogen capacity (c).

$$pLCOH2_{X,cap} = \frac{\sum_i ICC_i \cdot CRF}{c} \quad (18)$$

As a result of the 100% capacity factors of the stations, there is no distinction between fixed and variable O&M costs, so the $pLCOH2_{X,O\&M}$ is just the division of the yearly O&M costs by the hydrogen dispensing capacity. Furthermore, there is no up front payment for the fuel costs, nor any fuel disposal costs as there were in the case of nuclear fuel in Section 4.1. So, the $pLCOH2_{X,fuel}$ also follows from simply dividing the annual fuel costs by the hydrogen throughput.

Besides the breakdown of the pLCOH2 into the components related to the type of technology – storage, compression, trucking – the pLCOH2 is also split into the levelized cost of packaging (at the distribution terminal), distribution, and dispensing. Of course, there will be only dispensing costs for on-site production and the trucking and distribution costs are equal in our model, as only trucking is considered for distribution.

Again, Monte Carlo simulations are performed to account for the uncertainty in the cost estimates simultaneously. Yet in this section, the simulations use 5 000 samples because of the increased model complexity and run times – in contrast to the Monte Carlo simulations of Section 4 that used 50 000 samples. The results are reported in the same manner, though, as $\mu \pm \sigma\ [m, M]$ where μ is the average of the distribution, σ the standard deviation, m the minimum, and M the maximum. In addition, sensitivity analyses are performed where all parameters but one are fixed, with the remaining parameter being varied by ± 30% of their original value.

Again, cost estimates from external sources were adjusted for inflation using the US Bureau of Economic Analysis implicit price deflators for gross domestic product [15]. Thus, all costs reported here are given in Q2 2022 USD.

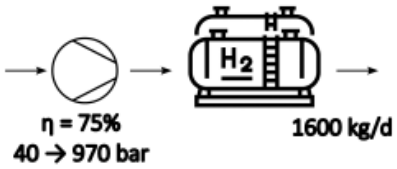

Figure 69 Schematic representation of the distributed production model

5.3. Modeling the storage and transport of hydrogen

As discussed in Section 5.1, our scope is limited to gaseous hydrogen transport and storage with a single compression step in the refueling station. And even in this limited scope, not all components of the hydrogen infrastructure are modeled. In fact, only the compressors, trucks, and main storage tanks are accounted for in the model because the compressor and tank costs make up the majority of the levelized cost of refueling anyways [61]. Figure 69 shows the components considered in the distributed model. A medium-pressure tank could be used as a buffer to lower the need for high-pressure storage – with the added cost of needing another compressor [2]. For simplicity, this configuration is not considered.

The storage requirements for a refueling station with on-site production will be different to those for a station that gets hydrogen delivered to it. So, a Gurobi [62] model of the storage and delivery is made for both scenarios to estimate the difference in storage needs. This model solves for the mass in all tanks for each hour and aims to find the minimal tank capacity that still allows the station to meet demand with a 10% margin. In order to do so in a physical manner, constraints must be specified, which will be outlined below.

Starting with the simple on-site model, there is no leakage accounted for in the model, so it is clear that mass must be conserved in the tank:

$$M_{i+1} = M_i + \Delta t \cdot (P - D_i) \tag{19}$$

Where M_i is the mass at hour i, D_i is the hydrogen demand in hour i, and P is the hydrogen production rate – which is assumed to be constant. Note that Δt is fixed at one hour in both models, but written for completeness. Of course, the stored mass cannot exceed the tank capacity at any time:

$$M_i \leq C \tag{20}$$

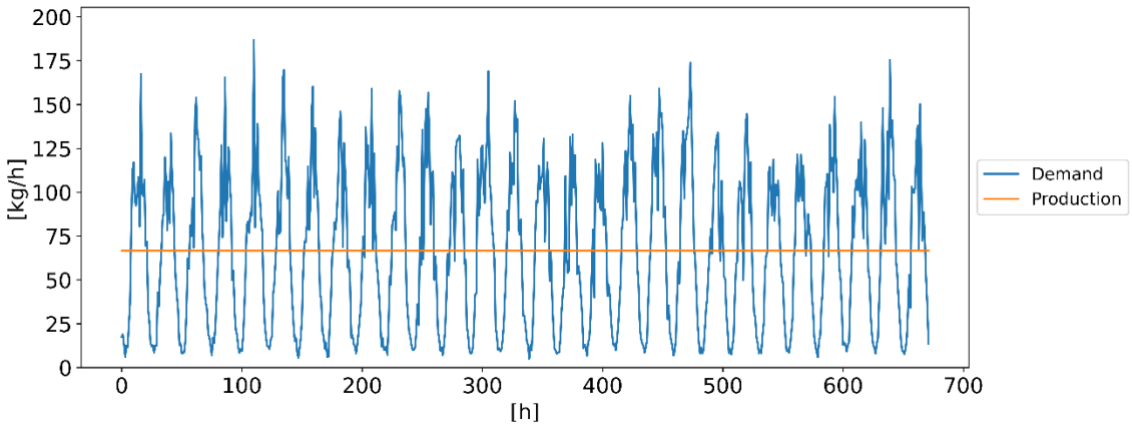

Figure 70 Demand profile used in the sensitivity analyses of the transport and storage model with distributed production

There is also a lower limit on the tank mass as the pressure in the tank cannot get arbitrarily low. The lower limit follows from the tank capacity through the ratio of the minimum and maximum allowed pressure:

$$M_i \geq C \cdot \left(\frac{P_{min}}{P_{max}}\right) \tag{21}$$

Finally, the model allows to specify a buffer margin B separate from the 10% margin mentioned before, such that the B percent of the minimal needed capacity is kept full at all times:

$$M_i \geq C \cdot f_{min} \text{ where } f_{min} = \frac{1}{1+\frac{100}{B}} \tag{22}$$

For a given demand (and production) profile, the above constraints allow to find the time evolution of the mass stored in the tanks and by extension, allow to find the tank capacities. The demand profiles are made using hour-to-hour and day-to-day demand data for gasoline stations reported in the work of Mintz et al. [63].

Samuelsen et al. [64] show that the demand profiles can substantially affect the LCOH2. So, the profiles are varied in the Monte Carlo analyses by adding random noise to the Mintz et al. base profiles and the average daily demand is varied between each sample. For the sensitivity analyses, on the other hand, the added noise is kept constant and only the average daily demand is varied. Figure 70 shows a demand profile used for the on-site model.

For simplicity, the production profile is constant and equal to the average demand over the entire model horizon to avoid drift in the tank levels over time due to over-/underproduction. Furthermore, seasonal variation in hydrogen demand and plant outages are not taken into account.

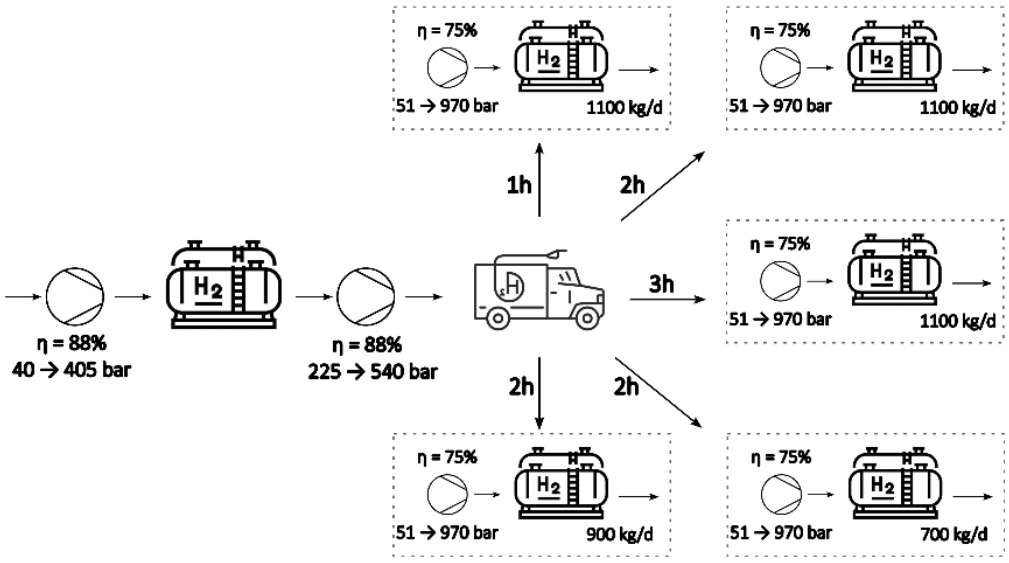

Figure 71 The model components in centralized production where a quarter of the production plant that supplies five separate stations is modeled

Moving on to the model for centralized production with trucking delivery, the model becomes more complex, Figure 71. The centralized plant in the models of Section 4 has a capacity of 25 000 kg/d, which can serve many stations. So, instead of modeling the delivery of the entire output, only five stations are considered, which have a cumulative demand of 4900 kg/d – about a fifth of the facility output. More specifically, there are three stations with a 1100 kg/d capacity, one with a 900 kg/d capacity, and one with a 700 kg/d capacity. The capacities are chosen to correspond to the gaseous hydrogen trailer capacities used in the HDSAM model [65]. As a result, each station needs one truck delivery per day. In the Monte Carlo, simulations, the station capacity can be lowered, in which case there is still one truck delivery per day but with a partially filled trailer. This is done to reduce the model complexity.

So, there are five refueling stations (indexed 1 to 5) as well as the production plant (index 0). These have different constraints because the plant has constant hydrogen production and sees demand in the form of trucks being filled, whereas the stations are subjected a varying demand profile with hydrogen brought in at specific delivery times. For the central plant, the conservation of mass constraint for the tank looks as follows:

$$M_{0,i+1} = M_{0,i} + \Delta t \cdot \left(P \; - \sum\nolimits_j x_{p\;j,i} \frac{TC_j}{\Delta t_f} \right) \tag{23}$$

Again, $M_{0,i}$ denotes the mass at hour i, P is the constant production rate, and Δt is constant at one hour. The demand term comes from the filling of truck with capacity TC_j over a fixed filling time Δt_f of three hours. However, a truck j can, of course, only be filled if it is at the plant. This is denoted by the binary value $x_{p\;j,i}$, which is one if truck j is at the plant in hour i and is zero otherwise.

Besides the conservation of mass, the system has to abide by the constraints set by the maximum and minimum levels, as well as the buffer margin (if specified):

$$M_{0,i} \leq C_0 \tag{24}$$

$$M_{0,i} \geq C_0 \cdot \left(\frac{P_{min,p}}{P_{max,p}}\right) \tag{25}$$

$$M_{0,i} \geq C_0 \cdot f_{min} \text{ where } f_{min} = \frac{1}{1+\frac{100}{B}} \tag{26}$$

The conservation of mass looks different for the storage tanks of the refueling stations:

$$M_{j,i+1} = M_{j,i} + \Delta t \cdot \left(\delta(i - t_{del}) \cdot TC_j \ - D_{j,i}\right) \tag{27}$$

Where Δt, and TC_j have the same meaning as before and $D_{i,j}$ is the hydrogen demand at station j in hour i. However, $M_{j,i}$ does not represent the hydrogen mass in the storage tanks, but the mass in the tanks *and* trailer. This is done such that mass flows between the trailer and high-pressure storage tanks do not need to be modeled. The $\delta(i - t_{del})$ function is one at the times of delivery and is zero otherwise. Thus, the product $\delta(i - t_{del}) \cdot TC_j$ represents the influx of mass when a full trailer arrives.

As a result of combining the hydrogen stored in the high-pressure tanks and in the trailer, the maximum capacity constraint on $M_{j,i}$ is now time dependent:

$$M_{j,i} \ \leq C_j + x_{s\ j,i} \cdot TC_j \tag{28}$$

$x_{s\ j,i}$ is a binary value that represents when a trailer is available in the station. Once more, there is a lower withdrawal limit set by the minimum allowable pressure in the tanks and the user can specify a buffer margin:

$$M_{j,i} \geq C_j \cdot \left(\frac{P_{min,t}}{P_{max,s}}\right) \tag{29}$$

$$M_{j,i} \geq C_j \cdot f_{min} \text{ where } f_{min} = \frac{1}{1+\frac{100}{B}} \tag{30}$$

Note that the pressure limits for the high-pressure tanks of the refueling station are different to those of the distribution terminal because storage in the terminal is at lower pressure.

The demand profiles $D_{j,i}$ (Figure 72) are generated in the same way as for the on-site model – i.e., by adding random noise to the average profiles reported by Mintz et al. [63] – and they are varied in the same way during Monte Carlo simulations and sensitivity analyses. Furthermore, the production is again assumed to be constant and equal to total consumption to avoid drift in the hydrogen mass over time.

Optimizing the trucking network is a complex challenge that is outside the scope of this work. However, an inefficient trucking schedule – e.g., all trucks being filled simultaneously at the plant – will inflate distribution costs. So, the filling and delivery schedules of the trucks are cherry-picked as an approximation of schedule optimization. More specifically, the filling of the trucks is spread evenly throughout the day, Figure 73, which reduces the storage requirements at the centralized plant considerably.

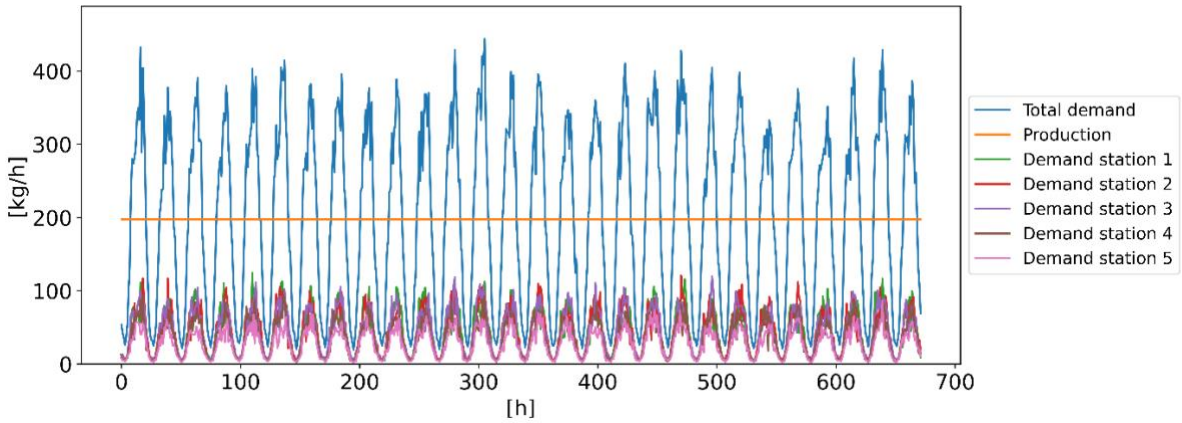

Figure 72 Demand profiles used in the sensitivity analyses of the transport and storage model with centralized production

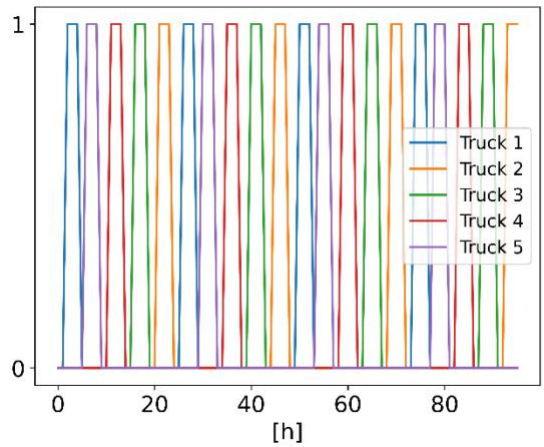

Figure 73 The evolution of the binary values $x_{p\ j,i}$ as a function of time over four days, a value of one indicates the truck is at the production plant

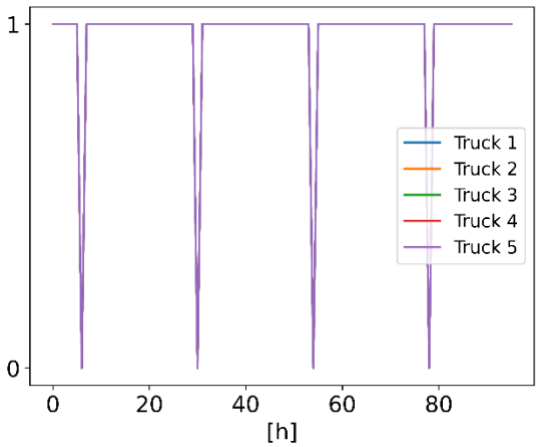

Figure 74 The evolution of the binary values $x_{s\ j,i}$ as a function of time over four days, a value of zero indicates that the old trailer is being replaced with a new one and is hence unavailable

In addition, for each refueling station, the delivery times are fixed at 6 AM – just before the morning demand peak – to lower the storage requirements on the station side. Furthermore, the model assumes that decoupling an old trailer and installing a new one takes one hour. So, after delivery, $x_{s\ j,i}$ dips to zero for one hour in all stations, Figure 74.

As a final simplification, the driving times to each refueling station are constant for each station and shown (in units of hours) in Figure 71. Note that the driving times are rather short because the community-scale facility is assumed to be close to demand centers.

5.4. Distributed production

The cost assumptions and results of the storage and dispensing cost model for on-site production are discussed in this section. Table 12 lists the ranges used in Monte Carlo simulations and much like in the tables of Section 4, the parameter is fixed when only the mode is given, it has a uniform distribution when the minimum and maximum are given, and it has a triangular distribution if the minimum, mode, and maximum are given.

Table 12 Model assumptions for on-site hydrogen production using NBs

Parameter	Unit	Min	Mode	Max	Source
Discount rate	%	2	6	12	
Avg. daily demand	kg/d	1440	1600	1760	[3]
High-pressure tank	$/kg	2335	2919	3502	[65]
Tank O&M	$\%_{CAPEX}$	0.8	1	1.2	[65], [66]
Tank lifetime	y	12	15	18	[65]
LCOE	$/MWh	126	192	277	
P_{min}	bar		40		[24]
P_{max}	bar		969		[65]
Compressor O&M	$\%_{CAPEX}$	3.2	4	4.8	[65]
Compressor lifetime	y	12	15	18	[65]

To be consistent with the work of Section 4, the same discount rate distribution is used and the average daily demand matches the output of the distributed production units – i.e., 1600 kg/d. Although, in contrast to Section 4, the daily output is varied in the Monte Carlo simulations too – rather than in the sensitivity analyses only. The difference between the highest and lowest average daily station demands reported by Mintz et al. [63] is 15.6%. Because the daily demand in our model represents a monthly average, we expect it to be less volatile. Hence, only a 10% variation from the mode is used. Note that while the discount rate and capacity are consistent with the distributed production projects of Section 4, the component lifetimes in this section do not match the lifetime of those projects.

Our model is heavily based on the cost assumptions used in the HDSAM model [65], with about half of the parameters having their mode based on the HDSAM assumptions with a 20% deviation for the width of the distribution: the tank capital cost, tank O&M fractions, compressor lifetime and compressor O&M fraction. In addition, the compressor capital cost is calculated using the HDSAM correlation for 700 bar refueling station compressors:

$$CAPEX\ [2013\$] = 1.3 \cdot 40035 \cdot (n_{working} + n_{backup}) \cdot MR^{0.6038} \quad (31)$$

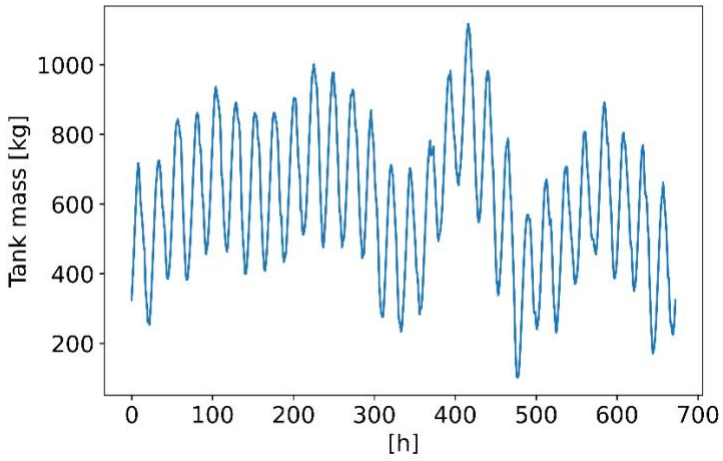

Figure 75 The mass of hydrogen stored in the station's tank as a function of time throughout the month when the station is subjected to the reference profile of used in sensitivity analyses

Where MR is the rating of the compressor motor. The calculation of MR assumes an isentropic efficiency of 75%, a motor efficiency of 94%, and motor safety factor of 1.1. The factor 1.3 is an installation factor and the number of working and backup compressors are two and one, respectively. Again, all these assumptions are in line with the HDSAM model [65].

Furthermore, the LCOE distribution is derived from Monte Carlo simulations of the LCOE for a single UO_2-fueled NB claiming an ITC. And finally, minimum pressure – which is the electrolyzer operating pressure – is taken in the midrange of operating pressures of commercial electrolyzers listed by Buttler et al. [24], and the maximum pressure follows from the tank pressure limits used in the HDSAM model [65].

Figure 75 shows the mass in the refueling station tank for the base demand profile that is used in the sensitivity analyses (Figure 70). Of course, there are clear daily swings in the tank levels, but there are also significant drifts occurring over multiple days as a result of sustained high/low demand. Note that the y-axis does not start at 0 kg because the tank is never drawn down that far, which is a direct result of specifying a buffer margin (see Section 5.3). A 10% margin is used because the model also assumes up to 10% variation in daily demand averaged over the entire month.

Monte Carlo simulations result in an average tank capacity of 1181 ± 147 [814, 1911] kg. The tank capacity associated with Figure 75, however, is 1229 kg, which is on the higher end due to the period of low demand, as this increases the tank levels under constant production. In reality, the production could be ramped down in periods of low demand, which would allow to lower the tank size. Of course, the decrease in tank sizing has to be balanced against lowered production. Another simplification that will inflate our tank costs, is that the model only uses high-pressure tanks.

Figure 76 shows the cost breakdown of the pLCOH2 over the different components. Overall, the pLCOH2 is low at 1.63 ± 0.18 [1.10, 2.37] $/kg, with the capital costs making up the lion share (66%), followed by the energy cost of the compressors (20%). Note that the spread in pLCOH2 values is about 1.5 $/kg which is much lower than the uncertainties related to the production costs of Sections 4.3 to 4.5. The breakdown between packaging, distribution, and dispensing is trivial in this case, as there are only dispensing costs.

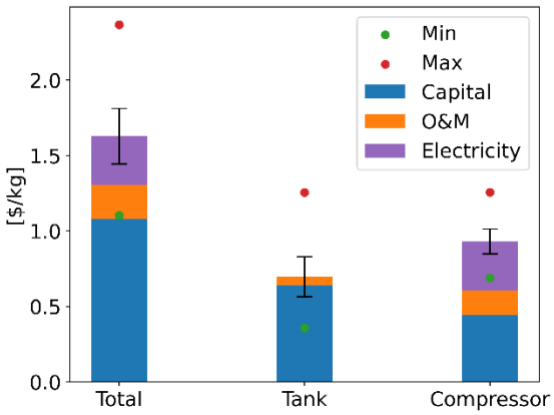

Figure 76 Component-wise pLCOH2 breakdown for distributed production resulting from a MC simulation with 5000 samples

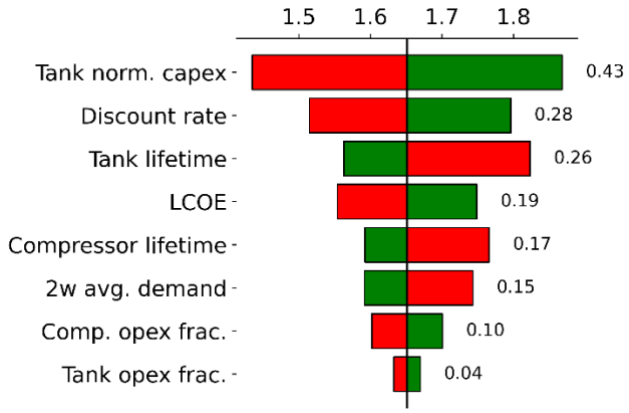

Figure 77 Tornado chart for the pLCOH2 (in $/kg) of a station with on-site hydrogen production

Additionally, the compressors are the more expensive component, although the pLCOH2 is split relatively evenly between the tank and compressor. As mentioned before, there are reasons that point to an overestimation of the tank costs, so it is expected that the compressor costs will dominate over the tank cost, as it does in a study by Reddi et al. [58] and in calculations for gaseous delivery networks performed with the HDSAM model. However, comparing the cost breakdown to literature is rather complicated as this scenario is tailor-made to our needs. Instead, the results of the more traditional model of centralized production will be compared to other studies in Section 5.5.

Four out of the five most influential parameters are related to the capital costs, Figure 77, which is unsurprising given the 66% share of the capital costs. Note that the compressor capital cost does not show up in the sensitivity analysis because the cost correlation of Equation (31) is kept constant in the model. Hence, the tank parameters show up as the most influential, even though the tank costs make up a smaller share of the pLCOH2 than the compressor cost. However, the high energy intensity of the compression – accounting for 20% of the pLCOH2 – leads to a sizable impact of the LCOE.

Surprisingly, the station capacity – i.e., the daily demand – does not have a large influence on the pLCOH2, in contrast, many studies find that increasing the station capacity significantly decreases the cost of refueling [14], [58], [67]–[69]. Yet, this is a direct result of neglecting many fixed costs that are shared between stations supplied by centralized or on-site production in the calculation of the pLCOH2.

5.5. Centralized production

This section discusses the cost assumptions and results of the storage and dispensing cost model for centralized production. Table 13 lists the ranges used in Monte Carlo simulations, where again, the parameter is fixed when only the mode is given, it has a uniform distribution when the minimum and maximum are given, and it has a triangular distribution if the minimum, mode, and maximum are given.

As mentioned in Section 5.3, the demands are linked to the truck capacities such that there is one delivery per day. As a result, the distributions of the daily demands are capped at this maximum trucking capacity, and the distributions are no longer triangular, instead leaning toward keeping this maximum capacity. There is still potential for lower capacities, with up to a 10% deviation of the mean, in accordance with the demand variation assumptions of Section 5.4. Note that the truck capacity limit is also imposed in the sensitivity analyses.

Table 13 Model assumptions for community-scale hydrogen production with gaseous truck delivery

Parameter	Unit	Min	Mode	Max	Source
Discount rate	%	2	6	12	
Avg. daily demand st. 1	kg/d	990	1100	1100	
Avg. daily demand st. 2	kg/d	990	1100	1100	
Avg. daily demand st. 3	kg/d	990	1100	1100	
Avg. daily demand st. 4	kg/d	810	900	900	
Avg. daily demand st. 5	kg/d	630	700	700	
High-pressure tank	$/kg	2335	2919	3502	[65]
Medium-pressure tank	$/kg	1557	1946	2335	[65]
Tank O&M	$\%_{CAPEX}$	0.8	1	1.2	[65], [66]
Tank lifetime	y	12	15	18	[65]
LCOE plant	$/MWh	83	119	175	
LCOE station	$/MWh	162	184	200	[5]
$P_{min,\ plant}$	bar		40		[24]
$P_{max,\ plant}$	bar		405.3		[65]
$P_{min,\ station}$	bar		50.7		[65]
$P_{max,\ station}$	bar		969		[65]
Compressor O&M	$\%_{CAPEX}$	3.2	4	4.8	[65]

Compressor lifetime	y	12	15	18	[65]
Tractor cost	k$	113	140	169	[65]
Tractor lifetime	y	4	5	6	[65]
250 bar trailer	k$	518	647	777	[65]
350 bar trailer	k$	644	805	966	[65]
540 bar trailer	k$	1117	1396	1675	[65]
Trailer lifetime	y	16	20	24	[65]
Fuel cost	$/l	0.72	0.90	1.08	[65]
Driver rate	$/h	20	25	29	[65]
Truck loading infra-structure	k$	56	70	84	[65]

The cost of the high-pressure tanks used in the refueling stations is equal to that discussed in Section 5.4, as they have the same pressure rating. However, the storage tank in the production plant is assumed to be at a lower pressure and uses the HDSAM cost data for 350 bar cascade storage tanks. The lifetime and fractional O&M cost of both types of tanks are taken to be the same, though.

Compression at the production plant is powered by the NBs and thus, the LCOE distribution at the plant is taken from a Monte Carlo simulation of the LCOE for centralized production with UO_2-fueled NBs claiming an ITC. The stations, on the other hand, will draw power from the grid. So, the LCOE there is based on the cost projections for the Californian electricity rates by Marshall [5].

Again, the operating pressure of the electrolyzers is considered the minimum pressure in the production loop and the maximum pressures are taken from the pressure limits in the HDSAM model. The lower pressure limit of the refueling stations is now set by the minimum pressure in the tube trailers (50 atm [65]).

A different compressor cost function is used for the plant compressors because the plant storage tank is at lower pressure:

$$CAPEX\ [2013\$] = \ 1.3 \cdot 40528 \cdot (n_{working} + n_{backup}) \cdot MR^{0.4603} \tag{32}$$

Where MR is the rating of the compressor motor. Now, the calculation of MR assumes an isentropic efficiency of 88% in contrast to 75% used for the refueling station compressors. All other parameters are the same as for the refueling station compressors, i.e., a motor efficiency of 94%, motor safety factor of 1.1, two working compressors, and one backup. Additionally, there are compressors to fill the trucks at the plant, their costs are calculated with the same assumptions with the exception of the number of compressors, as there are only 4+1 loading compressors for the four loading bays at the plant.

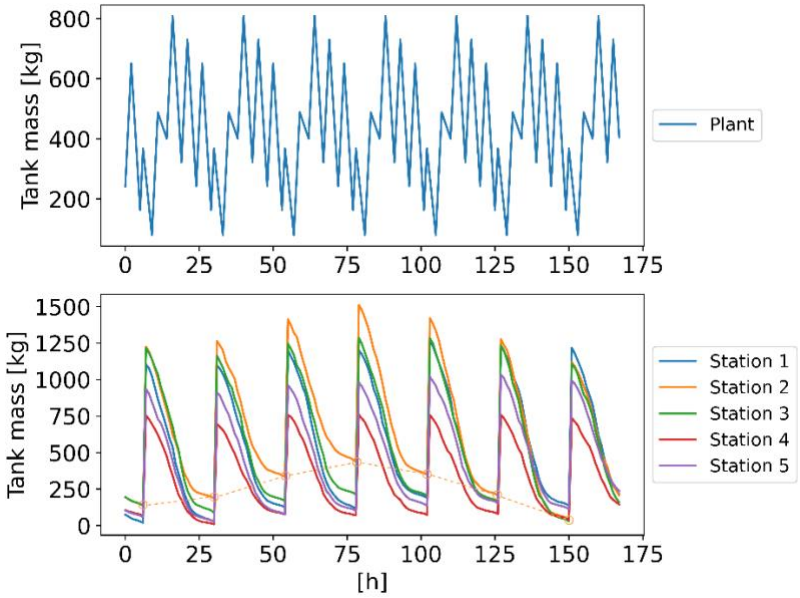

Figure 78 The mass of hydrogen stored in the tanks as a function of time throughout a single week when the station is subjected to the reference profile of used in sensitivity analyses. The dashed line indicates which moments define the station tank capacity

For the trucking cost, the tractor and trailer are treated separately, because they have different lifetimes and the trailer pressure rating determines its cost. Additionally, the pressure rating dictates its capacity with the 250 bar, 350 bar, and 540 bar trailers having a maximum capacity of 700 kg, 900 kg, 1100kg, respectively. As a result of the different pressure levels of the trailers, varying amounts of compressive work will be needed to fill them and possibly even different compressors. However, this is neglected in the model and all loading bays are treated the same. Besides the loading bays, the cost of truck scales and administrative buildings is included in the truck loading infrastructure.

Note that again, many of the parameters have their mode taken from the HDSAM model with a 20% deviation for the minimum and maximum of the distribution.

The hydrogen mass stored at the production plant in the scenario with the demand profiles of Figure 72 is shown in Figure 78. A first thing to note is that there are no irregularities in the level over time, which is a result from the regular truck filling schedule combined with the flat production profile. Additionally, the uniformly spaced-out filling of the trucks lowers the storage requirements significantly, resulting in a relatively low average capacity of 761 ± 30 [646, 859] kg even though the total demand shows day-to-day large variations, Figure 72.

A first thing to note from the refueling station mass levels (Figure 78) is that they show sudden upward peaks. These peaks are a direct result of tracking both the mass in the station tank and trailer, and they occur when a new trailer is brought to the station. The tanks are thus not sized based on the height of the peaks in Figure 78, but based on the lows, as they occur at the time that the trailer is empty or unavailable due to being switched for a new one – these moments are highlighted by the dashed line.

Again, the trailers help relieve some of the storage requirements by acting as mobile tanks, as evidenced by the far lower station tank capacities, e.g., 420 ± 91 [174, 914] kg for the 1100 kg/d station – compared to 1181 kg for the station with on-site production. A high-pressure tank capacity of around 400 kg is similar to the size of high-pressure tanks the HDSAM model for a station with the same

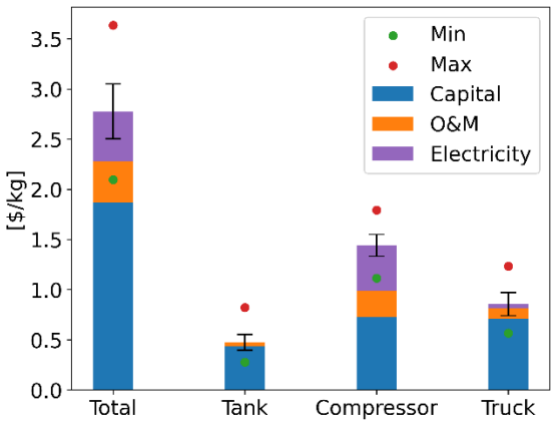

Figure 79 Component-wise pLCOH2 breakdown for centralized production resulting from a MC simulation with 5000 samples

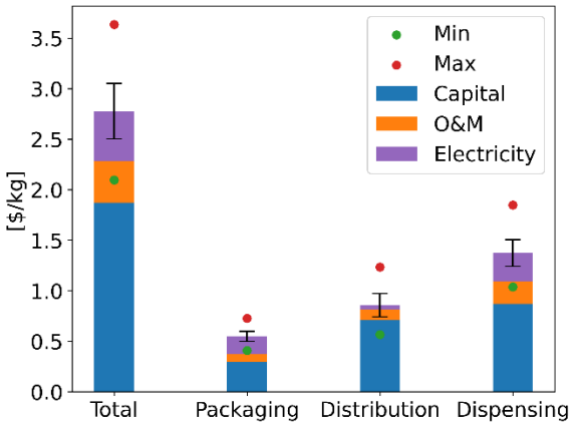

Figure 80 Logistical pLCOH2 breakdown for centralized production resulting from a MC simulation with 5000 samples

capacity. However, the HDSAM model assumes two trailers are present at gaseous stations. Using two trailers in our model negates the need for any high-pressure storage. So, the high-pressure tanks of HDSAM model are likely not sized based on storage capacity considerations as is done in our model.

As expected, the pLCOH2 of storage and delivery is higher than in the case with on-site production at 2.78 ± 0.27 [2.10, 3.64] $/kg versus 1.63 $/kg. The component-wise cost breakdown is shown in Figure 79. Much like was the case for on-site production, the compressor makes up the largest share of the levelized storage and dispensing cost – a result also seen by Reddi et al. [58].

For a gaseous refueling station of similar size (1000 kg/d), Reddi et al. [58] estimate the levelized cost of compression and storage to be 2.21 $/kg, which is higher than our 1.44 $/kg. Two reasons that help explain the cost difference are: our model does not account for up-front overhead costs such as engineering and design, and they use different financial assumptions – namely, a higher discount rate as well as a ramp-up of the station capacity, both of which increase the levelized costs. Additionally, our results show a higher relative fuel cost for compression due to the simplifying assumption that compression always occurs from the minimal to maximal pressure, while Bartolucci et al. [67] show that pressure cascades can have a significant impact on the compressor energy use.

Furthermore, Reddit et al. [58] report a levelized tank cost of 0.27 $/kg, which is in the same ballpark as our 0.39 $/kg for the station tanks. Our higher cost is not unexpected as all storage occurs at in high-pressure tanks with slight oversizing compared to the HDSAM model – which they use as the basis of their study. Note that the tank costs have come down 31% compared to the on-site model due to the trailers taking on some of the storage needs.

Finally, the 0.86 $/kg trucking costs are in line with the findings of Refs. [60], [70]. So, our simplified model provides reasonable ballpark cost estimates for all three components.

Figure 80 shows the cost breakdown over the different steps in the hydrogen supply chain. The dispensing cost is the highest at 1.4 $/kg, which is still relatively close to the cost of dispensing with on-site production of 1.63 $/kg. The distribution (trucking) cost is about 1.0 $/kg and the pLCOH2 of packaging at the plant is low at about 0.5 $/kg.

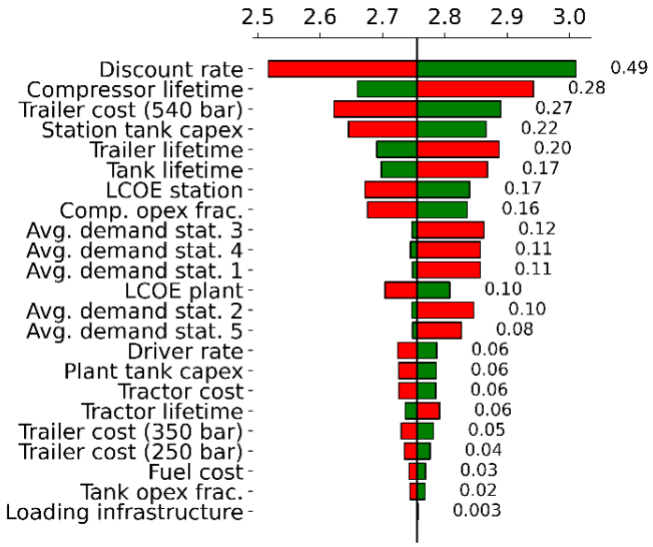

Figure 81 Tornado chart for the pLCOH2 (in $/kg) in a centralized production scheme

Again, the dominance of the capital costs is also reflected in the sensitivity analysis, Figure 81, with the discount rate, component lifetimes, and tank/trailer capital costs being the most influential parameters. Once more, the compressor capital cost does not show up in the sensitivity analysis as the correlations and their parameters remain unchanged in the model. The compressor fuel cost does show, though, in the form of the LCOE sensitivities. Note that the LCOE at the stations is far more impactful than the LCOE at the plant because at the plant the compressors do not need to reach as high pressures.

Overall, the tank cost parameters have lost importance compared to the on-site production case, and the compressor and trucking parameters have gained importance. Note that the production plant tank cost ("plant tank capex") has a limited impact on the pLCOH2, so the optimistic assumption of a uniform truck filling schedule likely does not affect the results much.

Finally, note the upward limit on the station capacities to prevent the stations from needing more than one delivery per day. As a result, there is a skewed influence between increases and decreases in the capacity. Overall, their effect is again rather limited because many of the fixed costs associated with hydrogen storage, transport, and refueling have been left out of the model.

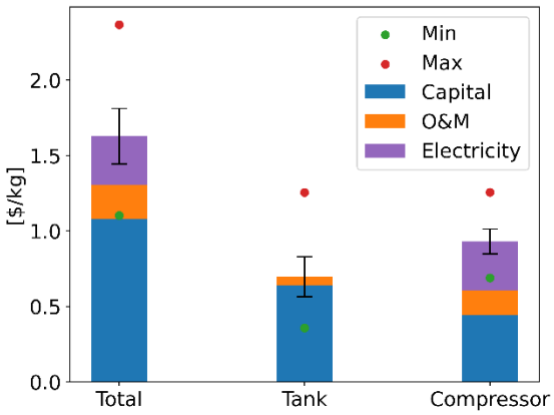

Figure 82 Component-wise pLCOH2 breakdown for distributed production resulting from a MC simulation with 5000 samples

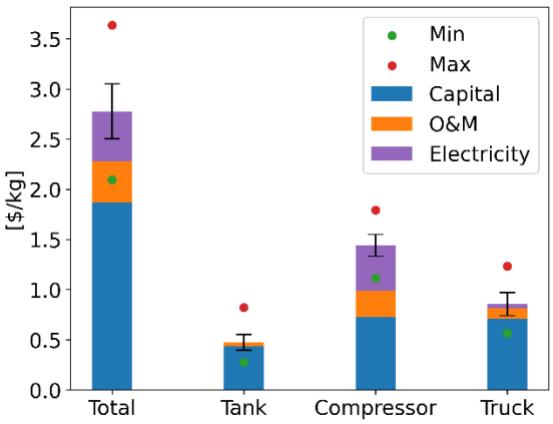

Figure 83 Component-wise pLCOH2 breakdown for centralized production resulting from a MC simulation with 5000 samples

5.6. Total hydrogen cost comparison and discussion

In this section, the production cost results are combined with the storage and delivery costs to evaluate the total cost differences between distributed and centralized production between NBs. While the term "total" hydrogen cost is used here to refer to the sum of both costs, the reader is reminded that the storage costs are partial costs, as discussed in Section 5.2.

A noticeable difference when comparing the pLCOH2 breakdown for the on-site and centralized cases, is the 31% lower tank cost with centralized production, Figure 82 Figure 83, which is a result of the trailers acting as mobile tanks. Comparing the costs breakdown in terms of supply chain steps shows that the partial dispensing costs of both cases are quite similar, Figure 84.

As mentioned in Section 4.9, the cost difference between cases with shared cost parameters cannot be determined by comparing their respective distributions directly. Instead, a new Monte Carlo simulation is run where the shared cost parameters (e.g., station tank cost) are varied identically. The resulting pLCOH2 difference is relatively small at 1.14 ± 0.17 [0.59, 1.73] $/kg. Note that the on-site production is disadvantaged in this comparison because our model is unable to account for economies of scale as it does not consider fixed costs, as discussed in Section 5.3. With the inclusion of economies of the cost difference is expected to grow.

The production costs by far dominate the pLCOH2, Figure 84. However, they will not necessarily make up the lion share if the full transport, storage and dispensing costs are considered. For PEM electrolysis, the LCOH2 difference between the lowest cost options for on-site production and centralized production found in Section 4.4 is 3.80 $/kg, which is larger than the storage, transport and dispensing cost differences. As a result, centralized production is the cheaper option compared to on-site production with a total hydrogen cost difference of 2.64 ± 1.22 [-0.50, 7.14] $/kg, Figure 85.

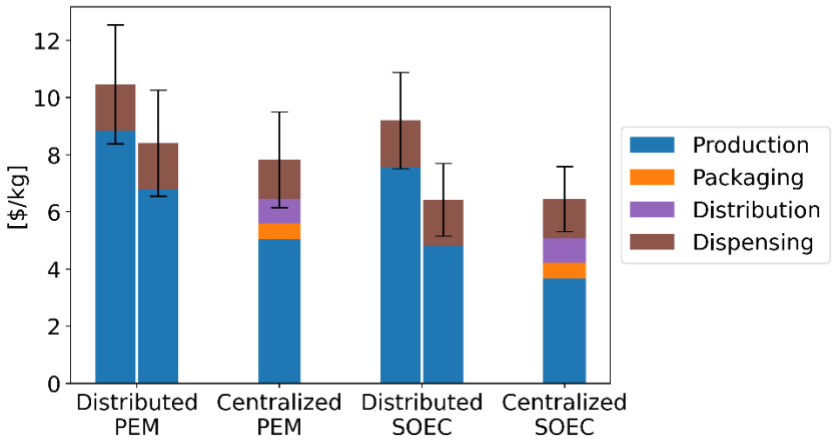

Figure 84 Comparison of the total LCOH2 between centralized and distributed production with PEM and SOEC. For the distributed production, the left bar represents production with a single NB and the right bar represents production with two NBs

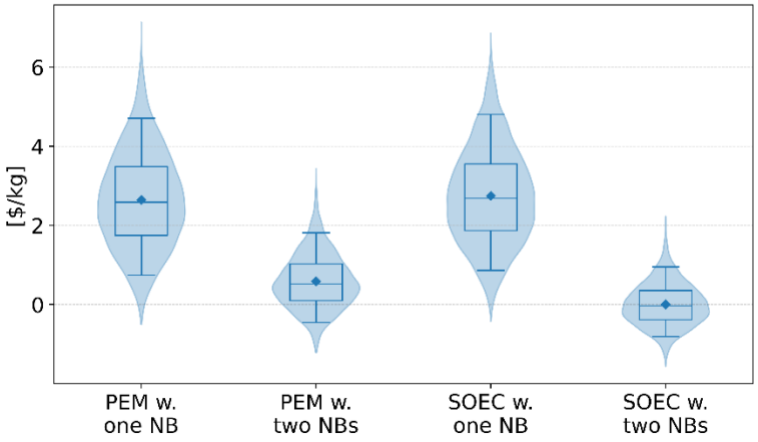

Figure 85 Box plots of the total LCOH2 difference between centralized and distributed production as determined from Monte Carlo simulations with consistent sampling. Centralized PEM/SOEC production is the reference for the differences, with the labels denoting what type of distributed production is used

Centralized production is cheaper than using on-site production with two NBs in 99% of the cases. Yet, the difference has decreased to 1.73 ± 0.68 [-0.12, 4.63] $/kg, making the production cost increase for on-site production is similar to its 1.14 $/kg storage and delivery cost saving. Unsurprisingly, then, there is no significant difference between on-site and centralized production anymore when comparing both on a total hydrogen cost basis – the difference between both is 0.59 ± 0.70 [-1.21, 3.43] $/kg. Note that Monforti et al. [59] also find that on-site production becomes more attractive at higher capacities due to economies-of-scale in their biomass gasification – however, the capacities in their work are far lower than what is discussed here.

Our finding that centralized production is cheaper than on-site production on a total hydrogen cost basis depending on the on-site production capacity goes against the findings of Simunovic et al. [68] who compare, amongst other paradigms, on-site production and centralized production with wind energy. They find that on-site production is cheaper over all capacities. This discrepancy again underscores the importance of case-by-case examination.

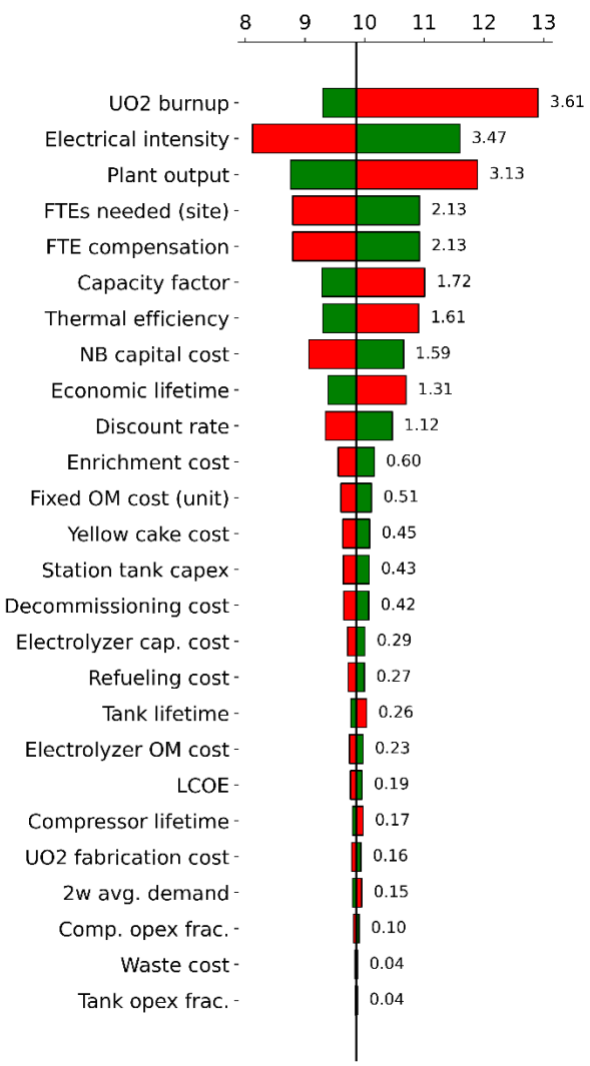

Figure 86 Tornado chart of the total cost (in $/kg) model for distributed PEM electrolysis with a single UO_2-fueled NOAK NB claiming mixed subsidies

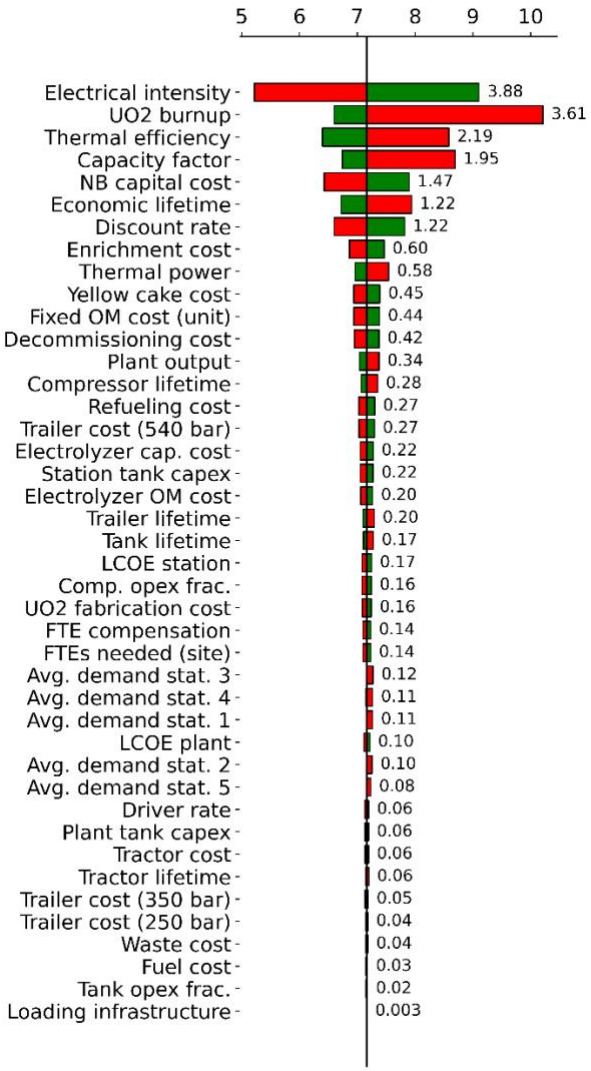

Figure 87 Tornado chart of the total cost (in $/kg) model for centralized PEM electrolysis with UO_2-fueled NOAK NBs claiming mixed subsidies

Analogously, when using SOEC electrolysis, the large (3.91 $/kg) production cost between centralized and distributed production overschadows the storage and delivery cost difference, and centralized production is 2.75 ± 1.20 [-0.43, 6.86] $/kg cheaper on a total hydrogen cost basis, Figure 85. Moreover, the production cost difference when using two NBs for on-site production is again similar to the delivery cost savings, thereby precluding any definitive conclusion on the cheaper option – the total cost difference is 0.00 ± 0.54 [-1.56, 2.23] $/kg.

Figure 86 Figure 87 show the sensitivity analyses carried out on the total hydrogen cost models for centralized and distributed production using PEM and claiming mixed subsidies. Given that production costs make up the majority of the total cost, it is no surprise to see that the NB cost parameters are dominant. The 9 most influential parameters for centralized production are related to the production cost, and for distributed production, it is the 13 most influential parameters. In centralized production, there is also a higher upward LCOH2 potential than downward one, which is mainly driven by the UO_2 burnup, thermal efficiency, and capacity factor.

In conclusion, the production costs are the predominant driver for cost differences in our total hydrogen cost model, and the total hydrogen cost shows the largest sensitivity to them. Our results indicate a preference for centralized production, though this preference disappears at higher on-site production capacities. Given the model's many simplifying assumptions and the multitude of neglected cost items in the pLCOH2, it is premature to decisively say whether centralized or on-site production will always be the most economical. What is clear, though, is that the storage and dispensing cost difference is not as large as initially expected based on the immense current costs. In part, the limited cost saving is due to the fact that the centralized facility is close to demand and does not need transmission over long distances.

6. Conclusion and future work

This report shows the current state of the feasibility study for using NBs in hydrogen production on a community scale or collocated with the customer. As part of the study, a set of requirements is developed for the NBs, which is only discussed qualitatively at this stage. For now, no technical requirements have been identified that are unique to hydrogen production as opposed to electricity production for the grid, and it is thus expected that NBs will be able to live up to the process specifications for electrolysis. However, the economic requirements for the NB system are strict, as there will be fierce competition with other hydrogen production methods.

For this reason, simple levelized cost models have been developed to get preliminary cost estimates for using NBs. Based on a review of hydrogen economy growth projections for CA, two hypothetical projects are chosen: a community-scale facility producing hydrogen relatively close to the demand with an average output of 25 000 kg/d, and a hydrogen fueling station having a capacity of 1600 kg/d with hydrogen produced on-site.

The preliminary results show that the use of NBs in community-scale production reaches cost of 3.67 $/kg, which is lower than the cost when grid electricity (in CA) and similar to the estimates for solar, but higher than cost estimates for steam methane reforming with carbon capture or large-scale nuclear hydrogen production. In distributed production, the economic attractiveness of using NBs is lower due to the lack of scaling of the NB O&M costs. The least costly distributed project uses SOEC and claims mixed IRA credits, resulting in an LCOH2 of 7.56 $/kg. Doubling the facility capacity lowers the LCOH2 4.81 $/kg by diluting the large fixed O&M costs. In view of those fixed costs, projects with a larger number of NBs will be more economical. Yet, large projects compete with technologies that benefit from economies of scale. So, projects with a handful of NBs will likely be most economical.

A simple hydrogen storage and transport model was developed to evaluate the benefit of local power production in the context of hydrogen production for refueling stations, and to compare the storage, transport, and dispensing costs between a community-scale facility and a station with on-site hydrogen production.

For hydrogen production, negating distribution costs is not sufficient to make on-site production more economical, as the total cost (differences) remain dominated by the hydrogen production costs. For larger on-site production projects with two NBs, the production cost increase compared to centralized production roughly matches the storage and transport cost saving, leading to no clearly preferred option.

However, the on-site production is disadvantaged as a result of the simplifying model setup that negates many fixed costs, as its larger capacity would result in lower levelized costs compared to the smaller stations that are refueled via truck delivery. Consequently, the storage and transport cost saving associated with distributed production will be underestimated – even more so for the large double capacity stations with two NBs. This makes it difficult to crown either centralized or distributed production as the cheapest option based on our rudimentary model. Yet, it is clear that the cost saving for distributed production is less than expected based on the huge current cost of transport and dispensing due to the proximity of the community-scale production plant to the demand.

To summarize, the competitiveness of using NBs for hydrogen production is found to depend heavily on four aspects. The first is policy and regulation because of the security requirements and subsidies, with the former dictating the economics of small-scale NB projects and the latter being required for competitiveness with other low-carbon power sources. Second, there are the learning rates in the economics of multiples of the NBs, which are needed to push down the prices compared to FOAK models. Third, is the use-case of the NBs, where NBs seem most fit for off-grid application that valorize the high-temperature heat of the NBs directly in, e.g., SOEC electrolysis. And lastly, there is the benefit of local power production – which in the context of electricity production in CA, makes the use of NBs competitive despite their LCOE that far exceed wholesale electricity prices.

There are many possible improvements to the economic models as future work, some of which are listed below:

- Expanding the scope of the hydrogen storage, transport, and dispensing cost model to include more cost items
- Performing a more detailed grid integration study that includes the optimization of buying electricity, other secondary revenue streams (e.g., black-start payments) and the interconnection costs
- Investigating the direct use of high-temperature heat in thermochemical processes such as SMR
- Considering the effects of using TRISO fuels on the licensing process and associated second-order cost effects
- Improving the cost estimates for the NBs, TRISO fuel and the FTE requirements and compensation in particular
- Improving the cost estimates for the electrolyzers, e.g., taking into account the electrolyzer replacement costs

In addition, the requirements for the NBs should also be quantified and treated in greater detail.

7. References

[1] N. Rustagi, A. Elgowainy, and J. Vickers, “Current Status of Hydrogen Delivery and Dispensing Costs and Pathways to Future Cost Reductions,” Department of Energy, 18003, Dec. 2018.

[2] K. Reddi, M. Mintz, A. Elgowainy, and E. Sutherland, “13 - Building a hydrogen infrastructure in the United States,” in *Compendium of Hydrogen Energy*, M. Ball, A. Basile, and T. N. Veziroğlu, Eds., in Woodhead Publishing Series in Energy. , Oxford: Woodhead Publishing, 2016, pp. 293–319. doi: 10.1016/B978-1-78242-364-5.00013-0.

[3] “Annual Evaluation of Fuel Cell Electric Vehicle Deployment and Hydrogen Fuel Station Network Development,” California Air Resources Board, Sep. 2021. Accessed: Oct. 03, 2022. [Online]. Available: https://ww2.arb.ca.gov/resources/documents/annual-hydrogen-evaluation

[4] J. Vickers, D. Peterson, and K. Randolph, “Cost of Electrolytic Hydrogen Production with Existing Technology,” Department of Energy, 20004, Sep. 2020.

[5] L. Marshall, “Electricity Rate Scenarios.” California Energy Commission, Sep. 30, 2021.

[6] A. Abou-Jaoude *et al.*, “Assessment of Factory Fabrication Considerations for Nuclear Microreactors,” *Nucl. Technol.*, vol. 209, no. 11, pp. 1697–1732, Nov. 2023, doi: 10.1080/00295450.2023.2206779.

[7] J. Buongiorno, B. Carmichael, B. Dunkin, J. Parsons, D. Smit, and S. E. Aumeier, “Can Nuclear Batteries Be Economically Competitive in Large Markets?,” *Energ. 2021 Vol 14 Page 4385*, vol. 14, no. 14, p. 4385, Jul. 2021, doi: 10.3390/EN14144385.

[8] P. R. Mcclure, D. I. Poston, V. Dasari, R. Rao, and R. Stowers, “Design of Megawatt Power Level Heat Pipe Reactors,” Los Alamos National Lab, Los Alamos, Nov. 2015.

[9] A. T. Pham, L. Lovdal, T. Zhang, and M. T. Craig, “A techno-economic analysis of distributed energy resources versus wholesale electricity purchases for fueling decarbonized heavy duty vehicles,” *Appl. Energy*, vol. 322, Sep. 2022, doi: 10.1016/j.apenergy.2022.119460.

[10] J. G. Reed *et al.*, “Roadmap for the Deployment and Buildout of Renewable Hydrogen Production Plants in California,” California Energy Commission, Jun. 2020. Accessed: Oct. 03, 2022. [Online]. Available: www.apep.uci.edu

[11] M. F. Ruth *et al.*, “The Technical and Economic Potential of the H2@Scale Hydrogen Concept within the United States,” National Renewable Energy Laboratory, 2020.

[12] “Roadmap to a US hydrogen economy,” The Fuel Cell and Hydrogen Energy Association, 2020.

[13] “Hydrogen Strategy: Enabling A Low-Carbon Economy,” Office of Fossil Energy US Department of Energy, Washington DC, 2020.

[14] O. Tang, J. Rehme, and P. Cerin, “Levelized cost of hydrogen for refueling stations with solar PV and wind in Sweden: On-grid or off-grid?,” *Energy*, vol. 241, p. 122906, Feb. 2022, doi: 10.1016/j.energy.2021.122906.

[15] "Table 1.1.9. Implicit Price Deflators for Gross Domestic Product," US Bureau of Economic Analysis. Accessed: Oct. 15, 2022. [Online]. Available: https://www.bea.gov/itable/national-gdp-and-personal-income

[16] M. Nickel, C. M. Haus, D. McCormick, J. Spilman, M. Woodard, and H. Welch Arbogast, "Inflation Reduction Act Creates New Tax Credit Opportunities for Energy Storage Projects," McGuireWoods. Accessed: Jan. 14, 2023. [Online]. Available: https://www.mcguirewoods.com/client-resources/Alerts/2022/12/inflation-reduction-act-creates-new-tax-credit-opportunities-for-energy-storage-projects

[17] P. Gordon, R. Lighty, J. Sanders, S. Clausen, and W. Pearson, "Inflation Reduction Act of 2022 Boosts Nuclear Power with Tax Credits and Funding," Morgan Lewis. Accessed: Jan. 14, 2023. [Online]. Available: https://www.morganlewis.com/pubs/2022/08/inflation-reduction-act-of-2022-boosts-nuclear-power-with-tax-credits-and-funding

[18] "Hydrogen-Related Provisions of the Inflation Reduction Act of 2022," King & Spaiding. Accessed: Jan. 14, 2023. [Online]. Available: https://www.kslaw.com/news-and-insights/hydrogen-related-provisions-of-the-inflation-reduction-act-of-2022

[19] K. Martin, "Bonus Tax Credits and the Inflation Reduction Act | Project Finance NewsWire," Norton Rose Fulbright. Accessed: Jan. 14, 2023. [Online]. Available: https://www.projectfinance.law/publications/2022/october/bonus-tax-credits-and-the-inflation-reduction-act/

[20] H. Cooper, C. Fleming, and A. Perlman, "Clean Hydrogen Tax Benefits under the Inflation Reduction Act," McDermott Will & Emery. Accessed: Jan. 20, 2023. [Online]. Available: https://www.mwe.com/insights/clean-hydrogen-tax-benefits-under-the-inflation-reduction-act/#_edn6

[21] A. Bergman, B. C. Prest, and K. Palmer, "How Can Hydrogen Producers Show That They Are Clean?," Resources. Accessed: Mar. 09, 2023. [Online]. Available: https://www.resources.org/common-resources/how-can-hydrogen-producers-show-that-they-are-clean/

[22] "Life Cycle Assessment of Electricity Generation Options," United Nations Economics Commission For Europe, Geneva, 2021.

[23] B. Parkinson, P. Balcombe, J. F. Speirs, A. D. Hawkes, and K. Hellgardt, "Levelized cost of CO2 mitigation from hydrogen production routes," *Energy Environ. Sci.*, vol. 12, no. 1, pp. 19–40, Jan. 2019, doi: 10.1039/c8ee02079e.

[24] A. Buttler and H. Spliethoff, "Current status of water electrolysis for energy storage, grid balancing and sector coupling via power-to-gas and power-to-liquids: A review," *Renew. Sustain. Energy Rev.*, vol. 82, pp. 2440–2454, Feb. 2018, doi: 10.1016/j.rser.2017.09.003.

[25] D. DeSantis, B. James, and G. Saur, "Current (2015) Hydrogen Production from Central PEM Electrolysis." in H2A Model. National Renewable energy Laboratory, 2019.

[26] D. DeSantis, B. James, and G. Saur, "Future (2040) Hydrogen Production from Central PEM Electrolysis," National Renewable energy Laboratory, 2019.

[27] J. M. Lee *et al.*, "Environ-economic analysis of high-temperature steam electrolysis for decentralized hydrogen production," *Energy Convers. Manag.*, vol. 266, Aug. 2022, doi: 10.1016/j.enconman.2022.115856.

[28] D. Peterson, J. Vickers, and D. Desantis, "Hydrogen Production Cost From PEM Electrolysis," Department of Energy, 19009, Feb. 2020. [Online]. Available: http://www.hydrogen.energy.gov/h2a_prod_studies.html:

[29] "Electricity Data Browser." U.S. Energy Information Administration, Washington DC, Jan. 11, 2023. Accessed: Jan. 11, 2023. [Online]. Available: https://www.eia.gov/electricity/data/browser/

[30] "The Role of Nuclear Power in the Hydrogen Economy: Cost and Competitiveness," Organisation for Economic Co-operation and Development, 2022.

[31] "California Greenhouse Gas Emissions for 2000 to 2020 Trends of Emissions and Other Indicators," California Air Resources Board, Sacramento, Oct. 2022. [Online]. Available: https://ww2.arb.ca.gov/ghg-inventory-data.

[32] D. DeSantis, B. James, and G. Saur, "Future (2040) Hydrogen Production from Distributed Grid PEM Electrolysis," National Renewable energy Laboratory, 2019.

[33] K. Shirvan *et al.*, "UO2-fueled microreactors: Near-term solutions to emerging markets," *Nucl. Eng. Des.*, vol. 412, p. 112470, Oct. 2023, doi: 10.1016/j.nucengdes.2023.112470.

[34] "Cost Competitiveness of Micro-Reactors for Remote Markets," Nuclear Energy Institute, Apr. 2019.

[35] "Projected Costs of Generating Electricity," Nuclear Energy Agency, 2020.

[36] "Nuclear Costs in Context," Nuclear Energy Institute, Washington D.C., 2022.

[37] B. Eric Ingersoll and K. Gogan, "Missing Link to a Livable Climate How Hydrogen-Enabled Synthetic Fuels Can Help Deliver the Paris Goals," Lucid Catalyst, Sep. 2020.

[38] J. Aborn *et al.*, "An Assessment of the Diablo Canyon Nuclear Power Plant for Zero Carbon Energy, Desalination, and Hydrogen," 2021.

[39] A. Abou Jaoude, A. W. Foss, Y. Arafat, and B. W. Dixon, "An Economics-by-Design Approach Applied to a Heat Pipe Microreactor Concept," Idaho National Laboratory, Idaho Falls, INL/EXT-21-63067, Jul. 2021. Accessed: Oct. 02, 2022. [Online]. Available: https://www.osti.gov/servlets/purl/1811894/

[40] D. DeSantis, B. James, and G. Saur, "Solid Oxide Electrolysis Case (Current)," National Renewable energy Laboratory, 2019.

[41] D. DeSantis, B. James, and G. Saur, "Solid Oxide Electrolysis Case (Future)," National Renewable energy Laboratory, 2019.

[42] R. Pinsky, P. Sabharwall, J. Hartvigsen, and J. O'Brien, "Comparative review of hydrogen production technologies for nuclear hybrid energy systems," *Prog. Nucl. Energy*, vol. 123, p. 103317, May 2020, doi: 10.1016/J.PNUCENE.2020.103317.

[43] J. J. Powers and B. D. Wirth, “A review of TRISO fuel performance models,” *J. Nucl. Mater.*, vol. 405, no. 1, pp. 74–82, Oct. 2010, doi: 10.1016/j.jnucmat.2010.07.030.

[44] “What is spent nuclear fuel?,” Deep Isolation. Accessed: Nov. 21, 2023. [Online]. Available: https://www.deepisolation.com/about-nuclear-waste/what-is-spent-nuclear-fuel/

[45] C. A. Condon *et al.*, “Fate and transport of unruptured tri-structural isotropic (TRISO) fuel particles in the event of environmental release for advanced and micro reactor applications,” *J. Environ. Radioact.*, vol. 234, p. 106630, Aug. 2021, doi: 10.1016/j.jenvrad.2021.106630.

[46] D. E. Shropshire *et al.*, “Advanced Fuel Cycle Cost Basis,” Idaho National Lab. (INL), Idaho Falls, ID (United States), INL/EXT-07-12107, Apr. 2007. doi: 10.2172/911948.

[47] S. Cole, L. Chow, S. Brant, M. Kito, and M. Sterkel, “2021 Resource Adequacy Report,” CAISO, Apr. 2023. [Online]. Available: https://www.cpuc.ca.gov/RA/

[48] T. Nguyen, Z. Abdin, T. Holm, and W. Mérida, “Grid-connected hydrogen production via large-scale water electrolysis,” *Energy Convers. Manag.*, vol. 200, p. 112108, Nov. 2019, doi: 10.1016/j.enconman.2019.112108.

[49] P. Gagnon, B. Cowiestoll, and M. Schwarz, “Cambium 2022 Scenario Descriptions and Documentation,” National Renewable Energy Laboratory (NREL), Golden, CO (United States), NREL/TP-6A40-84916, Jan. 2023. doi: 10.2172/1915250.

[50] J. Seel and A. D. Mills, “Integrating Cambium Marginal Costs into Electric Sector Decisions: Opportunities to Integrate Cambium Marginal Cost Data into Berkeley Lab Analysis and Technical Assistance,” Lawrence Berkeley National Lab. (LBNL), Berkeley, CA (United States), Nov. 2021. doi: 10.2172/1828856.

[51] S. Mosquera-López and A. Nursimulu, “Drivers of electricity price dynamics: Comparative analysis of spot and futures markets,” *Energy Policy*, vol. 126, pp. 76–87, Mar. 2019, doi: 10.1016/j.enpol.2018.11.020.

[52] M. Kopp, D. Coleman, C. Stiller, K. Scheffer, J. Aichinger, and B. Scheppat, “Energiepark Mainz: Technical and economic analysis of the worldwide largest Power-to-Gas plant with PEM electrolysis,” *Int. J. Hydrog. Energy*, vol. 42, no. 19, pp. 13311–13320, May 2017, doi: 10.1016/j.ijhydene.2016.12.145.

[53] E. Lewis *et al.*, “Comparison of Commercial, State-of-the-art, Fossil-based Hydrogen Production Technologies,” National Energy Technology Laboratory, Apr. 2022.

[54] C. Forsberg, A. Foss, and A. Abou-Jaoude, “Fission battery economics-by-design,” *Prog. Nucl. Energy*, vol. 152, Oct. 2022, doi: 10.1016/j.pnucene.2022.104366.

[55] “Annual Technology Baseline: Hydrogen Fuel Cost,” National Renewable Energy Laboratory. Accessed: Oct. 15, 2022. [Online]. Available: https://atb.nrel.gov/transportation/2020/hydrogen

[56] M. Genovese and P. Fragiacomo, “Hydrogen station evolution towards a poly-generation energy system,” *Int. J. Hydrog. Energy*, vol. 47, no. 24, pp. 12264–12280, Mar. 2022, doi: 10.1016/j.ijhydene.2021.06.110.

[57] “Noth American Gas Outlook to 2030 H1 2019,” McKinsey.

[58] K. Reddi, A. Elgowainy, N. Rustagi, and E. Gupta, “Impact of hydrogen refueling configurations and market parameters on the refueling cost of hydrogen,” *Int. J. Hydrog. Energy*, vol. 42, no. 34, pp. 21855–21865, Aug. 2017, doi: 10.1016/j.ijhydene.2017.05.122.

[59] A. Monforti Ferrario, S. Rajabi Hamedani, L. Del Zotto, G. Santori Simone, and Bocci, “Techno-economic analysis of in-situ production by electrolysis, biomass gasification and delivery systems for Hydrogen Refuelling Stations: Rome case study,” *Energy Procedia*, vol. 148, pp. 82–89, Aug. 2018, doi: 10.1016/j.egypro.2018.08.033.

[60] J. J. Brey, A. F. Carazo, and R. Brey, “Exploring the marketability of fuel cell electric vehicles in terms of infrastructure and hydrogen costs in Spain,” *Renew. Sustain. Energy Rev.*, vol. 82, pp. 2893–2899, Feb. 2018, doi: 10.1016/j.rser.2017.10.042.

[61] T. Mayer, M. Semmel, M. A. Guerrero Morales, K. M. Schmidt, A. Bauer, and J. Wind, “Techno-economic evaluation of hydrogen refueling stations with liquid or gaseous stored hydrogen,” *Int. J. Hydrog. Energy*, vol. 44, no. 47, pp. 25809–25833, Oct. 2019, doi: 10.1016/j.ijhydene.2019.08.051.

[62] “Gurobi Optimization.” Gurobi Optimization LLC, 2023. [Online]. Available: https://www.gurobi.com

[63] M. Mintz, A. Elgowainy, and M. Gardiner, “Rethinking Hydrogen Fueling: Insights from Delivery Modeling,” *Transp. Res. Rec. J. Transp. Res. Board*, vol. 2139, no. 1, pp. 46–54, Jan. 2009, doi: 10.3141/2139-06.

[64] S. Samuelsen, B. Shaffer, J. Grigg, B. Lane, and J. Reed, “Performance of a hydrogen refueling station in the early years of commercial fuel cell vehicle deployment,” *Int. J. Hydrog. Energy*, vol. 45, no. 56, pp. 31341–31352, Nov. 2020, doi: 10.1016/j.ijhydene.2020.08.251.

[65] “HYDROGEN DELIVERY SCENARIO ANALYSIS MODEL (HDSAM).” UChicago Argonne, LLC. [Online]. Available: https://hdsam.es.anl.gov/

[66] D. S. Mallapragada, E. Gençer, P. Insinger, D. W. Keith, and F. M. O’Sullivan, “Can Industrial-Scale Solar Hydrogen Supplied from Commodity Technologies Be Cost Competitive by 2030?,” *Cell Rep. Phys. Sci.*, vol. 1, no. 9, p. 100174, Sep. 2020, doi: 10.1016/j.xcrp.2020.100174.

[67] L. Bartolucci, S. Cordiner, V. Mulone, C. Tatangelo, M. Antonelli, and S. Romagnuolo, “Multi-hub hydrogen refueling station with on-site and centralized production,” *Int. J. Hydrog. Energy*, vol. 48, no. 54, pp. 20861–20874, Jun. 2023, doi: 10.1016/j.ijhydene.2023.01.094.

[68] J. Šimunović, I. Pivac, and F. Barbir, “Techno-economic assessment of hydrogen refueling station: A case study in Croatia,” *Int. J. Hydrog. Energy*, vol. 47, no. 57, pp. 24155–24168, Jul. 2022, doi: 10.1016/j.ijhydene.2022.05.278.

[69] C. F. Guerra, L. Reyes-Bozo, E. Vyhmeister, J. L. Salazar, M. J. Caparrós, and C. Clemente-Jul, “Sustainability of hydrogen refuelling stations for trains using electrolysers,” *Int. J. Hydrog. Energy*, vol. 46, no. 26, pp. 13748–13759, Apr. 2021, doi: 10.1016/j.ijhydene.2020.10.044.

[70] J. Munster and M. Blieske, “Shell Hydrogen Refueling Station Cost Reduction Roadmap,” 2018.

[71] K. Shirvan, “Email Communication with Prof. Shirvan,” May 05, 2023.

[72] “Mitsubishi Nuclear Fuel Co., Ltd. | PWR Fuel.” Accessed: Nov. 27, 2023. [Online]. Available: https://www.mhi.com/group/mnf/products/pwr.html

[73] “Home | NWMO.” Accessed: Nov. 27, 2023. [Online]. Available: https://www.nwmo.ca/www.nwmo.ca/https://nwmo-jss-nextjs-le085xyny-nwmo-tg.vercel.app

[74] L. Lallemant, J. Buongiorno, and S. Islam, “Design of a Fission Batteries Process (FIBAPRO) facility,” CANES, MIT-198-ANP, Nov. 2023.

[75] H. Choi, W. I. Ko, and M. S. Yang, “Economic Analysis on Direct Use of Spent Pressurized Water Reactor Fuel in CANDU Reactors—I: DUPIC Fuel Fabrication Cost,” *Nucl. Technol.*, vol. 134, no. 2, pp. 110–129, May 2001, doi: 10.13182/NT01-A3190.

[76] H. Choi, W. I. Ko, M. S. Yang, I. Namgung, and B.-G. Na, “Economic Analysis on Direct Use of Spent Pressurized Water Reactor Fuel in CANDU Reactors—II: DUPIC Fuel-Handling Cost,” *Nucl. Technol.*, vol. 134, no. 2, pp. 130–148, May 2001, doi: 10.13182/NT01-A3191.

[77] W. I. Ko, H. Choi, and M. S. Yang, “Economic Analysis on Direct Use of Spent Pressurized Water Reactor Fuel in CANDU Reactors—IV: DUPIC Fuel Cycle Cost,” *Nucl. Technol.*, vol. 134, no. 2, pp. 167–186, May 2001, doi: 10.13182/NT01-A3193.

[78] W. I. Ko, H. Choi, G. Roh, and M. S. Yang, “Economic Analysis on Direct Use of Spent Pressurized Water Reactor Fuel in CANDU Reactors—III: Spent DUPIC Fuel Disposal Cost,” *Nucl. Technol.*, vol. 134, no. 2, pp. 149–166, May 2001, doi: 10.13182/NT01-A3192.

Appendix A Waste and refueling cost calculations

A.1 Waste cost

Even when using the conventional UO_2 fuel, the NB waste will be different from traditional light water reactor waste in its form and burnup – with the lower burnup leading to a larger waste volume on a per-MWh basis. Both of these factors could lead to a significantly increased waste cost. Therefore, we estimate the cost of waste disposal from a bottom-up analysis rather than using a flat spent nuclear fuel fee – as is commonly done in the context of large-scale power reactors.

More specifically, the cost of dry storage is estimated, not the cost of permanent disposal in a geological repository, as for now, there is no permanent repository in the US. The dry storage cost is estimated by calculating the number of dry casks needed per core, which, given the cost of a dry cask translates immediately to a waste cost per core. Note that the cost associated with the emptying of the NB and filling of the casks is not treated here, but is instead covered under the broader refueling and servicing cost covered in Appendix A.2. In addition, any costs associated with developing the waste strategy for NBs is assumed to be amortized, since our main focus is on NOAK NBs.

The design chosen for this analysis is the liquid metal cooled, graphite moderated reactor with UO_2 fuel treated by Shirvan et al. [33], Figure 88. As for the casks, the focus is on readily available casks that are made for current power reactors. It is unlikely that these casks will be the optimal storage system for the different fuel form of NBs, but the design of a NB-specific cask is outside the scope of this work. In addition, as will be shown later, the waste cost is so low that the cost savings with an optimal cask will not materially affect the work.

The end-of-life (EOL) burnup of the NB fuel is on the order of 5 – 15 MWd/kg HM, which is comparable to the roughly 8 MWd/kg HM EOL burnup of CANDU fuel. So, we first look at the disposal cost when using CANDU waste cannisters – a schematic of which is shown in Figure 89. One CANDU cask can hold 48 CANDU fuel bundles, each of which are about 48 cm long and have a radius of 5.2 cm, Table 14. By contrast, the NB assemblies are about three times longer at 150 cm and fit in a circle of diameter 5.3 cm. A single cask can thus also hold 48 NB assemblies assuming that three NB assemblies fit in the same cross-sectional area as one bundle – see Figure 90 – and the length of each assembly is three bundles.

Table 14 Geometric parameters of the fuel assemblies of different reactor types

	NB	**CANDU**	**PWR**
Cross-sectional assembly shape	Hexagonal	Circular	Square
Side length/radius [cm]	2.65	5.17	21.4
Assembly/bundle length [cm]	150	48	410
Source	[33]	[71]	[72]

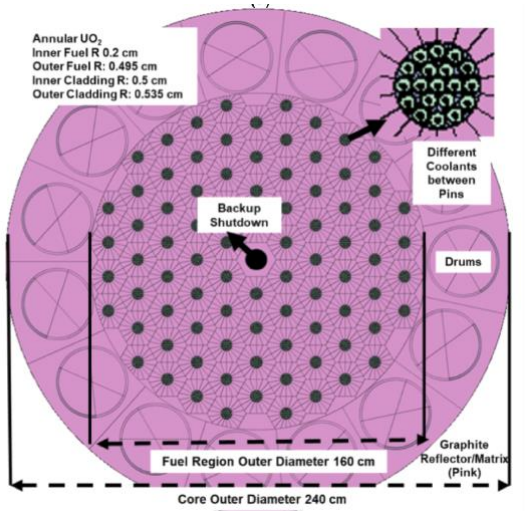

Figure 88 Liquid metal and FLiBe core design of Shrivan et al. [33]

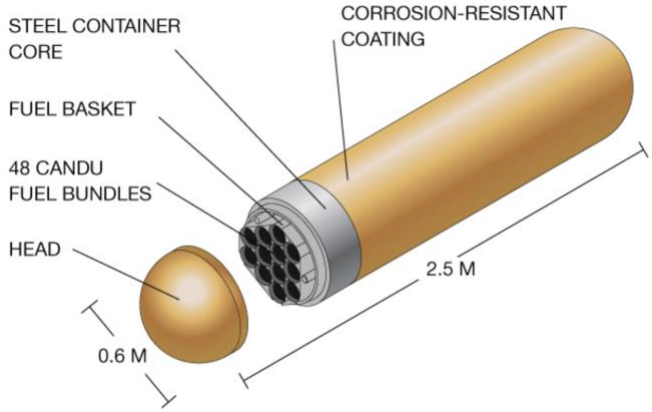

Figure 89 Schematic of a CANDU disposal cask, taken from Ref. [73]

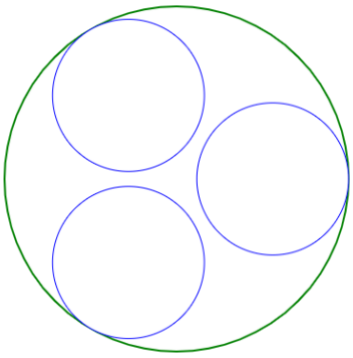

Figure 90 Schematic showing the positions of the NB assemblies in the CANDU bundle slot, the radii of the blue and green circles match the radii of the NB assemblies and CANDU bundles

Yet there is another constraint, namely that the decay heat limits of the cask cannot be exceeded. After shutdown of the reactor, the fuel will still generate heat due to the decay of radioactive fission products created during operation. The decay power decreases as a function of time and increases with increasing burnup, see Figure 91. The CANDU bundles have an average end-of-life (EOL) of 8 MWd/kg HM, whereas the NB fuel has a higher average EOL burnup of 11.7 MWd/kg HM. After two years of cooled storage (in line with the 18 months assumed by Lallemant et al. [74]), the decay power of the NB fuel is about 1.5 times higher than that of the CANDU fuel. Accounting for equal total decay power, the CANDU cask can only hold 36 NB assemblies. At a cost of 160 k$/cask [71], this puts the total cost of waste disposal at 377 k$/core, or 0.74 $/MWh.

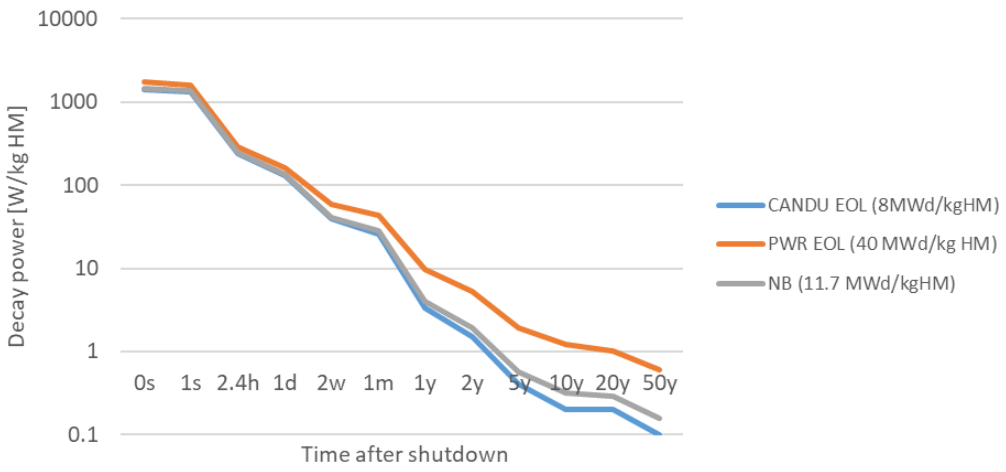

Figure 91 Decay power as a function of time based on decay power calculations from Ref. [71]

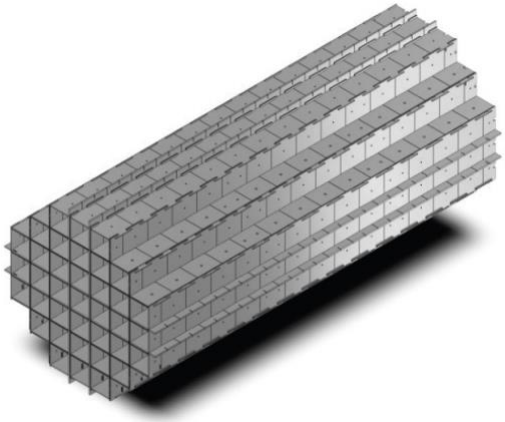

Figure 92 Rendering of the NUHOMS® EOS P37, taken from Ref. [74]

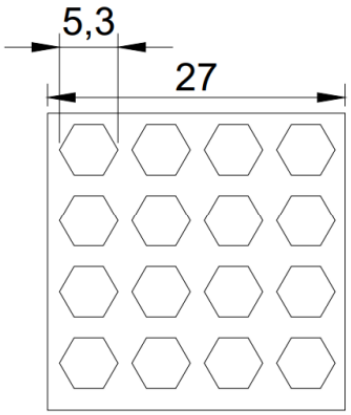

Figure 93 Schematic showing the positions of the NB assemblies in the PWR assembly slot, taken from Ref. [74]

Alternatively, we consider the use of PWR dry casks – more specifically, the NUHOMS® EOS P37 type casks (Figure 92) in line with the work of Lallemant et al. [74]. Each of the 37 slots for PWR assemblies can hold up to 16 NB assemblies, see Figure 93. In addition, the PWR assemblies are about three times longer than the NB assemblies, so three layers of NB assemblies fit in a NUHOMS cask, resulting in a total of 1776 NB assemblies per cask.

Unlike the CANDU casks, the burnup of the NB fuel is now below the burnup of the fuel that normally fills the volume, so the only constraint will be volumetric. With 1776 assemblies per PWR cask, it can fit about 21 cores worth of NB assemblies. At a cost of 1 M$ per PWR dry cask (the lower end of costs assumed in Ref. [74]), the casks cost per NB is low at about 47 300 $/core, which equates to about 0.09 – 0.28 $/MWh for the highest and lowest burnup respectively.

Based on these results, we assume a uniform distribution of the waste cost between 50 k$ and 400 k$ per core in the economic model. So, despite the higher waste volume per unit energy, the costs associated with it remain low and comparable to those seen in the industry today. Of course, the analysis presented

here is rough and is only meant to provide an order of magnitude for the waste cost. In addition, it only considers the cask cost, so the real waste cost (that includes labor etc.) will be higher.

In the above analysis, we assumed that the assemblies are stored as a whole. However, one could remove the fuel pins from the graphite to store only pins. Not only does this lead to a lesser amount of dry casks needed, it also allows for the graphite to be stored as a lower waste class. However, we expect that the cost of developing and operating a pin separation line in the central servicing facility will far outweigh the decrease in the (already low) waste cost. Furthermore, the analysis implicitly assumes that waste disposal and associated costs for TRISO fuels will be identical to those of UO_2 fuel.

A.2 Refueling cost

The NBs will be refueled, inspected and serviced in a central facility rather than on-site and the cost of doing so will be passed on to the project owners. Hence, this section evaluates what the refueling (and servicing) cost will be to have a better picture of the NB economics.

As was the case for Appendix A.1, the analysis is closely related to the work on the design of the central facility by Lallemant et al. [74], as it evolved together. In his work, the levelized cost of refueling is estimated through an analogy with the DUPIC process [75]–[78] – with the main emphasis on the cost analysis of Ko et al. [77]. Here, the work is expanded by adding ranges to the cost estimates and running Monte Carlo simulations of the model. The resulting distribution of outcomes is used in our cost calculations.

The levelized cost of refueling LCRF is split in a capital and O&M contribution

$$LCRF = LCRF_{cap} + LCRF_{O\&M} \tag{33}$$

To calculate the levelized capital cost of the facility, the overnight capital costs and decommissioning costs are annualized using a capital recovery factor CRF and sinking fund factor SFF, respectively. Both can be determined using the discount rate r and the economic lifetime of the project t_{ec}:

$$CRF = \frac{r \cdot (1+r)^{t_{ec}}}{(1+r)^{t_{ec}} - 1} \tag{34}$$

$$SFF = \frac{r}{(1+r)^{t_{ec}} - 1} \tag{35}$$

After annualizing the overnight and decommissioning costs, $LCRF_{cap}$ follows as:

$$LCRF_{cap} = (1+c) \cdot \frac{CRF \cdot (b + l + eq + pc) + SFF \cdot (b + l)}{N_{ref}} \tag{36}$$

Where c is the contingency, d the decommission cost fraction, N_{ref} the yearly number of refueled NBs, b is the building cost, l is the land cost, eq is the equipment cost, and pc is the preconstruction cost. The $LCRF_{O\&M}$ is simpler to calculate:

$$LCRF_{O\&M} = (1+c) \cdot \frac{s + u + mat + m}{N_{ref}} \tag{37}$$

Where c is the contingency, N_{ref} the yearly number of refueled NBs, s is the annual staff cost, u is the annual utilities cost, mat is the annual materials cost, and m is the annual maintenance cost. Table 15 shows the cost ranges used. The mode of each distribution is taken from Ref. [74] and the width of the ranges is 20% to 30% of the mean depending on the perceived rigor of the estimation in Ref. [74]. The only exception is the discount rate, which is chosen according to the same distribution as used throughout this work.

Table 15 Assumptions for the central facility cost model

Parameter	Unit	Min	Mode	Max	Source
Facility output	NBs/y		200		[74]
Facility lifetime	y	55	60	65	[74]
Discount rate	%	2	6	12	
Contingency	%	20	30	40	[74]
Land cost	M$	20.7	25.8	31.0	[74]
Building cost	M$	358.6	512.3	665.9	[74]
Equipment cost	M$	204.0	291.6	379.0	[74]
Preconstruction cost	M$	57.7	72.2	86.6	[74]
Staff cost	M$/y	43.0	61.4	79.9	[74]
Utilities	M$/y	10.2	12.8	15.3	[74]
Materials	M$/y	17.5	25.0	32.5	[74]
Maintenance	M$/y	8.9	12.8	16.6	[74]
Decommissioning	%	40	50	60	[74]

Figure 94 shows the resulting distribution of levelized refueling costs, with a drawn overlay of the approximate triangular distribution that will be used in further cost modeling. The minimum assumed refueling cost in the triangular distribution is 0.84 M$/core, the mode is 1.09 M$/core and the maximum is 1.45 M$/core.

For completeness, the cost breakdown and tornado chart of the LCRF are shown in Figure 95 Figure 96. The O&M costs take up about two thirds of the levelized refueling cost, with the capital cost making up the remaining third. In addition, the most important parameter, by far, is the facility output. It will thus be important to avoid delays on the refueling lines.

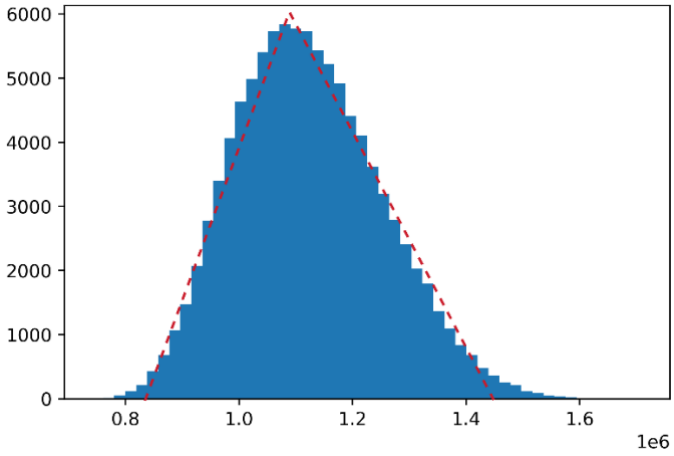

Figure 94 The LCRF (in $/NB) distribution resulting from a Monte Carlo simulation with an overlay of the approximate triangular distribution

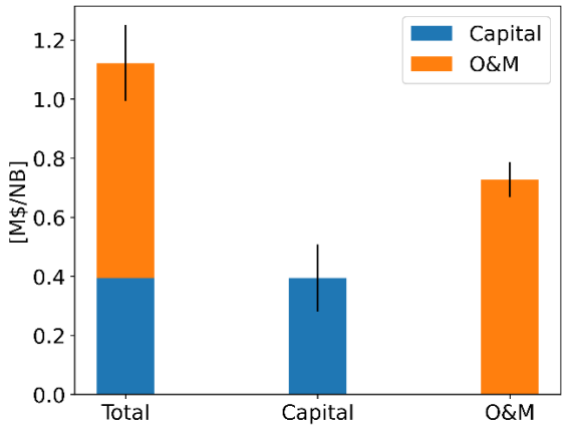

Figure 95 The cost breakdown of the LCRF resulting from Monte Carlo simulations with 50 000 samples

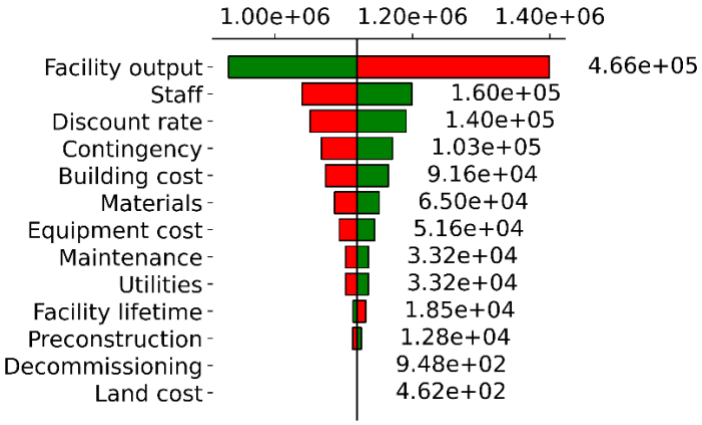

Figure 96 Tornado chart of the LCRF (in $/NB)

Appendix B LCOE Results

B.1 Nuclear batteries

As detailed in Section 4.1, reported levelized costs are the result of Monte Carlo simulations with 50 000 samples and are reported as μ ± σ [m, M] with μ being the average cost, σ the standard deviation of the cost distribution, m the minimum cost, and M the maximum cost.

B.1.1 Community-scale production

Table 16 LCOE breakdown for community-scale PEM electrolysis with UO_2-fueled NBs, LCOE given in $/MWh as μ ± σ [m, M]

NB Type	IRA Subsidy	Total	Capital	O&M	Fuel
NOAK	None	159 ± 25 [88, 290]	86 ± 20 [34, 179]	28 ± 4 [19, 53]	44 ± 11 [25, 109]
	PTC	142 ± 25 [73, 266]	86 ± 20 [33, 182]	28 ± 4 [18, 55]	44 ± 11 [25, 107]
	ITC	135 ± 21 [77, 252]	62 ± 14 [25, 123]	28 ± 4 [18, 53]	44 ± 11 [26, 108]
FOAK	None	134 ± 20 [76, 229]	62 ± 14 [25, 124]	28 ± 4 [18, 51]	44 ± 11 [25, 109]
	PTC	257 ± 40 [148, 435]	185 ± 37 [89, 339]	28 ± 4 [18, 53]	44 ± 11 [25, 111]
	ITC	240 ± 40 [127, 435]	185 ± 37 [86, 354]	28 ± 4 [17, 50]	44 ± 11 [26, 110]

Table 17 LCOE breakdown for community-scale PEM electrolysis with TRISO-fueled NBs, LCOE given in $/MWh as μ ± σ [m, M]

NB Type	IRA Subsidy	Total	Capital	O&M	Fuel
NOAK	None	170 ± 26 [91, 291]	86 ± 20 [31, 177]	27 ± 3 [17, 42]	57 ± 13 [26, 119]
	PTC	154 ± 26 [72, 285]	86 ± 20 [32, 182]	27 ± 3 [17, 41]	57 ± 13 [27, 113]
	ITC	147 ± 21 [78, 251]	62 ± 14 [26, 122]	27 ± 3 [17, 43]	57 ± 13 [26, 118]

FOAK	None	147 ± 21 [81, 243]	62 ± 14 [22, 123]	27 ± 3 [17, 41]	57 ± 13 [27, 118]
	PTC	269 ± 41 [154, 463]	185 ± 37 [81, 340]	27 ± 3 [18, 42]	57 ± 13 [27, 118]
	ITC	252 ± 41 [132, 447]	184 ± 37 [87, 350]	27 ± 3 [16, 44]	57 ± 13 [26, 116]

B.1.2 Distributed production

Table 18 LCOE breakdown for distributed PEM electrolysis with UO_2-fueled NBs, LCOE given in $/MWh as μ ± σ [m, M]

NB Type	IRA Subsidy	Total	Capital	O&M	Fuel
NOAK	None	231 ± 36 [124, 406]	92 ± 22 [32, 198]	95 ± 24 [33, 175]	44 ± 11 [25, 109]
	PTC	215 ± 36 [101, 375]	92 ± 22 [37, 194]	95 ± 24 [35, 177]	44 ± 11 [26, 107]
	ITC	206 ± 32 [111, 374]	66 ± 15 [25, 136]	95 ± 24 [36, 182]	44 ± 11 [26, 105]
FOAK	None	206 ± 32 [105, 352]	66 ± 15 [26, 132]	95 ± 24 [34, 179]	44 ± 11 [26, 112]
	PTC	338 ± 50 [187, 568]	199 ± 41 [87, 384]	95 ± 24 [36, 180]	44 ± 11 [25, 105]
	ITC	322 ± 50 [175, 589]	199 ± 41 [87, 394]	95 ± 24 [35, 178]	44 ± 11 [25, 106]

Table 19 LCOE breakdown for distributed PEM electrolysis with TRISO-fueled NBs, LCOE given in $/MWh as μ ± σ [m, M]

NB Type	IRA Subsidy	Total	Capital	O&M	Fuel
NOAK	None	244 ± 36 [132, 414]	92 ± 22 [37, 195]	94 ± 24 [34, 178]	58 ± 13 [27, 117]
	PTC	227 ± 36 [108, 374]	92 ± 22 [38, 200]	94 ± 24 [34, 172]	57 ± 13 [27, 116]
	ITC	218 ± 32 [114, 369]	66 ± 15 [27, 144]	94 ± 24 [34, 175]	58 ± 13 [28, 117]

FOAK	None	218 ± 32 [113, 353]	66 ± 15 [26, 133]	94 ± 24 [35, 176]	58 ± 13 [27, 115]
	PTC	350 ± 50 [189, 589]	199 ± 40 [92, 408]	94 ± 24 [35, 174]	58 ± 13 [27, 115]
	ITC	334 ± 51 [165, 568]	199 ± 41 [89, 392]	94 ± 24 [34, 174]	58 ± 12 [28, 115]

B.1.3 Distributed production with two NBs

Table 20 LCOE breakdown for distributed PEM electrolysis with two UO_2-fueled NBs, LCOE given in $/MWh as μ ± σ [m, M]

NB Type	IRA Subsidy	Total	Capital	O&M	Fuel
NOAK	None	193 ± 30 [105, 347]	92 ± 22 [36, 189]	58 ± 13 [25, 122]	44 ± 11 [25, 111]
	PTC	177 ± 30 [90, 333]	92 ± 22 [35, 194]	58 ± 13 [24, 122]	44 ± 11 [26, 107]
	ITC	168 ± 26 [93, 308]	66 ± 15 [26, 132]	58 ± 13 [23, 119]	44 ± 11 [25, 105]
FOAK	None	168 ± 26 [86, 315]	66 ± 15 [25, 132]	58 ± 13 [24, 126]	44 ± 11 [26, 109]
	PTC	300 ± 47 [165, 566]	199 ± 41 [91, 400]	58 ± 13 [24, 127]	44 ± 11 [25, 108]
	ITC	284 ± 47 [141, 501]	199 ± 41 [89, 378]	58 ± 13 [23, 123]	44 ± 11 [25, 108]

Table 21 LCOE breakdown for distributed PEM electrolysis with two TRISO-fueled NBs, LCOE given in $/MWh as μ ± σ [m, M]

NB Type	IRA Subsidy	Total	Capital	O&M	Fuel
NOAK	None	206 ± 31 [111, 378]	92 ± 22 [36, 195]	56 ± 13 [23, 117]	57 ± 13 [27, 115]
	PTC	189 ± 31 [88, 346]	92 ± 22 [34, 195]	56 ± 13 [23, 117]	57 ± 13 [26, 118]
	ITC	180 ± 26 [98, 305]	66 ± 15 [26, 136]	56 ± 13 [23, 114]	57 ± 13 [26, 118]

FOAK	None	180 ± 26 [91, 312]	66 ± 15 [26, 135]	56 ± 13 [23, 113]	57 ± 13 [27, 116]
	PTC	312 ± 47 [157, 551]	199 ± 41 [95, 400]	56 ± 13 [23, 115]	57 ± 13 [27, 115]
	ITC	296 ± 47 [155, 532]	199 ± 41 [89, 400]	56 ± 13 [24, 113]	57 ± 13 [26, 114]

B.2 Nuclear batteries used in SOEC electrolysis

The LCOE when using NBs for SOEC electrolysis is derived from the LCOH as $LCOE = LCOH/\eta$. The parameters of the NBs haven't changed between PEM and SOEC electrolysis, but the number of NBs needed for the more-efficient SOEC electrolysis is lower than for PEM electrolysis. As a result, the LCOE between both cases differ due to economies of scale – in particular for spreading the fixed O&M costs. At the community scale and for distributed production with two NBs the differences remain below 1%, so the results are not repeated.

B.2.1 Distributed production

Table 22 LCOE breakdown for distributed SOEC electrolysis with UO_2-fueled NBs, LCOE given in $/MWh as μ ± σ [m, M]

NB Type	IRA Subsidy	Total	Capital	O&M	Fuel
NOAK	None	255 ± 41 [130, 443]	92 ± 22 [34, 190]	118 ± 31 [43, 222]	45 ± 11 [26, 107]
	PTC	239 ± 41 [112, 414]	92 ± 22 [35, 204]	118 ± 31 [41, 228]	45 ± 11 [26, 109]
	ITC	230 ± 37 [119, 395]	66 ± 15 [24, 133]	118 ± 31 [43, 223]	45 ± 11 [26, 111]
FOAK	None	230 ± 37 [118, 390]	67 ± 15 [26, 132]	118 ± 31 [43, 226]	45 ± 11 [26, 107]
	PTC	362 ± 54 [188, 597]	199 ± 41 [83, 394]	118 ± 31 [43, 225]	45 ± 11 [26, 108]
	ITC	346 ± 54 [176, 610]	199 ± 41 [95, 396]	119 ± 31 [44, 228]	45 ± 11 [26, 107]

Table 23 LCOE breakdown for distributed SOEC electrolysis with TRISO-fueled NBs, LCOE given in $/MWh as μ ± σ [m, M]

NB Type	IRA Subsidy	Total	Capital	O&M	Fuel
NOAK	None	268 ± 41 [142, 451]	92 ± 22 [37, 196]	117 ± 31 [43, 219]	59 ± 13 [28, 121]
	PTC	252 ± 41 [120, 438]	92 ± 22 [33, 200]	117 ± 31 [39, 219]	59 ± 13 [29, 115]
	ITC	243 ± 37 [122, 402]	66 ± 15 [26, 134]	117 ± 31 [43, 223]	59 ± 13 [28, 113]
FOAK	None	243 ± 38 [119, 398]	66 ± 15 [25, 135]	117 ± 31 [42, 222]	59 ± 13 [28, 117]
	PTC	375 ± 54 [209, 613]	199 ± 41 [87, 390]	117 ± 31 [41, 219]	59 ± 13 [28, 116]
	ITC	359 ± 54 [181, 602]	199 ± 41 [90, 389]	117 ± 31 [41, 217]	59 ± 13 [28, 116]

Appendix C LCOH2 Results

As detailed in Section 4.1, reported levelized costs are the result of Monte Carlo simulations with 50 000 samples and are reported as μ ± σ [m, M] with μ being the average cost, σ the standard deviation of the cost distribution, m the minimum cost, and M the maximum cost.

C.1 PEM electrolysis with grid electricity

Table 24 LCOH2 for PEM electrolysis using grid electricity in $/kg as μ ± σ [m, M]

Paradigm	IRA Subsidy	Total	Capital	O&M	Fuel
Community-scale	None	10.03 ± 0.42 [8.81, 11.34]	0.36 ± 0.09 [0.16, 0.77]	0.33 ± 0.08 [0.17, 0.57]	9.34 ± 0.40 [8.31, 10.26]
	PTC	6.18 ± 0.42 [4.93, 7.44]	0.36 ± 0.09 [0.15, 0.83]	0.33 ± 0.08 [0.17, 0.57]	8.49 ± 0.40 [7.47, 9.41]
	ITC	9.91 ± 0.41 [8.73, 11.06]	0.24 ± 0.06 [0.10, 0.53]	0.33 ± 0.08 [0.17, 0.57]	9.34 ± 0.40 [8.31, 10.25]
Distributed	None	10.12 ± 0.42 [8.81, 11.50]	0.44 ± 0.11 [0.19, 0.94]	0.34 ± 0.09 [0.17, 0.62]	9.34 ± 0.40 [8.33, 10.25]
	PTC	6.27 ± 0.42 [4.99, 7.66]	0.44 ± 0.11 [0.19, 0.97]	0.34 ± 0.09 [0.17, 0.60]	8.49 ± 0.40 [7.47, 9.40]
	ITC	9.97 ± 0.41 [8.76, 11.24]	0.30 ± 0.07 [0.12, 0.63]	0.34 ± 0.09 [0.17, 0.60]	9.34 ± 0.40 [8.31, 10.26]

C.1.1 Community-scale production

Comparison

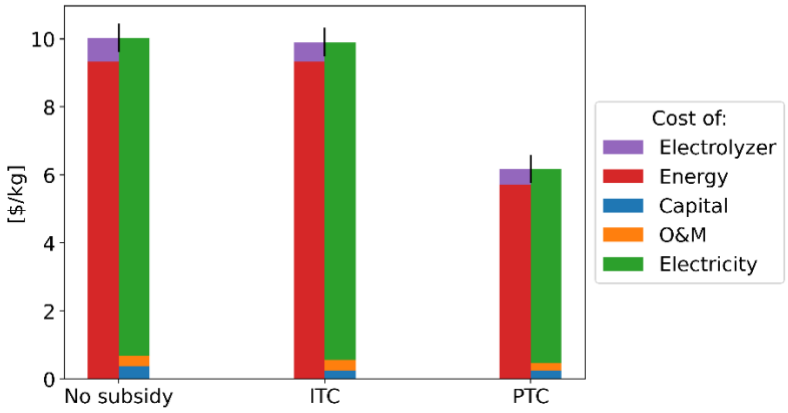

Figure 97 Comparison of the LCOH2 for community-scale PEM electrolysis using grid electricity when claiming different types of IRA subsidies, the LCOH2 is broken up in two columns for each case to show share of the levelized cost of the electrolyzers versus energy and to show the distribution between the levelized costs of capital, O&M, and fuel

C.1.2 Distributed production

Comparison

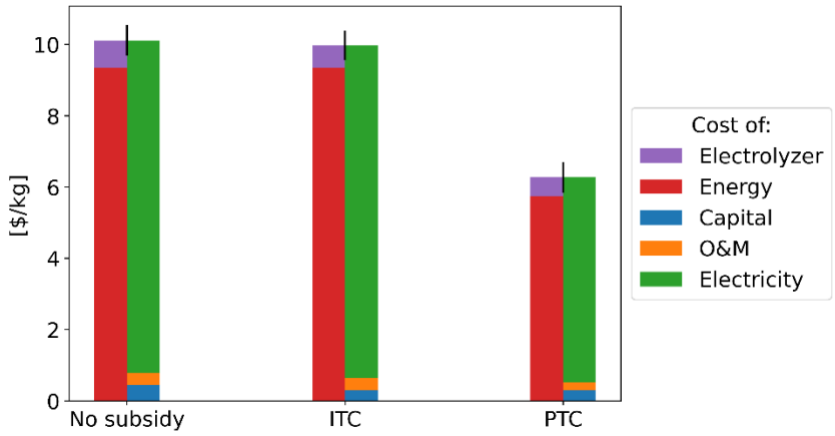

Figure 98 Comparison of the LCOH2 for distributed PEM electrolysis using grid electricity when claiming different types of IRA subsidies, the LCOH2 is broken up in two columns for each case to show share of the levelized cost of the electrolyzers versus energy and to show the distribution between the levelized costs of capital, O&M, and fuel

C.2 PEM electrolysis with nuclear batteries

C.2.1 Community-scale production

Table 25 LCOH2 breakdown for community-scale PEM electrolysis with UO_2-fueled NBs, LCOH2 given in $/kg as μ ± σ [m, M]

NB Type	IRA Subsidy	Total	Capital	O&M	Fuel
NOAK	None	8.85 ± 1.33 [5.11, 15.86]	0.38 ± 0.10 [0.17, 0.83]	0.34 ± 0.09 [0.17, 0.60]	8.13 ± 1.30 [4.52, 14.86]
	PTC	5.41 ± 1.83 [1.39, 13.57]	0.38 ± 0.10 [0.16, 0.83]	0.34 ± 0.09 [0.17, 0.59]	7.27 ± 1.30 [3.76, 13.62]
	ITC	7.50 ± 1.07 [4.47, 13.72]	0.25 ± 0.06 [0.11, 0.55]	0.34 ± 0.09 [0.17, 0.60]	6.91 ± 1.05 [3.96, 12.91]
	Mixed	5.04 ± 1.65 [1.35, 11.75]	0.38 ± 0.10 [0.16, 0.79]	0.34 ± 0.09 [0.17, 0.60]	6.89 ± 1.04 [3.88, 11.77]
FOAK	None	13.90 ± 2.13 [8.16, 23.41]	0.38 ± 0.10 [0.16, 0.82]	0.34 ± 0.09 [0.17, 0.60]	13.19 ± 2.08 [7.58, 22.31]
	PTC	10.47 ± 2.46 [4.04, 22.57]	0.38 ± 0.10 [0.16, 0.79]	0.34 ± 0.09 [0.17, 0.60]	12.32 ± 2.07 [6.54, 22.29]
	ITC	10.86 ± 1.52 [6.36, 19.37]	0.25 ± 0.06 [0.11, 0.55]	0.34 ± 0.09 [0.17, 0.60]	10.27 ± 1.49 [5.95, 18.55]
	Mixed	8.44 ± 1.99 [3.50, 17.60]	0.38 ± 0.10 [0.17, 0.82]	0.34 ± 0.09 [0.17, 0.60]	10.29 ± 1.49 [5.93, 17.70]

UO_2 NOAK comparison

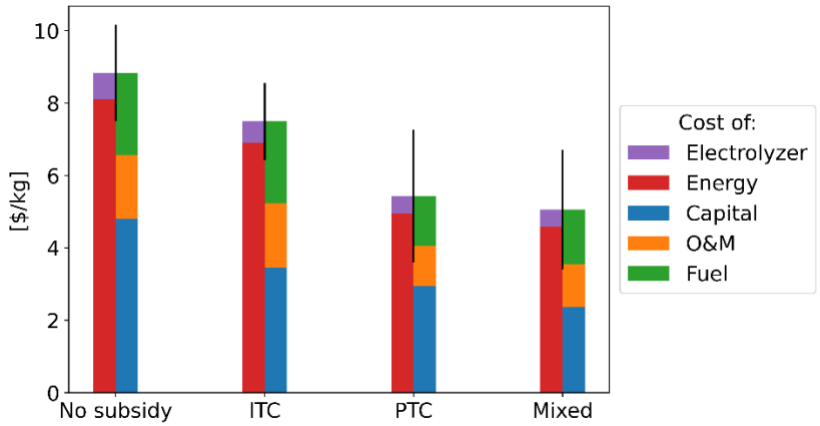

Figure 99 Comparison of the LCOH2 for community-scale PEM electrolysis using NOAK UO_2-fueled NBs when claiming different types of IRA subsidies, the LCOH2 is broken in two ways to show share of the levelized cost of the electrolyzers versus energy and to show the distribution between the levelized costs of capital, O&M, and fuel

UO_2 FOAK comparison

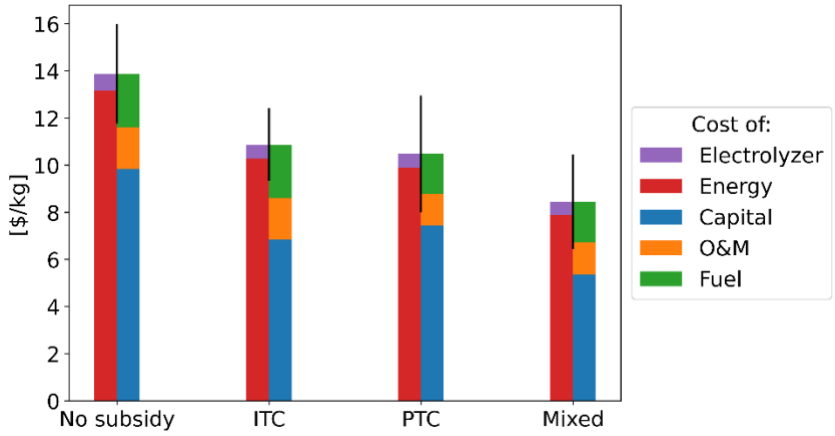

Figure 100 Comparison of the LCOH2 for community-scale PEM electrolysis using FOAK UO_2-fueled NBs when claiming different types of IRA subsidies, the LCOH2 is broken in two ways to show share of the levelized cost of the electrolyzers versus energy and to show the distribution between the levelized costs of capital, O&M, and fuel

Table 26 LCOH2 breakdown for community-scale PEM electrolysis with TRISO-fueled NBs, LCOH2 given in $/kg as μ ± σ [m, M]

NB Type	IRA Subsidy	Total	Capital	O&M	Fuel
NOAK	None	9.45 ± 1.37 [5.23, 15.77]	0.38 ± 0.10 [0.16, 0.81]	0.34 ± 0.09 [0.17, 0.60]	8.73 ± 1.33 [4.65, 14.93]
	PTC	5.60 ± 1.36 [1.24, 12.49]	0.38 ± 0.10 [0.16, 0.82]	0.34 ± 0.09 [0.17, 0.60]	7.88 ± 1.33 [3.67, 14.62]
	ITC	8.11 ± 1.10 [4.42, 13.50]	0.25 ± 0.06 [0.11, 0.52]	0.34 ± 0.09 [0.17, 0.60]	7.52 ± 1.07 [4.00, 12.86]
	Mixed	5.24 ± 1.10 [1.69, 10.18]	0.38 ± 0.10 [0.16, 0.82]	0.34 ± 0.09 [0.17, 0.59]	7.52 ± 1.07 [4.18, 12.45]
FOAK	None	14.50 ± 2.16 [8.54, 24.66]	0.38 ± 0.10 [0.17, 0.83]	0.34 ± 0.09 [0.17, 0.60]	13.79 ± 2.10 [7.91, 23.74]
	PTC	10.65 ± 2.17 [4.56, 20.76]	0.38 ± 0.10 [0.17, 0.81]	0.34 ± 0.09 [0.17, 0.60]	12.93 ± 2.12 [6.78, 22.95]
	ITC	11.50 ± 1.56 [6.33, 18.66]	0.25 ± 0.06 [0.11, 0.55]	0.34 ± 0.09 [0.17, 0.59]	10.91 ± 1.53 [5.94, 17.86]
	Mixed	8.62 ± 1.57 [3.70, 15.24]	0.38 ± 0.10 [0.17, 0.79]	0.34 ± 0.09 [0.17, 0.60]	10.91 ± 1.52 [6.15, 17.53]

TRISO NOAK comparison

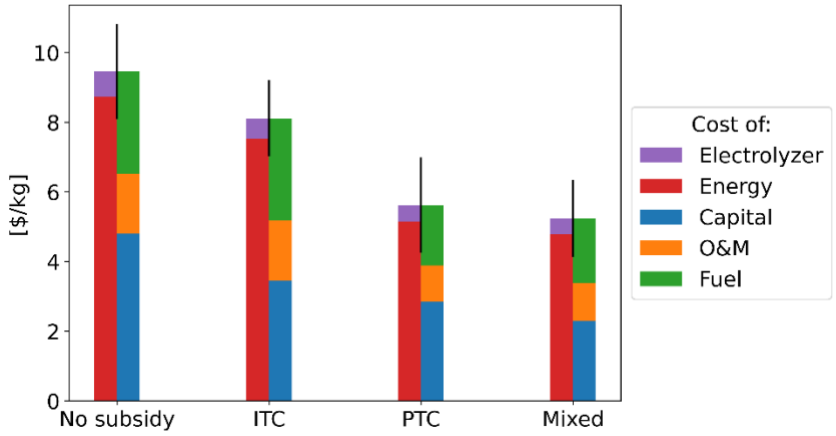

Figure 101 Comparison of the LCOH2 for community-scale PEM electrolysis using NOAK TRISO-fueled NBs when claiming different types of IRA subsidies, the LCOH2 is broken in two ways to show share of the levelized cost of the electrolyzers versus energy and to show the distribution between the levelized costs of capital, O&M, and fuel

TRISO FOAK comparison

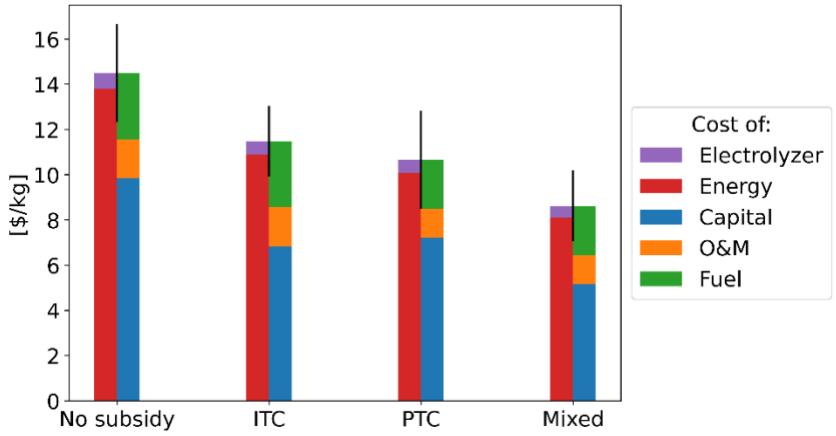

Figure 102 Comparison of the LCOH2 for community-scale PEM electrolysis using FOAK TRISO-fueled NBs when claiming different types of IRA subsidies, the LCOH2 is broken in two ways to show share of the levelized cost of the electrolyzers versus energy and to show the distribution between the levelized costs of capital, O&M, and fuel

C.2.2 Distributed production

Table 27 LCOH2 breakdown for distributed PEM electrolysis with UO_2-fueled NBs, LCOH2 given in $/kg as μ ± σ [m, M]

NB Type	IRA Subsidy	Total	Capital	O&M	Fuel
NOAK	None	12.73 ± 1.88 [6.98, 21.80]	0.48 ± 0.12 [0.21, 1.01]	0.39 ± 0.10 [0.18, 0.73]	11.86 ± 1.84 [6.36, 20.82]
	PTC	9.33 ± 2.27 [2.90, 19.41]	0.48 ± 0.12 [0.20, 1.07]	0.39 ± 0.10 [0.19, 0.73]	11.02 ± 1.84 [5.17, 19.24]
	ITC	11.26 ± 1.65 [6.37, 20.06]	0.32 ± 0.08 [0.14, 0.68]	0.39 ± 0.10 [0.18, 0.73]	10.55 ± 1.63 [5.70, 19.17]
	Mixed	8.87 ± 2.08 [3.19, 18.00]	0.48 ± 0.12 [0.21, 1.06]	0.39 ± 0.10 [0.19, 0.74]	10.56 ± 1.63 [5.39, 18.05]
FOAK	None	18.19 ± 2.63 [10.18, 30.10]	0.48 ± 0.12 [0.21, 1.06]	0.39 ± 0.10 [0.19, 0.73]	17.33 ± 2.56 [9.59, 29.12]
	PTC	14.80 ± 2.91 [6.50, 30.31]	0.48 ± 0.12 [0.21, 1.06]	0.39 ± 0.10 [0.18, 0.74]	16.49 ± 2.56 [8.96, 30.21]
	ITC	14.91 ± 2.04 [8.31, 24.03]	0.32 ± 0.08 [0.14, 0.71]	0.39 ± 0.10 [0.19, 0.74]	14.20 ± 2.00 [7.82, 23.16]
	Mixed	12.52 ± 2.42 [5.29, 24.68]	0.48 ± 0.12 [0.20, 1.07]	0.38 ± 0.10 [0.18, 0.74]	14.21 ± 2.01 [7.62, 24.59]

UO_2 NOAK comparison

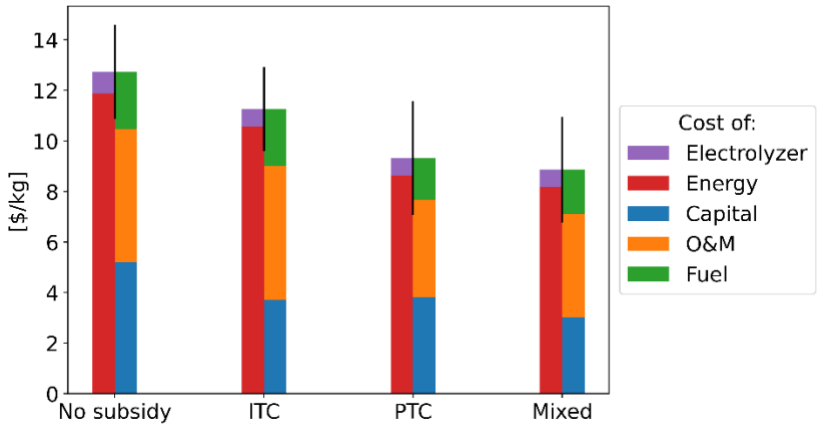

Figure 103 Comparison of the LCOH2 for distributed PEM electrolysis using NOAK UO_2-fueled NBs when claiming different types of IRA subsidies, the LCOH2 is broken in two ways to show share of the levelized cost of the electrolyzers versus energy and to show the distribution between the levelized costs of capital, O&M, and fuel

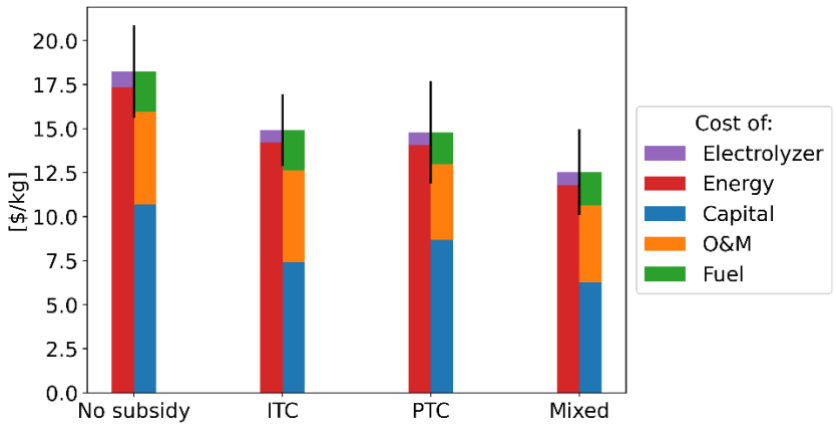

Figure 104 Comparison of the LCOH2 for distributed PEM electrolysis using FOAK UO_2-fueled NBs when claiming different types of IRA subsidies, the LCOH2 is broken in two ways to show share of the levelized cost of the electrolyzers versus energy and to show the distribution between the levelized costs of capital, O&M, and fuel

Table 28 LCOH2 breakdown for distributed PEM electrolysis with TRISO-fueled NBs, LCOH2 given in $/kg as μ ± σ [m, M]

NB Type	IRA Subsidy	Total	Capital	O&M	Fuel
NOAK	None	13.38 ± 1.90 [7.53, 22.27]	0.48 ± 0.12 [0.20, 1.02]	0.39 ± 0.10 [0.19, 0.73]	12.51 ± 1.86 [6.78, 21.22]
	PTC	9.49 ± 1.89 [3.42, 17.14]	0.48 ± 0.12 [0.20, 1.06]	0.38 ± 0.10 [0.19, 0.74]	11.63 ± 1.84 [5.54, 19.17]
	ITC	11.89 ± 1.66 [6.55, 20.05]	0.32 ± 0.08 [0.14, 0.71]	0.39 ± 0.10 [0.19, 0.73]	11.18 ± 1.64 [5.85, 18.91]
	Mixed	9.04 ± 1.67 [3.53, 16.51]	0.48 ± 0.12 [0.20, 1.06]	0.39 ± 0.10 [0.19, 0.73]	11.18 ± 1.64 [5.78, 18.11]
FOAK	None	18.84 ± 2.64 [10.33, 31.21]	0.48 ± 0.12 [0.21, 1.03]	0.38 ± 0.10 [0.19, 0.73]	17.97 ± 2.58 [9.72, 30.21]
	PTC	14.98 ± 2.66 [6.02, 27.55]	0.48 ± 0.12 [0.20, 1.04]	0.39 ± 0.10 [0.19, 0.74]	17.11 ± 2.60 [8.44, 29.13]
	ITC	15.53 ± 2.07 [8.28, 25.35]	0.32 ± 0.08 [0.14, 0.71]	0.39 ± 0.10 [0.19, 0.74]	14.82 ± 2.03 [7.59, 24.61]
	Mixed	12.70 ± 2.09 [5.96, 22.20]	0.48 ± 0.12 [0.21, 1.04]	0.39 ± 0.10 [0.19, 0.73]	14.84 ± 2.04 [8.28, 24.34]

TRISO NOAK comparison

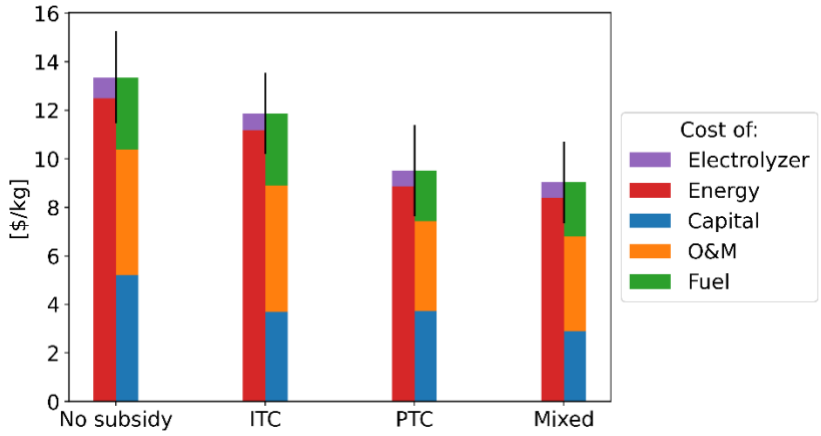

Figure 105 Comparison of the LCOH2 for distributed PEM electrolysis using NOAK TRISO-fueled NBs when claiming different types of IRA subsidies, the LCOH2 is broken in two ways to show share of the levelized cost of the electrolyzers versus energy and to show the distribution between the levelized costs of capital, O&M, and fuel

TRISO FOAK comparison

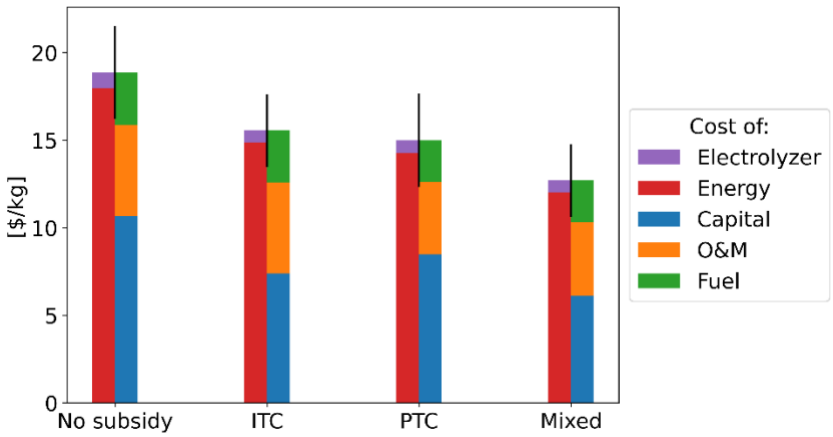

Figure 106 Comparison of the LCOH2 for distributed PEM electrolysis using FOAK TRISO-fueled NBs when claiming different types of IRA subsidies, the LCOH2 is broken in two ways to show share of the levelized cost of the electrolyzers versus energy and to show the distribution between the levelized costs of capital, O&M, and fuel

C.2.3 Distributed production with two NBs

Table 29 LCOH2 breakdown for distributed PEM electrolysis with two UO_2-fueled NBs, LCOH2 given in $/kg as μ ± σ [m, M]

NB Type	IRA Subsidy	Total	Capital	O&M	Fuel
NOAK	None	10.65 ± 1.60 [5.87, 18.63]	0.36 ± 0.09 [0.15, 0.83]	0.37 ± 0.10 [0.18, 0.71]	9.92 ± 1.55 [5.38, 17.80]
	PTC	7.25 ± 2.03 [2.24, 16.93]	0.36 ± 0.09 [0.15, 0.83]	0.37 ± 0.10 [0.18, 0.71]	9.08 ± 1.55 [4.61, 17.09]
	ITC	9.24 ± 1.34 [5.28, 16.72]	0.24 ± 0.06 [0.09, 0.55]	0.37 ± 0.10 [0.18, 0.72]	8.63 ± 1.31 [4.76, 15.79]
	Mixed	6.79 ± 1.85 [2.13, 16.26]	0.36 ± 0.09 [0.15, 0.87]	0.37 ± 0.10 [0.18, 0.72]	8.62 ± 1.31 [4.41, 16.16]
FOAK	None	16.14 ± 2.46 [8.98, 29.92]	0.36 ± 0.09 [0.14, 0.83]	0.37 ± 0.10 [0.18, 0.73]	15.41 ± 2.40 [8.48, 29.04]
	PTC	12.75 ± 2.76 [4.79, 25.50]	0.36 ± 0.09 [0.15, 0.82]	0.37 ± 0.10 [0.18, 0.72]	14.58 ± 2.39 [7.25, 25.73]
	ITC	12.89 ± 1.83 [7.46, 23.57]	0.24 ± 0.06 [0.10, 0.57]	0.37 ± 0.10 [0.18, 0.71]	12.28 ± 1.78 [6.82, 22.94]
	Mixed	10.45 ± 2.22 [4.03, 21.27]	0.36 ± 0.09 [0.14, 0.84]	0.37 ± 0.10 [0.18, 0.70]	12.28 ± 1.78 [6.51, 21.46]

UO_2 NOAK comparison

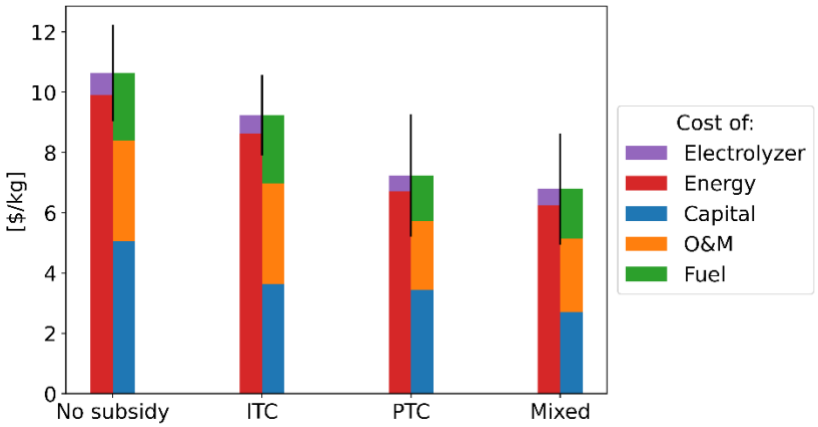

Figure 107 Comparison of the LCOH2 for distributed PEM electrolysis using two NOAK UO_2-fueled NBs when claiming different types of IRA subsidies, the LCOH2 is broken in two ways to show share of the levelized cost of the electrolyzers versus energy and to show the distribution between the levelized costs of capital, O&M, and fuel

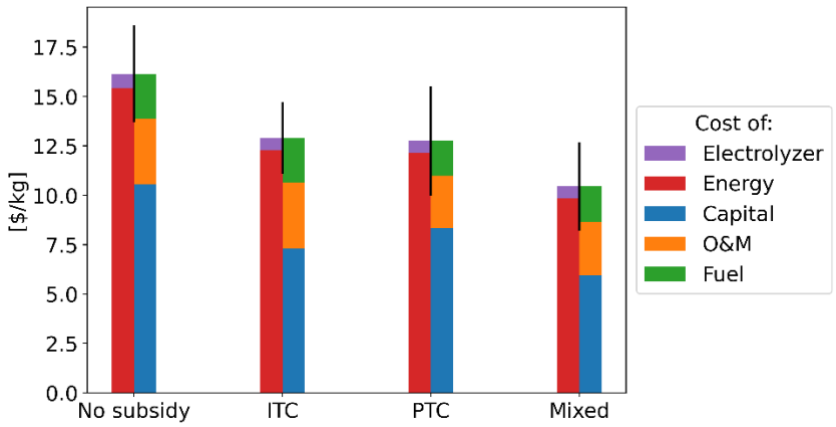

Figure 108 Comparison of the LCOH2 for distributed PEM electrolysis using two FOAK UO_2-fueled NBs when claiming different types of IRA subsidies, the LCOH2 is broken in two ways to show share of the levelized cost of the electrolyzers versus energy and to show the distribution between the levelized costs of capital, O&M, and fuel

Table 30 LCOH2 breakdown for distributed PEM electrolysis with two TRISO-fueled NBs, LCOH2 given in $/kg as μ ± σ [m, M]

NB Type	IRA Subsidy	Total	Capital	O&M	Fuel
NOAK	None	11.28 ± 1.63 [6.28, 20.43]	0.36 ± 0.09 [0.14, 0.79]	0.37 ± 0.10 [0.18, 0.71]	10.55 ± 1.58 [5.67, 19.39]
	PTC	7.44 ± 1.64 [2.08, 15.72]	0.36 ± 0.09 [0.15, 0.90]	0.37 ± 0.10 [0.18, 0.71]	9.71 ± 1.60 [4.52, 17.76]
	ITC	9.84 ± 1.37 [5.54, 16.34]	0.24 ± 0.06 [0.10, 0.54]	0.37 ± 0.10 [0.18, 0.71]	9.23 ± 1.34 [5.03, 15.63]
	Mixed	6.96 ± 1.38 [2.30, 13.91]	0.36 ± 0.09 [0.15, 0.84]	0.37 ± 0.10 [0.18, 0.70]	9.23 ± 1.34 [4.69, 16.00]
FOAK	None	16.74 ± 2.49 [8.61, 29.38]	0.36 ± 0.09 [0.15, 0.87]	0.37 ± 0.10 [0.18, 0.73]	16.01 ± 2.44 [8.07, 28.28]
	PTC	12.93 ± 2.49 [5.52, 25.29]	0.36 ± 0.09 [0.14, 0.84]	0.37 ± 0.10 [0.18, 0.72]	15.20 ± 2.43 [7.97, 27.29]
	ITC	13.50 ± 1.84 [7.60, 21.69]	0.24 ± 0.06 [0.10, 0.54]	0.37 ± 0.10 [0.17, 0.72]	12.89 ± 1.80 [7.23, 21.00]
	Mixed	10.64 ± 1.87 [4.52, 19.93]	0.36 ± 0.09 [0.14, 0.82]	0.37 ± 0.10 [0.18, 0.72]	12.91 ± 1.82 [7.13, 21.97]

TRISO NOAK comparison

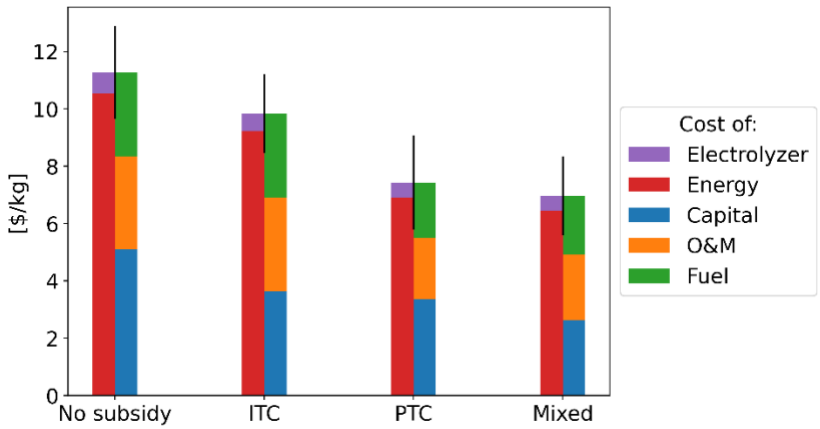

Figure 109 Comparison of the LCOH2 for distributed PEM electrolysis using two NOAK TRISO-fueled NBs when claiming different types of IRA subsidies, the LCOH2 is broken in two ways to show share of the levelized cost of the electrolyzers versus energy and to show the distribution between the levelized costs of capital, O&M, and fuel

TRISO FOAK comparison

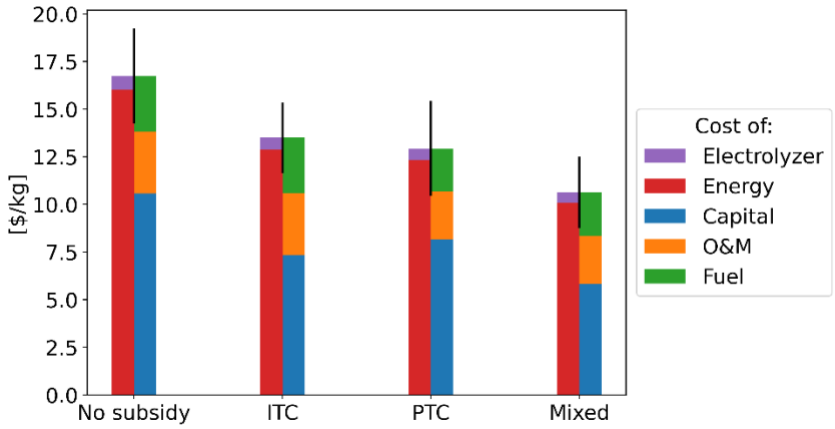

Figure 110 Comparison of the LCOH2 for distributed PEM electrolysis using two FOAK TRISO-fueled NBs when claiming different types of IRA subsidies, the LCOH2 is broken in two ways to show share of the levelized cost of the electrolyzers versus energy and to show the distribution between the levelized costs of capital, O&M, and fuel

C.3 SOEC electrolysis with nuclear batteries

C.3.1 Community-scale production

Table 31 LCOH2 breakdown for community-scale SOEC electrolysis with UO_2-fueled NBs, LCOH2 given in $/kg as μ ± σ [m, M]

NB Type	IRA Subsidy	Total	Capital	O&M	Fuel
NOAK	None	7.53 ± 1.07 [4.25, 13.07]	0.62 ± 0.12 [0.32, 1.05]	0.48 ± 0.05 [0.35, 0.64]	6.42 ± 1.01 [3.33, 11.68]
	PTC	3.99 ± 1.27 [0.83, 11.19]	0.62 ± 0.12 [0.33, 1.06]	0.48 ± 0.05 [0.34, 0.64]	5.79 ± 1.02 [2.88, 10.92]
	ITC	6.37 ± 0.84 [3.98, 10.65]	0.42 ± 0.08 [0.21, 0.70]	0.48 ± 0.05 [0.35, 0.64]	5.47 ± 0.81 [3.27, 9.67]
	Mixed	3.67 ± 1.09 [1.05, 9.92]	0.62 ± 0.12 [0.32, 1.05]	0.48 ± 0.05 [0.35, 0.64]	5.47 ± 0.81 [3.22, 9.65]
FOAK	None	11.50 ± 1.71 [6.73, 18.92]	0.62 ± 0.12 [0.32, 1.06]	0.48 ± 0.05 [0.35, 0.63]	10.39 ± 1.63 [5.83, 17.61]
	PTC	7.96 ± 1.83 [3.06, 18.15]	0.62 ± 0.12 [0.32, 1.05]	0.48 ± 0.05 [0.35, 0.64]	9.76 ± 1.61 [5.21, 17.70]
	ITC	9.03 ± 1.22 [5.32, 15.53]	0.42 ± 0.08 [0.21, 0.70]	0.48 ± 0.05 [0.35, 0.64]	8.13 ± 1.16 [4.66, 14.49]
	Mixed	6.33 ± 1.41 [2.58, 13.91]	0.62 ± 0.12 [0.32, 1.05]	0.48 ± 0.05 [0.35, 0.63]	8.13 ± 1.16 [4.76, 13.71]

UO_2 NOAK comparison

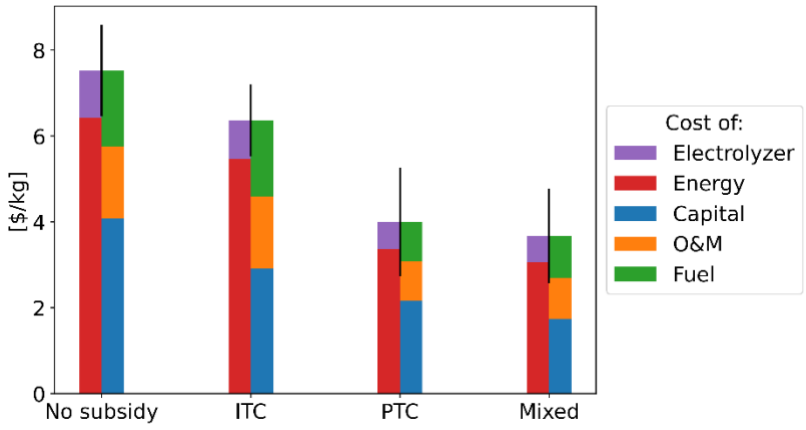

Figure 111 Comparison of the LCOH2 for community-scale SOEC electrolysis using NOAK UO_2-fueled NBs when claiming different types of IRA subsidies, the LCOH2 is broken in two ways to show share of the levelized cost of the electrolyzers versus energy and to show the distribution between the levelized costs of capital, O&M, and fuel

UO_2 FOAK comparison

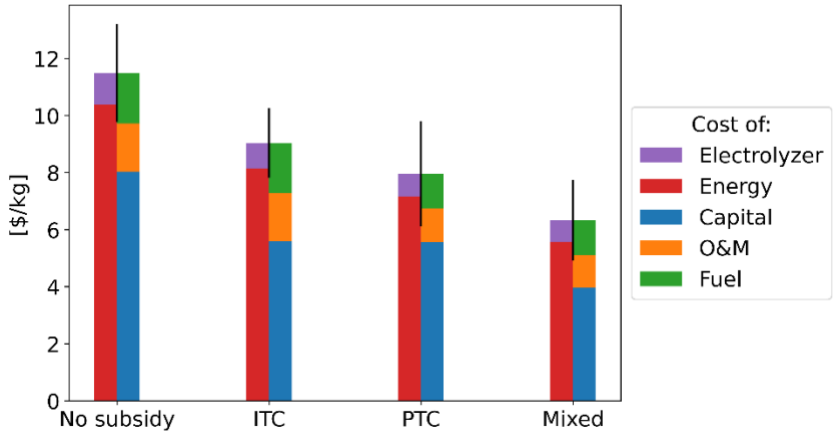

Figure 112 Comparison of the LCOH2 for community-scale SOEC electrolysis using FOAK UO_2-fueled NBs when claiming different types of IRA subsidies, the LCOH2 is broken in two ways to show share of the levelized cost of the electrolyzers versus energy and to show the distribution between the levelized costs of capital, O&M, and fuel

Table 32 LCOH2 breakdown for community-scale SOEC electrolysis with TRISO-fueled NBs, LCOH2 given in $/kg as μ ± σ [m, M]

NB Type	IRA Subsidy	Total	Capital	O&M	Fuel
NOAK	None	8.03 ± 1.09 [4.56, 13.27]	0.63 ± 0.12 [0.32, 1.06]	0.48 ± 0.05 [0.35, 0.63]	6.92 ± 1.03 [3.71, 11.86]
	PTC	4.40 ± 1.10 [1.08, 9.44]	0.63 ± 0.12 [0.32, 1.04]	0.48 ± 0.05 [0.35, 0.64]	6.29 ± 1.04 [3.07, 11.17]
	ITC	6.86 ± 0.86 [4.02, 11.14]	0.42 ± 0.08 [0.21, 0.72]	0.48 ± 0.05 [0.35, 0.64]	5.96 ± 0.83 [3.29, 10.18]
	Mixed	4.07 ± 0.89 [1.37, 8.46]	0.62 ± 0.12 [0.32, 1.05]	0.48 ± 0.05 [0.35, 0.64]	5.96 ± 0.84 [3.44, 10.06]
FOAK	None	11.99 ± 1.74 [7.02, 19.95]	0.63 ± 0.12 [0.32, 1.05]	0.48 ± 0.05 [0.35, 0.64]	10.89 ± 1.65 [6.16, 18.48]
	PTC	8.36 ± 1.73 [3.24, 16.00]	0.62 ± 0.12 [0.32, 1.07]	0.48 ± 0.05 [0.35, 0.64]	10.25 ± 1.64 [5.46, 17.60]
	ITC	9.52 ± 1.24 [5.51, 14.94]	0.42 ± 0.08 [0.22, 0.72]	0.48 ± 0.05 [0.35, 0.63]	8.62 ± 1.18 [4.81, 13.94]
	Mixed	6.72 ± 1.26 [2.96, 13.01]	0.62 ± 0.12 [0.33, 1.03]	0.48 ± 0.05 [0.34, 0.63]	8.62 ± 1.18 [5.04, 14.57]

TRISO NOAK comparison

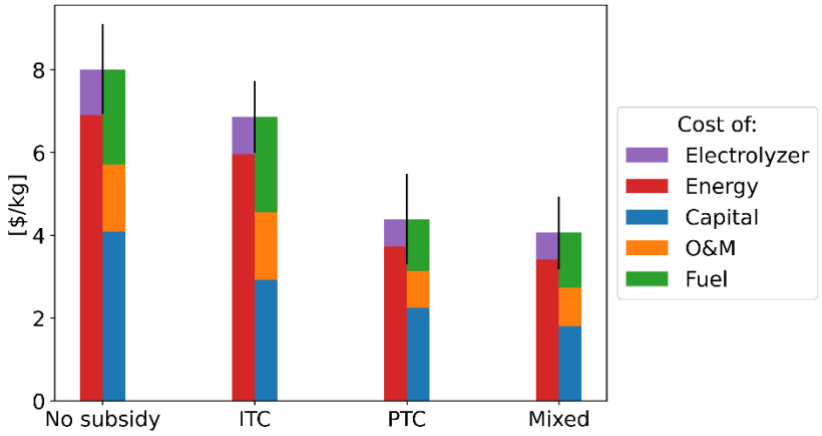

Figure 113 Comparison of the LCOH2 for community-scale SOEC electrolysis using NOAK TRISO-fueled NBs when claiming different types of IRA subsidies, the LCOH2 is broken in two ways to show share of the levelized cost of the electrolyzers versus energy and to show the distribution between the levelized costs of capital, O&M, and fuel

TRISO FOAK comparison

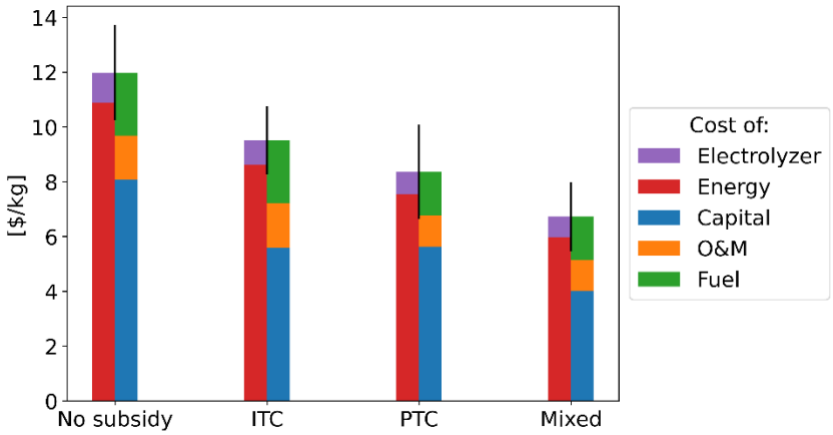

Figure 114 Comparison of the LCOH2 for community-scale SOEC electrolysis using FOAK TRISO-fueled NBs when claiming different types of IRA subsidies, the LCOH2 is broken in two ways to show share of the levelized cost of the electrolyzers versus energy and to show the distribution between the levelized costs of capital, O&M, and fuel

C.3.2 Distributed production

Table 33 LCOH2 breakdown for distributed SOEC electrolysis with UO_2-fueled NBs, LCOH2 given in $/kg as μ ± σ [m, M]

NB Type	IRA Subsidy	Total	Capital	O&M	Fuel
NOAK	None	11.49 ± 1.68 [6.22, 19.17]	0.67 ± 0.13 [0.35, 1.17]	0.54 ± 0.06 [0.37, 0.75]	10.29 ± 1.63 [5.29, 17.70]
	PTC	7.98 ± 1.82 [2.54, 16.92]	0.67 ± 0.13 [0.34, 1.21]	0.54 ± 0.06 [0.37, 0.76]	9.67 ± 1.64 [4.54, 16.65]
	ITC	10.24 ± 1.52 [5.69, 17.18]	0.45 ± 0.09 [0.23, 0.79]	0.54 ± 0.06 [0.37, 0.75]	9.26 ± 1.49 [4.83, 16.01]
	Mixed	7.56 ± 1.67 [2.79, 15.85]	0.67 ± 0.13 [0.34, 1.21]	0.54 ± 0.06 [0.38, 0.75]	9.26 ± 1.49 [4.79, 15.58]
FOAK	None	15.79 ± 2.24 [8.60, 25.71]	0.67 ± 0.13 [0.34, 1.15]	0.54 ± 0.06 [0.37, 0.74]	14.59 ± 2.15 [7.60, 24.14]
	PTC	12.28 ± 2.35 [5.11, 24.91]	0.67 ± 0.13 [0.35, 1.17]	0.54 ± 0.06 [0.37, 0.76]	13.98 ± 2.17 [7.12, 24.48]
	ITC	13.12 ± 1.81 [7.17, 20.93]	0.45 ± 0.09 [0.23, 0.78]	0.54 ± 0.06 [0.38, 0.75]	12.14 ± 1.77 [6.36, 19.74]
	Mixed	10.45 ± 1.94 [4.54, 20.81]	0.67 ± 0.13 [0.32, 1.16]	0.54 ± 0.06 [0.37, 0.74]	12.15 ± 1.75 [6.58, 20.34]

UO_2 NOAK comparison

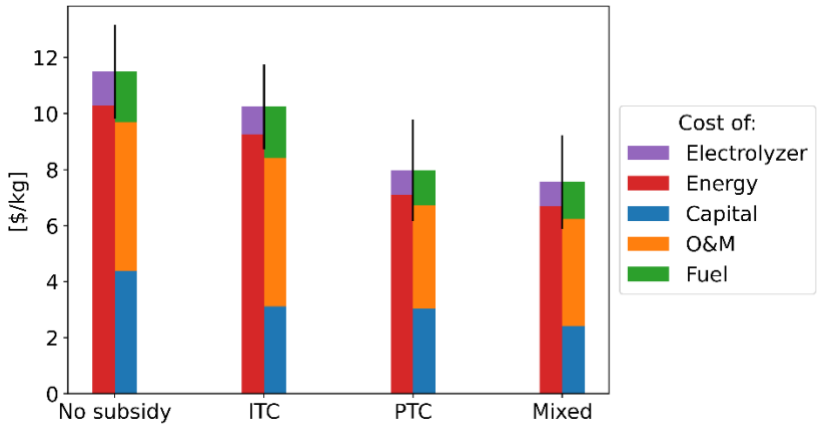

Figure 115 Comparison of the LCOH2 for distributed SOEC electrolysis using NOAK UO_2-fueled NBs when claiming different types of IRA subsidies, the LCOH2 is broken in two ways to show share of the levelized cost of the electrolyzers versus energy and to show the distribution between the levelized costs of capital, O&M, and fuel

UO_2 FOAK comparison

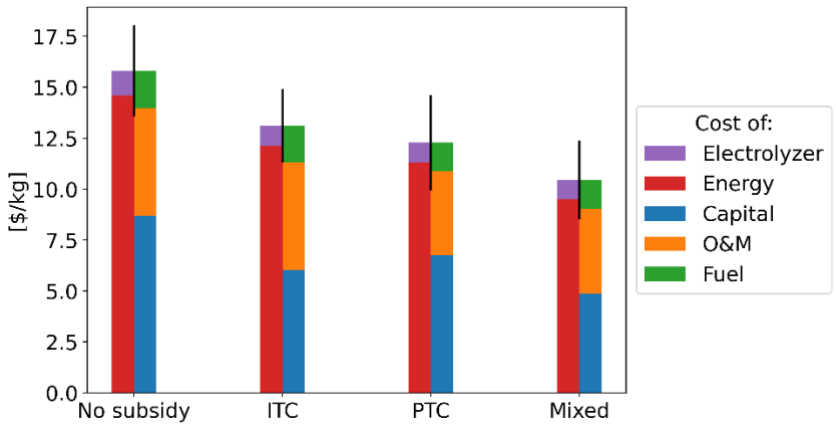

Figure 116 Comparison of the LCOH2 for distributed SOEC electrolysis using FOAK UO_2-fueled NBs when claiming different types of IRA subsidies, the LCOH2 is broken in two ways to show share of the levelized cost of the electrolyzers versus energy and to show the distribution between the levelized costs of capital, O&M, and fuel

Table 34 LCOH2 breakdown for distributed SOEC electrolysis with TRISO-fueled NBs, LCOH2 given in $/kg as μ ± σ [m, M]

NB Type	IRA Subsidy	Total	Capital	O&M	Fuel
NOAK	None	12.01 ± 1.69 [6.70, 19.55]	0.67 ± 0.13 [0.36, 1.13]	0.54 ± 0.06 [0.37, 0.76]	10.81 ± 1.64 [5.76, 18.03]
	PTC	8.39 ± 1.69 [3.01, 16.20]	0.67 ± 0.13 [0.34, 1.16]	0.54 ± 0.06 [0.37, 0.75]	10.19 ± 1.65 [4.88, 17.57]
	ITC	10.76 ± 1.52 [5.81, 17.01]	0.45 ± 0.09 [0.24, 0.77]	0.54 ± 0.06 [0.37, 0.75]	9.78 ± 1.50 [4.91, 16.05]
	Mixed	7.98 ± 1.54 [2.90, 14.36]	0.67 ± 0.13 [0.34, 1.15]	0.53 ± 0.06 [0.37, 0.75]	9.78 ± 1.50 [4.81, 15.96]
FOAK	None	16.31 ± 2.26 [9.37, 26.01]	0.67 ± 0.13 [0.36, 1.15]	0.54 ± 0.06 [0.38, 0.75]	15.11 ± 2.18 [8.36, 24.54]
	PTC	12.70 ± 2.27 [5.36, 23.18]	0.67 ± 0.13 [0.36, 1.19]	0.53 ± 0.06 [0.38, 0.75]	14.49 ± 2.19 [7.35, 24.45]
	ITC	13.63 ± 1.82 [7.72, 22.18]	0.45 ± 0.09 [0.23, 0.77]	0.54 ± 0.06 [0.37, 0.76]	12.65 ± 1.77 [6.87, 20.85]
	Mixed	10.86 ± 1.85 [5.23, 18.13]	0.67 ± 0.13 [0.34, 1.18]	0.54 ± 0.06 [0.37, 0.76]	12.65 ± 1.78 [7.10, 19.79]

TRISO NOAK comparison

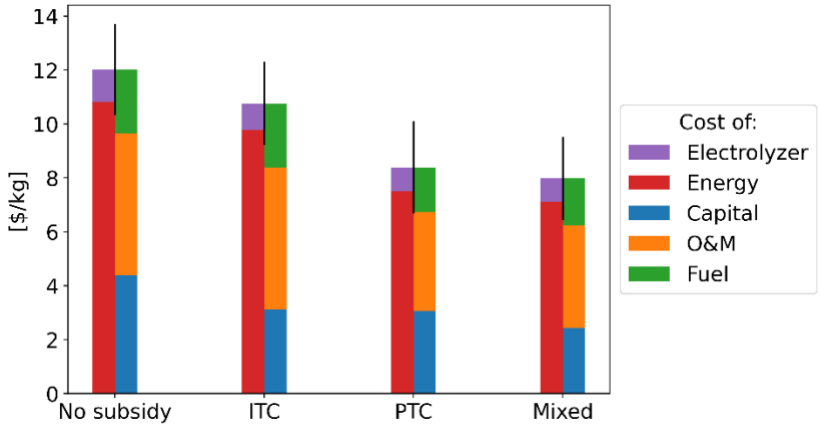

Figure 117 Comparison of the LCOH2 for distributed SOEC electrolysis using NOAK TRISO-fueled NBs when claiming different types of IRA subsidies, the LCOH2 is broken in two ways to show share of the levelized cost of the electrolyzers versus energy and to show the distribution between the levelized costs of capital, O&M, and fuel

TRISO FOAK comparison

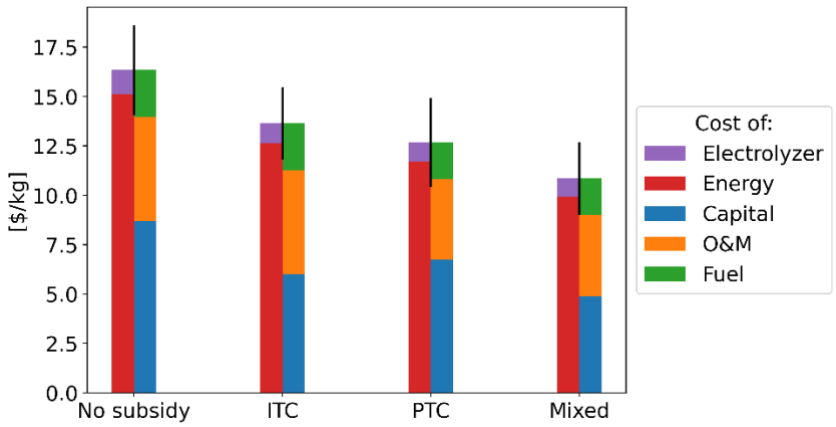

Figure 118 Comparison of the LCOH2 for distributed SOEC electrolysis using FOAK TRISO-fueled NBs when claiming different types of IRA subsidies, the LCOH2 is broken in two ways to show share of the levelized cost of the electrolyzers versus energy and to show the distribution between the levelized costs of capital, O&M, and fuel

C.3.3 Distributed production with two NBs

Table 35 LCOH2 breakdown for distributed SOEC electrolysis with two UO_2-fueled NBs, LCOH2 given in $/kg as μ ± σ [m, M]

NB Type	IRA Subsidy	Total	Capital	O&M	Fuel
NOAK	None	8.76 ± 1.27 [4.87, 15.21]	0.44 ± 0.09 [0.22, 0.83]	0.51 ± 0.06 [0.35, 0.73]	7.81 ± 1.22 [4.06, 13.82]
	PTC	5.22 ± 1.44 [1.20, 13.54]	0.44 ± 0.09 [0.21, 0.82]	0.51 ± 0.06 [0.35, 0.73]	7.18 ± 1.22 [3.36, 13.25]
	ITC	7.57 ± 1.05 [4.54, 14.08]	0.29 ± 0.06 [0.15, 0.55]	0.51 ± 0.06 [0.35, 0.72]	6.76 ± 1.02 [3.80, 12.92]
	Mixed	4.81 ± 1.26 [1.65, 13.01]	0.44 ± 0.09 [0.22, 0.79]	0.51 ± 0.06 [0.35, 0.72]	6.76 ± 1.01 [3.81, 12.79]
FOAK	None	13.05 ± 1.95 [7.22, 22.34]	0.44 ± 0.09 [0.23, 0.80]	0.51 ± 0.06 [0.35, 0.73]	12.10 ± 1.87 [6.46, 21.14]
	PTC	9.52 ± 2.06 [3.70, 20.42]	0.44 ± 0.09 [0.21, 0.84]	0.51 ± 0.06 [0.35, 0.73]	11.48 ± 1.87 [5.88, 20.26]
	ITC	10.45 ± 1.43 [5.84, 17.36]	0.29 ± 0.06 [0.15, 0.56]	0.51 ± 0.06 [0.36, 0.73]	9.64 ± 1.38 [5.18, 16.34]
	Mixed	7.69 ± 1.60 [3.31, 16.85]	0.44 ± 0.09 [0.21, 0.83]	0.51 ± 0.06 [0.35, 0.74]	9.65 ± 1.38 [5.58, 16.58]

UO_2 NOAK comparison

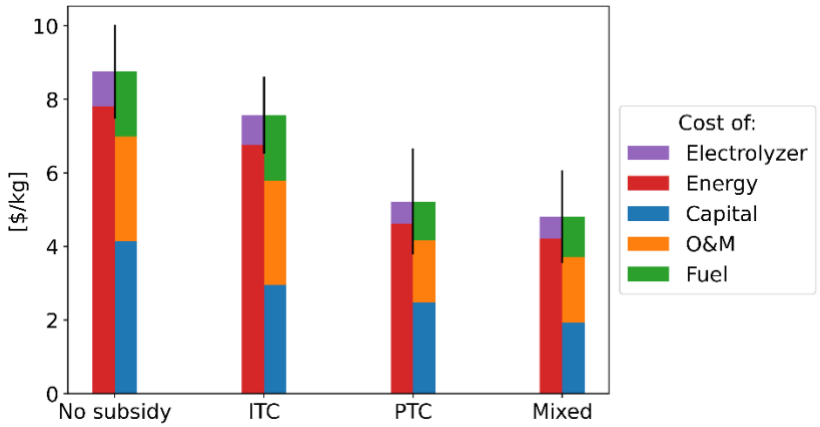

Figure 119 Comparison of the LCOH2 for distributed SOEC electrolysis using two NOAK UO_2-fueled NBs when claiming different types of IRA subsidies, the LCOH2 is broken in two ways to show share of the levelized cost of the electrolyzers versus energy and to show the distribution between the levelized costs of capital, O&M, and fuel

UO_2 FOAK comparison

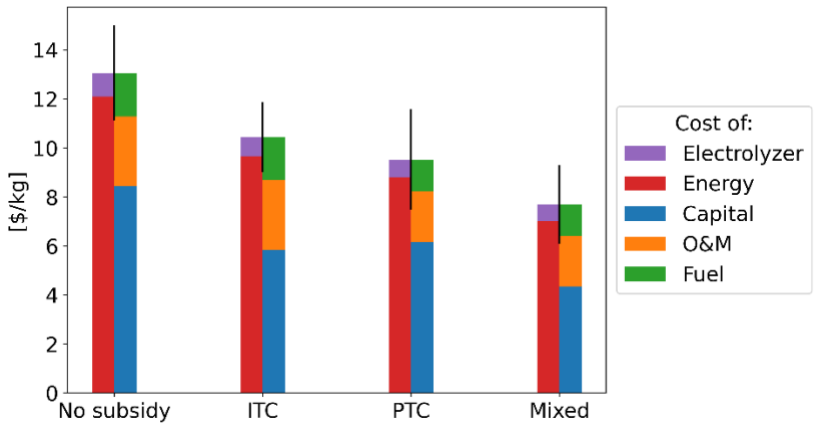

Figure 120 Comparison of the LCOH2 for distributed SOEC electrolysis using two FOAK UO_2-fueled NBs when claiming different types of IRA subsidies, the LCOH2 is broken in two ways to show share of the levelized cost of the electrolyzers versus energy and to show the distribution between the levelized costs of capital, O&M, and fuel

Table 36 LCOH2 breakdown for distributed SOEC electrolysis with two TRISO-fueled NBs, LCOH2 given in $/kg as μ ± σ [m, M]

NB Type	IRA Subsidy	Total	Capital	O&M	Fuel
NOAK	None	9.23 ± 1.29 [5.25, 15.27]	0.44 ± 0.09 [0.22, 0.84]	0.51 ± 0.06 [0.35, 0.72]	8.28 ± 1.24 [4.43, 14.03]
	PTC	5.61 ± 1.30 [1.24, 11.69]	0.44 ± 0.09 [0.22, 0.83]	0.51 ± 0.06 [0.36, 0.73]	7.66 ± 1.25 [3.43, 13.49]
	ITC	8.05 ± 1.08 [4.64, 13.81]	0.29 ± 0.06 [0.14, 0.54]	0.51 ± 0.06 [0.35, 0.72]	7.25 ± 1.04 [3.92, 12.90]
	Mixed	5.20 ± 1.09 [1.64, 11.11]	0.44 ± 0.09 [0.21, 0.82]	0.51 ± 0.06 [0.36, 0.72]	7.25 ± 1.04 [3.88, 13.04]
FOAK	None	13.52 ± 1.96 [7.60, 22.14]	0.44 ± 0.09 [0.21, 0.82]	0.51 ± 0.06 [0.35, 0.72]	12.57 ± 1.89 [6.88, 20.94]
	PTC	9.89 ± 1.96 [3.62, 19.23]	0.44 ± 0.09 [0.21, 0.81]	0.51 ± 0.06 [0.35, 0.72]	11.94 ± 1.89 [5.88, 20.94]
	ITC	10.93 ± 1.46 [6.41, 17.72]	0.29 ± 0.06 [0.14, 0.55]	0.51 ± 0.06 [0.35, 0.73]	10.12 ± 1.41 [5.75, 16.84]
	Mixed	8.06 ± 1.47 [3.61, 15.46]	0.44 ± 0.09 [0.22, 0.82]	0.51 ± 0.06 [0.35, 0.72]	10.12 ± 1.41 [5.87, 17.16]

TRISO NOAK comparison

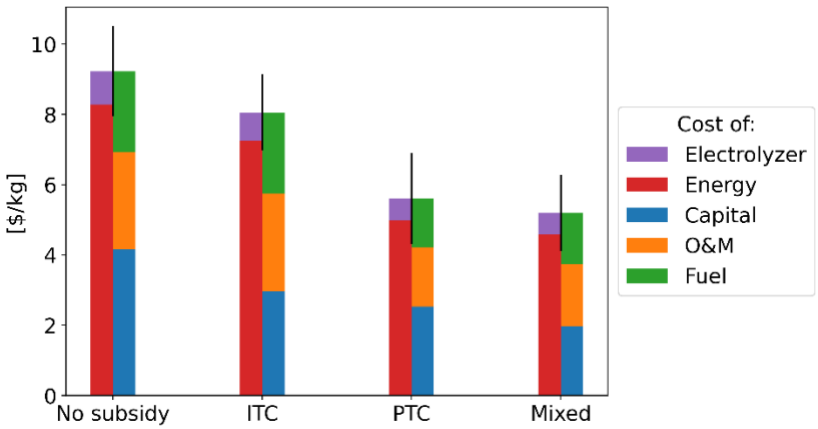

Figure 121 Comparison of the LCOH2 for distributed SOEC electrolysis using two NOAK TRISO-fueled NBs when claiming different types of IRA subsidies, the LCOH2 is broken in two ways to show share of the levelized cost of the electrolyzers versus energy and to show the distribution between the levelized costs of capital, O&M, and fuel

TRISO FOAK comparison

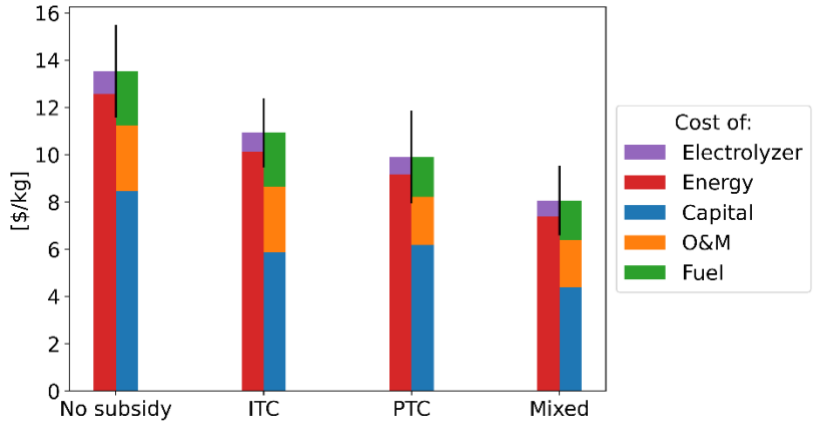

Figure 122 Comparison of the LCOH2 for distributed SOEC electrolysis using two FOAK TRISO-fueled NBs when claiming different types of IRA subsidies, the LCOH2 is broken in two ways to show share of the levelized cost of the electrolyzers versus energy and to show the distribution between the levelized costs of capital, O&M, and fuel